Materials Futures

TOPICAL REVIEW • OPEN ACCESS

Graphene quantum dots: preparations, properties, functionalizations and applications

To cite this article: Pin Tian *et al* 2024 *Mater. Futures* **3** 022301

OPEN ACCESS
IOP Publishing | Songshan Lake Materials Laboratory
Materials Futures
Mater. Futures 3 (2024) 022301 (49pp)
https://doi.org/10.1088/2752-5724/ad08cb

Topical Review

Graphene quantum dots: preparations, properties, functionalizations and applications

Pin Tian[1], Libin Tang[1,*], Kar-Seng Teng[2] and Shu-Ping Lau[3]

[1] Kunming Institute of Physics, 650223 Kunming, Yunnan, People's Republic of China
[2] Department of Electronic and Electrical Engineering, Faculty of Science and Engineering, Swansea University, Bay Campus, Fabian Way, Swansea SA1 8EN, United Kingdom
[3] Department of Applied Physics, The Hong Kong Polytechnic University, Hung Hom, Kowloon, Hong Kong, People's Republic of China

E-mail: scitang@163.com

Received 24 August 2023, revised 7 October 2023
Accepted for publication 18 October 2023
Published 7 February 2024

Abstract

Zero-dimensional graphene quantum dots (GQDs) exhibit many different properties, such as strong fluorescence, nonzero bandgap and solubility in solvents, compared to two-dimensional graphene. GQDs are biocompatible and have low toxicity; hence, they are widely used in the biomedical field. The edge effect of GQDs is of particular interest because edge modification can regulate the performance of nanomaterials. In this review, various preparation methods for GQDs, which can be divided into three main categories, namely top-down, bottom-up and chemical methods, are discussed. The unique optical, electrical, thermal and magnetic properties of GQDs are reviewed. The functionalization of GQDs by doping with heteroatoms and forming composites with other materials is studied, and the characteristics of these GQDs are also discussed. The applications of these GQDs in the fields of optics, electricity, optoelectronics, biomedicine, energy, agriculture and other emerging interdisciplinary fields are reviewed to highlight the enormous potential of nanomaterials. This review reports on the recent advancement in GQD research and suggests future directions for the development of GQDs.

Keywords: graphene quantum dots: preparations, properties, functionalizations and applications

1. Introduction

The discovery of new materials enables the realization of new physical and chemical phenomena that could result in the development of novel technologies and applications. For example, the discovery of graphene [1] in the 21st century has enabled the understanding of many excellent physical and chemical properties of two-dimensional materials [2–8], which led to the development of many exciting applications. Carbon materials have been of great scientific interest since the 1950s, particularly in the discovery of fullerene materials [9]. The fascinating properties of fullerenes have attracted the attention of researchers from around the world. Diamond [10], which is the oldest carbon material, has attracted scientists [11–20] from different fields because of its physical

* Author to whom any correspondence should be addressed.

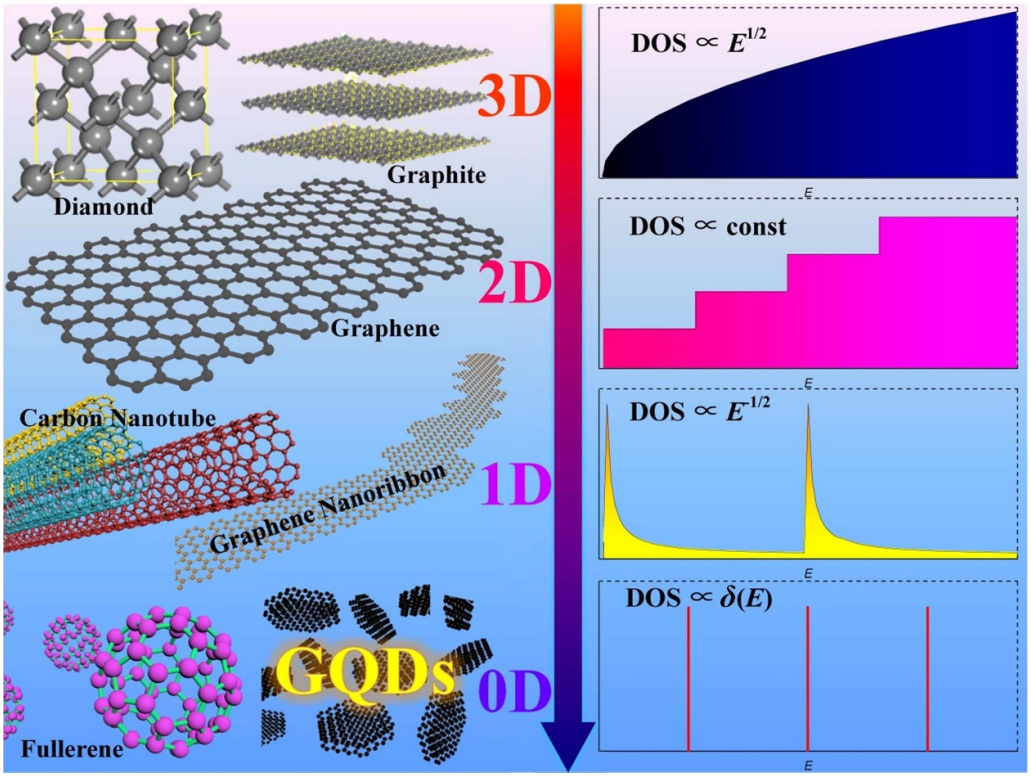

Figure 1. Different dimensions of carbon materials (left) and their related DOS against energy plots (right).

and chemical properties, such as hardness [21–24] and low dielectric constant [25–30]. Later, scientists from Japan [31] discovered a new one-dimensional carbon material, known as carbon nanotube, using the arc-discharge method. The high electron mobility in the one-dimensional material [32–36], chiral dependence [37–41] and other unique phenomena [42–46] have attracted enormous research interest. In 2004, the scientific community was filled with excitement upon the discovery of graphene [1], as its electrons exhibited the Dirac cone property of having no static mass [47]. Since then, carbon materials have been categorized according to different dimensions, such as three-dimensional bulk materials (e.g. graphite [48–50] and diamonds), two-dimensional nanosheets (e.g. graphene [51–53]), one-dimensional nanowires (e.g. carbon nanotube [54–56] and graphene nanoribbons [57–60]), and zero-dimensional dots (e.g. fullerenes [61–65] and graphene quantum dots (GQDs) [66–70]). These different dimensions of carbon materials can exhibit different electronic, physical and chemical properties. The electron densities of states (DOS) for the different dimensions of carbon materials are illustrated in figure 1. The electron DOS of a three-dimensional material is proportional to the 1/2 power of the energy. The DOS of a two-dimensional material is constant, whereas that of a one-dimensional material is negative 1/2 power relations. The DOS is quantized for a zero-dimensional material.

Among these carbon materials, graphene has attracted tremendous attention due to its excellent physical and chemical properties [71–78], which led to the development of many novel applications, such as magic-angle graphene superconductivity [79–81], ultrahigh-performance photodetector [82–84] and biomedical applications [85–90]. Although graphene has many excellent properties and applications, it has some limitations, such as a zero-bandgap structure [91], high preparation cost [92, 93] and difficulty in preparing large single crystals [73, 94, 95]. In 2008, Geim *et al* [96], who discovered graphene, used an electron beam etching technique to prepare zero-dimensional GQDs from graphene. GQDs, which are the newest members of the family of carbon materials, have received much attention because they inherit the excellent properties of graphene materials, such as high specific surface area, high carrier mobility, high inertia, high stability, nontoxicity and high light-to-heat conversion efficiency [91]. Due to the zero-dimensional properties of GQDs, these materials also exhibit quantum confinement in all three spatial directions and edge effects. Figure 2 depicts the characteristics of GQDs discussed in this review. Many excellent studies on GQDs have been reported [97–100] since the first demonstration of the nanomaterials. For example, Tang *et al* [100] reported a bottom-up synthesis technique (often known as the Tang–Lau method) that can effectively control the size of the GQDs, and hence their energy gap, which is an important parameter for many optoelectronic applications. Unlike carbon nanodots, GQDs exhibit crystalline properties with significant quantum confinement effects. The distinction between carbon dots and GQDs was discussed in a previous review [101]. The properties and potential applications of GQDs have not been fully realized because these nanomaterials are relatively new members of the carbon material family. In recent years, the physical and chemical properties of GQDs have been studied extensively, and their applications have been

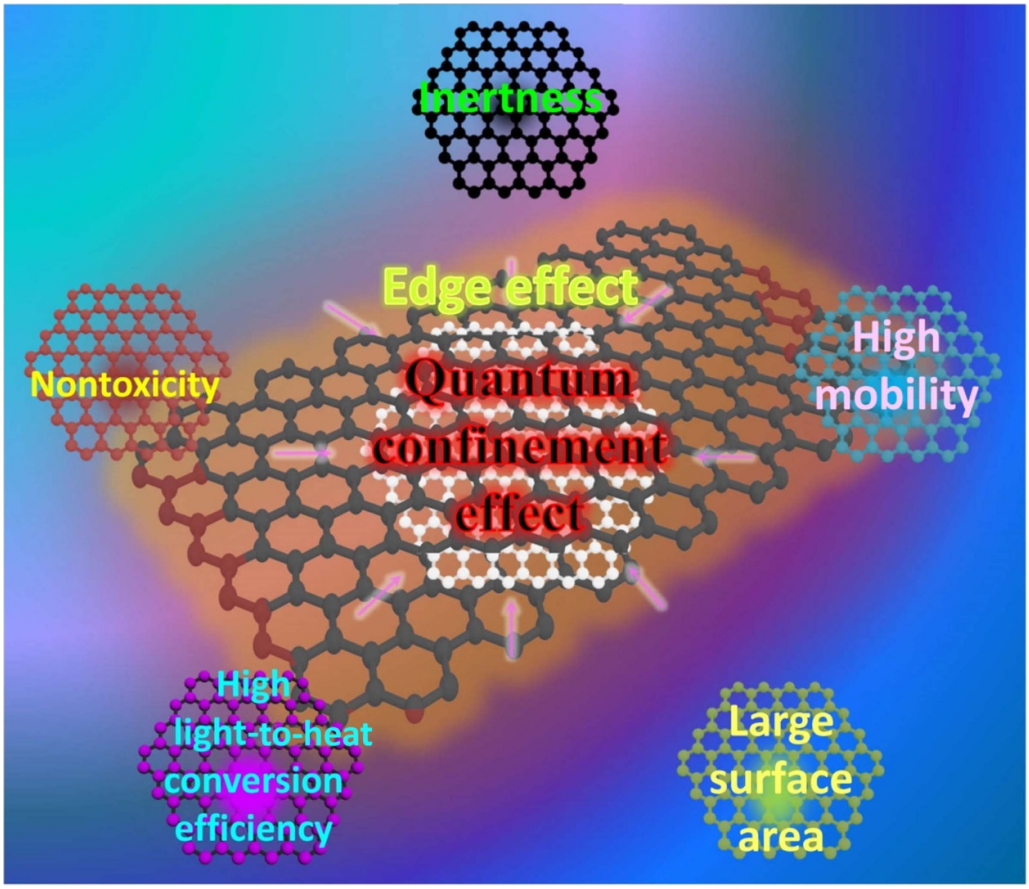

Figure 2. Schematic of the different properties of GQDs.

demonstrated. Although there already existed several excellent reviews [102–109] on GQDs, recent advancements in nanomaterials over the past two to three years have not been reviewed. Therefore, this review will provide an insight into recently reported remarkable studies on GQDs that are of significant interest to researchers working on similar nanomaterials, which offer many exciting and novel applications.

GQDs exhibit a strong fluorescence effect due to the quantum confinement of carriers in the nanomaterials. The excellent fluorescence properties of GQDs have drawn significant attention in the biomedical field, particularly in applications such as fluorescent probes [110], monitoring [98] and cancer treatment [111]. The edge effect of GQDs allows effective and simple functionalization of nanomaterials via doping of impurity atoms at the edge [112–116], thereby regulating the fluorescence wavelength of the GQDs. Such an edge effect also facilitates the formation of GQD-based composite materials by hybridizing with other substances [117–122], paving the way for many novel applications. Previous studies on GQDs have demonstrated many potential applications of these nanomaterials in a wide range of fields, such as energy environment [123], agriculture [124], biomedicine [125], photoelectric detection [126] and gas sensing [127], as depicted in figure 3. In this review, many new and exciting applications of GQDs over the past two to three years are introduced in detail. Research into GQDs continues to gain momentum, as many of their properties have not yet been fully understood [101]. This review examines recent advancements in the preparation, functionalization and application of GQDs.

2. Preparation methods

The preparation methodology of GQDs can significantly affect their widespread application, as it can influence the yield, cost and properties of the material. Most studies [108, 128–130] have divided the preparation methodology of GQDs into two categories: bottom-up and top-down methods. However, with the rapid development of new GQD preparation techniques, the two categories must be expanded to include other preparation methodologies. In this review, an additional category, which is a chemical method, is introduced. Chemistry is the science of reactions that produce changes in substances. Through the chemical reaction between two substances, an intermediate product or a precursor of GQDs is synthesized and subsequently converted into GQDs. This preparation methodology for GQDs is categorized as a chemical method. The bottom-up approach [131] for the preparation

Figure 3. Different applications of functionalized GQDs.

of GQDs is based on the polycondensation reaction of small molecular substances, whereas the top-down approach [132] is primarily based on the pyrolysis of bulk carbon materials. The main difference between these two methods and the chemical method is the formation of intermediates of GQDs in the latter method. The three categories that comprehensively classify the different preparation methodologies of GQDs are illustrated in figure 4. In the following sections, novel preparation methodologies of GQDs in all three categories developed over the last two years are introduced.

2.1. Top-down method

The top-down approach mainly involves the physical reduction of carbon materials, such as graphite [133], graphene [134], graphene oxide (GO) [135], carbon nanotubes [136] and fullerenes [137], into GQDs with sizes ranging from several nanometers to tens of nanometers by various means, as depicted in figure 5(a).

Laser ablation is a commonly used technique for preparing nanoparticles. It is simple, environmentally friendly, highly tunable and favored by many researchers for the preparation of nanomaterials. For example, Kang *et al* [138, 142] recently prepared GQDs using a technique involving the use of inexpensive graphene flakes as carbon source. Nitrogen-doped GQDs with improved optical properties were prepared in solution using the technique of laser ablation. Figure 5(b) shows the preparation method. Although this method is relatively simple and effective, the controllability of the GQD size is unfavorable. Transmission electron microscopy (TEM) images of the GQDs revealed good crystallinity of the materials but with nonuniformity in their sizes, as shown in figure 5(g); hence, GQDs prepared using the laser ablation method might not exhibit an obvious quantum confinement effect. Recently, some interesting techniques similar to the explosive method used for the preparation of diamond film [143–146] have been reported for the preparation of GQDs. Alidad *et al* [139] used graphite powder as carbon source, which underwent instantaneous explosive reaction with carbon dioxide to transform the graphite powder into GQDs. This preparation method, illustrated in figure 5(c), produced high-purity GQDs with a relatively uniform size distribution over a short period of time; however, it was difficult to control the size of the GQDs. He *et al* [147] prepared GQDs from carbon nanotubes. As depicted in figure 5(d), during the preparation process, the GQDs were functionalized with thiomalic acid (TA), which enhanced the fluorescent properties of the nanomaterials. Fullerene was also used to prepare GQDs, as

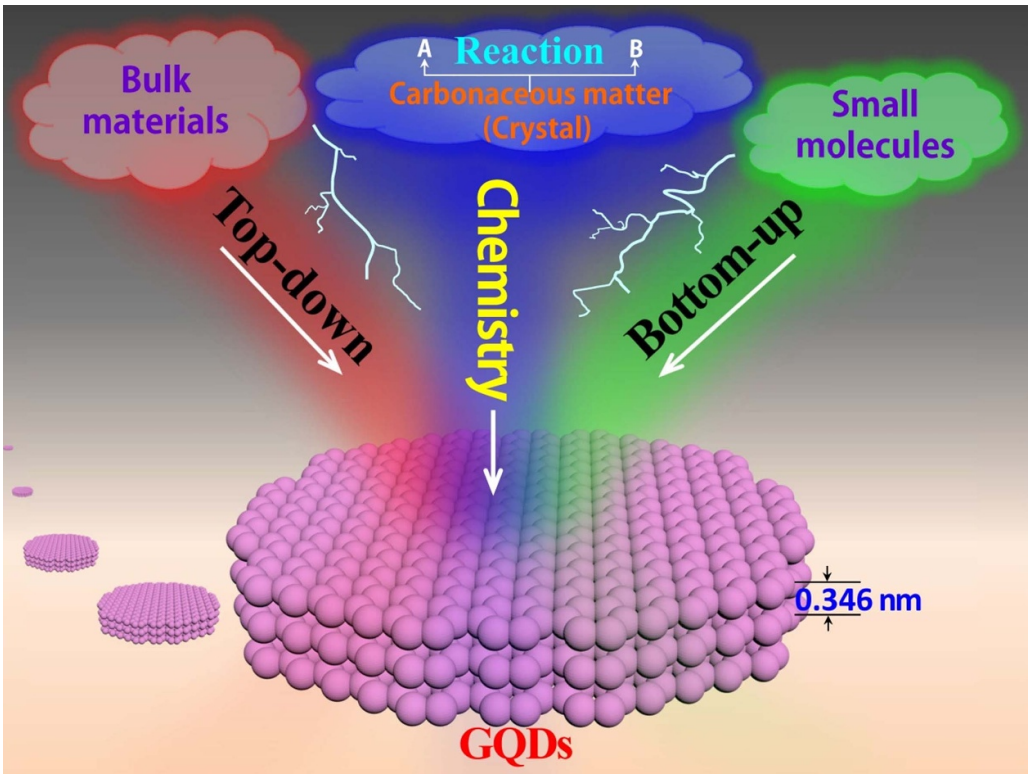

Figure 4. Schematic of the three categories of GQD preparation methods: top-down, bottom-up and chemical methods.

demonstrated for the first time by Loh *et al* [137]. Recently, Chen *et al* [141] prepared GQDs using fullerenes as a carbon source in a solvent thermal method (illustrated in figure 5(d)), which resulted in a high yield of GQDs at a relatively low cost; however, the nanomaterials were nonuniform in size, as shown in the atomic force microscope image in figure 5(f). The quantum yield of the GQDs prepared by this method was as high as 52.4% in the orange band (e.g. 617 nm), which is important for the future development of red-emission GQDs. The preparation of GQDs by electrolysis using carbon-based materials as electrodes has been reported [148, 149]; however, this process is time-consuming. Recently, Yang *et al* [140] developed a novel carbon cloth electrode coated with nitrogen-doped nanomesh graphene, which significantly improved the efficiency of GQD preparation and the carbon source utilization rate. The method, illustrated in figure 5(e), can produce a relatively high concentration of nitrogen-doped GQDs.

In summary, the top-down method allows rapid, low-cost mass production of GQDs [150–152], but the use of external energy to click carbon materials into GQDs results in poor controllability and nonuniformity of the GQD size. Therefore, this method is unsuitable for producing GQDs with well-controlled size, which is an essential requirement for optical applications.

2.2. Bottom-up method

The preparation of GQDs using bottom-up methods mainly involves the energy of small molecules with external energy. The formation of GQDs through condensation provides precise control of their sizes and morphologies, thus exhibiting an excellent quantum size effect. However, this method often requires the use of a ligand, similar to other quantum dot preparations [153–159], resulting in GQDs with a large number of ligands.

The size and morphology of GQDs can be controlled by selecting appropriate carbon sources and preparation conditions. Recently, Park *et al* [160] reported the preparation of the hexagonal structure of GQDs using D-glucose as a carbon source in a chemical liquid-phase catalytic condensation polymerization technique. The size of the GQDs was in the tens of nanometers with a uniform distribution. As shown in figures 6(a)–(d), the GQDs exhibited a hexagonal structure with an obvious grain boundary.

The use of microwaves in the synthesis of GQDs was first demonstrated by Tang *et al* [164–166], who also demonstrated the tunability of the optical bandgap of GQDs in their work. Recently, Gu *et al* [161] applied the microwave technique to prepare nitrogen-doped GQDs, as illustrated in figure 6(e). By regulating the proportion of the precursors, they reported the synthesis of C_3N_4 and graphite acetylene quantum dots, which are considered relatively new carbon materials. Using the microwave technique, Lee *et al* [167] prepared GQDs with functional groups passivated at their surfaces, and the GQDs were used in green-emitting lasers. The electrochemical method is another effective way to synthesize small molecules into GQDs, as shown in figure 6(f). Yang *et al* [162] used a microplasma-assisted electrochemical method to prepare GQDs with different sizes, which were dependent on the size of precursor molecules. Zhao *et al* [163]

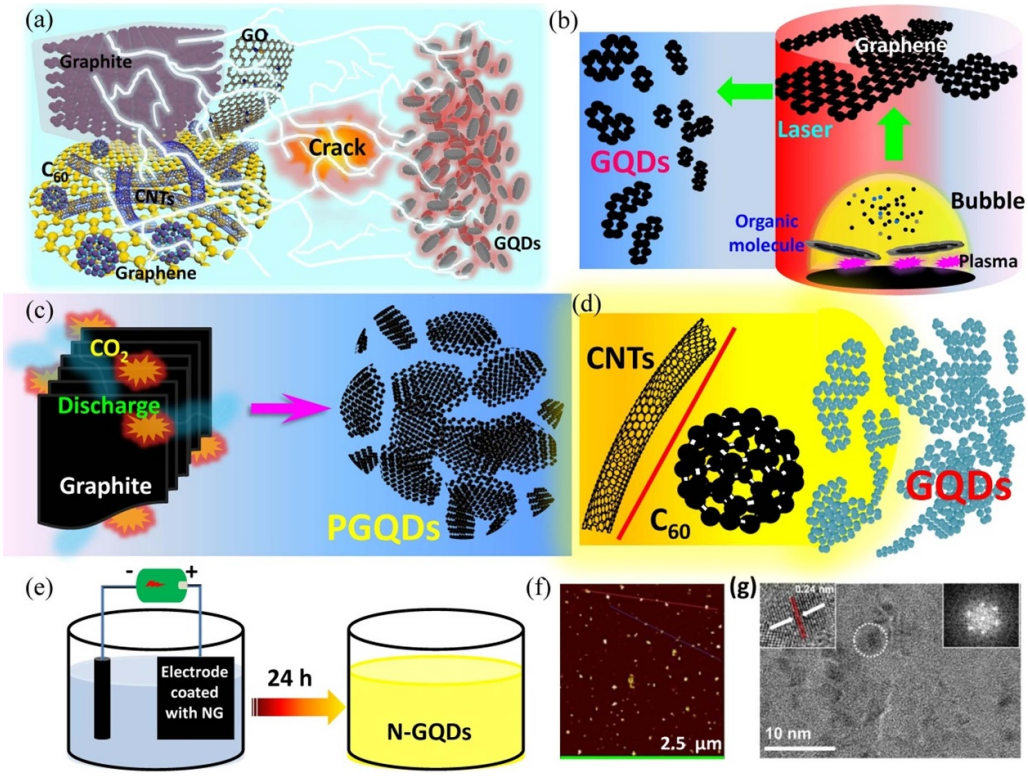

Figure 5. Top-down approach for the preparation of GQDs. (a) Schematic illustrating the preparation of GQDs, which involves the physical reduction of carbon materials. (b) Schematic depicting the use of laser ablation technique in the preparation of nitrogen-doped GQDs from graphite flakes. Reprinted from [138], © 2019 Elsevier B.V. All rights reserved. (c) Schematic of the exfoliation and cutting mechanism of graphite into GQDs using a shear mixer in supercritical CO_2. Reprinted from [139], © 2018 Elsevier B.V. All rights reserved. (d) Schematic depicting the synthesis of GQDs from carbon nanotubes or fullerene via a thiol-ene reaction or solvothermal treatment. (e) Schematic of nitrogen-doped GQD preparation process by electrolysis. Reproduced from [140], with permission from Springer Nature. (f) Atomic force microscope image of GQDs prepared by solvothermal method. Reprinted with permission from [141]. Copyright (2020) American Chemical Society. (g) High-resolution transmission electron microscope images of GQDs prepared by pulsed laser ablation. Reprinted from [138], © 2019 Elsevier B.V. All rights reserved.

revealed that the size of GQDs can be determined by precursor types. For example, GQDs prepared using a similar synthesis method but different precursors produced GQDs of different sizes and therefore producing GQDs that can generate blue, green and red fluorescent bands, as shown in figure 6(g). Extensive research activities [164–166] have shown that the bottom-up method is an effective technique for controlling the size and morphology of GQDs. This allows the tuning of the energy band structure of GQDs, which is invaluable for many applications.

2.3. Chemical method

In contrast to the first two methods, the chemical method mainly involves chemical changes of substances during the formation of GQDs. First, carbon-containing compounds are converted into the precursors of GQDs by a chemical method. Next, the precursors are converted into GQDs by external energy or other means. Many methods [168–172] reported previously on the preparation of GQDs fall into this category, but earlier papers often attribute their preparation methods to either top-down or bottom-up method, according to the precursors of GQDs. In this review, the preparation method of GQDs is classified as a chemical method if the starting materials undergo chemical changes. This review discusses recent advancements in chemical methods for preparing GQDs.

Inspired by the preparation of graphene from silicon carbide (SiC) epitaxy, Cho *et al* [173] prepared high-crystallinity and high-purity GQDs by hydrogen-assisted pyrolysis of SiC. The preparation process is illustrated in figure 7(a). GQDs were formed on the SiC surface by controlling the process conditions, such as annealing temperature and vacuum pressure. The morphology of the GQDs was characterized, as shown in figures 7(b)–(d), and they showed good uniformity in size. Another frequently used chemical method for the preparation of GQDs involves the use of small molecules that contain carbon to prepare graphene through hydrothermal synthesis, followed by etching or other techniques to prepare GQDs. Recently, Nie *et al* [174] reported the preparation of graphene by a hydrothermal method using L- or D-cysteine as a precursor; the graphene was subsequently etched into GQDs. Figure 7(e) shows the preparation process and morphology of the GQDs. The fluorescence quantum efficiency of the GQDs prepared using this method was as high as 41.26%. Because of the etching process, the

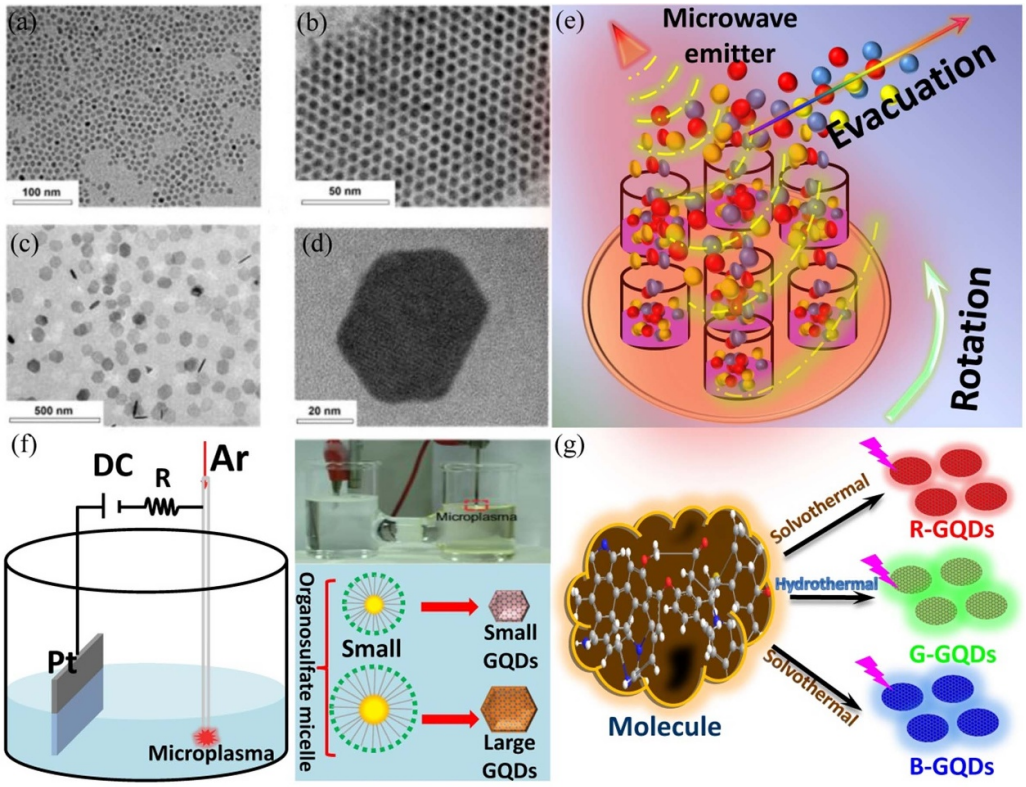

Figure 6. Bottom-up approach for the preparation of GQDs. (a) TEM image of 5 nm GQDs dispersed in methanol. (b) Self-assembled array of 5 nm GQDs upon solvent transfer to hexane. (c) Low-magnification and (d) high-resolution images of 70 nm GQDs in methanol. Reprinted with permission from [160]. Copyright (2019) American Chemical Society. (e) Schematic of the SPMA process used for the preparation of 2D nanostructures. Reproduced from [161] with permission from the Royal Society of Chemistry. (f) Synthesis of diameter-controlled colloidal GQDs using microplasmas. Schematic of the experimental setup for the microplasma-assisted electrochemical synthesis of colloidal GQDs (left). Photograph showing the experimental setup for microplasma-assisted electrochemical synthesis of GQDs (top right). Schematic of the microplasma-assisted electrochemical synthesis of diameter-controlled colloidal GQDs using organosulfate micelles (bottom right). Reproduced from [162] with permission from the Royal Society of Chemistry. (g) Schematic of the preparation of red, green and blue GQDs. Reprinted from [163], © 2020 Elsevier Inc. All rights reserved.

GQDs exhibited relatively poor crystallinity but good uniformity in size. Kapoor *et al* [175] demonstrated the synthesis of graphene nanosheets from graphite electrodes via electrochemical exfoliation method and subsequently performed hydrothermal cutting of the graphene into GQDs with controllable size and morphology. Natural materials are often used as source [176–180] for the preparation of GQDs. These materials would undergo chemical reactions to produce precursors necessary for the synthesis of GQDs. Therefore, it is possible to introduce dopants into GQDs using a chemical method, which can improve the doping efficiency. For example, Xu *et al* [176] used lignosulfonates as the source material, which underwent chemical reaction to produce precursors for hydrothermal synthesis of GQDs. During the synthesis, small molecules were condensed into GQDs doped with sulfur, as illustrated in figure 7(f). Recent advances in chemical methods have demonstrated many advantages, such as the large volume production of GQDs at a relatively low cost and good controllability.

In summary, the three methods of preparing GQDs have advantages and disadvantages, which are summarized in table 1. It can be seen from table 1 that the fluorescence properties of GQDs can be significantly affected by the preparation method, which can influence the morphology of the GQDs and therefore their essential properties [181–183], such as size (e.g. affecting quantum confinement), uniformity (e.g. affecting fluorescence peak width) and edge effect (e.g. affecting functionalization). Next, this review describes the recent work performed to study the new properties of GQDs to provide ideas for developing novel applications based on the use of GQDs.

3. Properties of GQDs

GQDs exhibit many unique properties because of the characteristics of graphene, which is confined to all three directions. The quantum confinement and edge effect of GQDs manifest extraordinary optical, electrical, thermal and magnetic properties. There has been a growing number of studies [200–208] exploring new properties of GQDs that could potentially lead to the development of novel applications. The optical and thermal properties of GQDs have been studied extensively because of their excellent fluorescent properties and high thermal efficiency. Other properties of GQDs have also received much attention over the past years. In this review, the

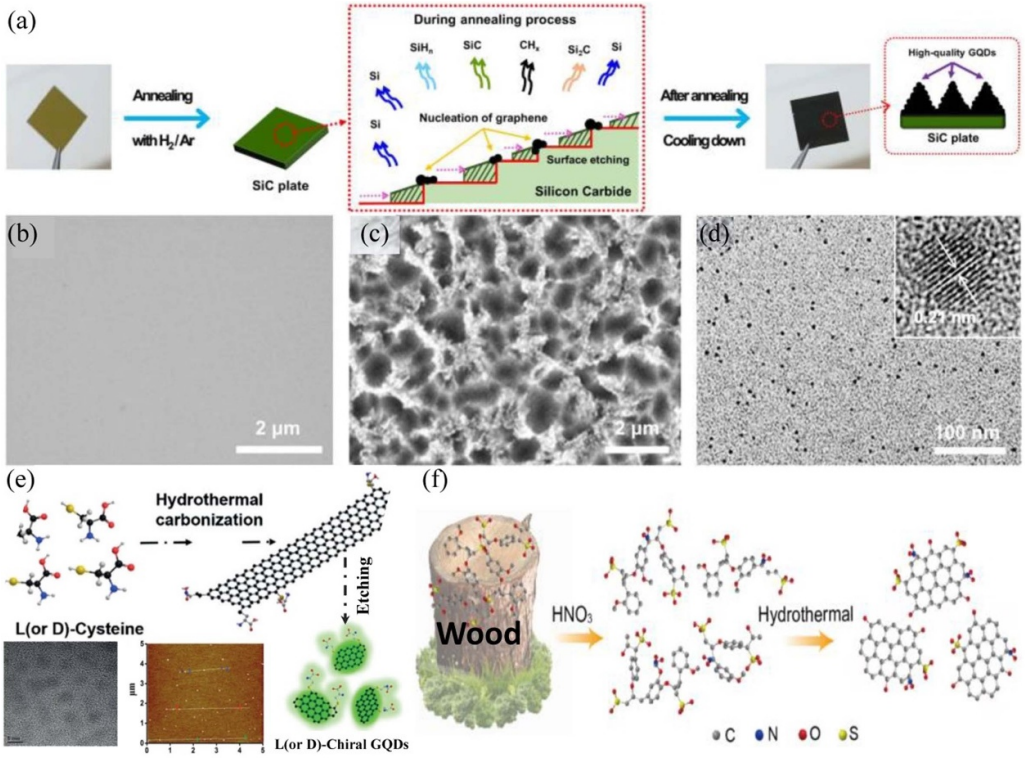

Figure 7. Preparation of GQDs using chemical methods. (a) Schematic layout of the synthesis of high-quality GQDs via hydrogen-assisted pyrolysis of SiC. Field-emission scanning electron microscope images of (b) pristine SiC plate and (c) GQDs on the SiC plate after annealing at 1500 °C in hydrogen etching gas. (d) Transmission electron microscope (TEM) image of the detached GQDs (inset: high-resolution transmission electron microscope image of the GQDs with their lattice spacing). Reproduced from [173]. CC BY 4.0. (e) Schematic (top) depicting the synthesis of chiral CDs by hydrothermal treatment of chiral cysteines. TEM (left) and atomic force microscope (middle) images of the GQDs. [174] John Wiley & Sons.© 2018 Wiley-VCH Verlag GmbH & Co. KGaA, Weinheim. (f) Two-step synthesis method of GQDs from lignosulfonates. Reprinted from [176], © 2019 Elsevier B.V. All rights reserved.

optical, thermal, electrical and magnetic properties of GQDs are discussed in detail.

3.1. Optical property

The optical properties of GQDs are completely different from those of graphene. This is because of the quantum confinement effect of GQDs, which leads to the opening of the energy bandgap in graphene. The optical absorption of GQDs can be in the UV-visible and near-infrared (NIR) range by controlling the size and functionalization of GQDs. In addition, GQDs also demonstrate excellent fluorescence properties because of their quantum confinement and edge effects. The optical properties of GQDs are focused on the modulation of the optical absorption band as well as the fluorescence band of GQDs and the improvement in their fluorescence efficiency. It often requires the understanding of the up-conversion luminescence mechanism, which involves the absorption of low-energy excitation light and the emission of high-energy ultraviolet or visible light [209–212].

The optical properties of GQDs have been studied extensively [213–216]. The size, functionalization (e.g. doping) and morphology of GQDs have a significant impact on their optical properties. For example, there is a relationship between the size of GQDs and their optical bandgap [216]. As shown in figure 8(a), the optical bandgap decreased as the transverse size of the GQDs increased. Sahu *et al* [217] demonstrated this remarkable fluorescence properties of GQDs, which showed different fluorescence wavelengths for the GQD solutions with varying nanomaterial sizes (e.g. from blue to red for GQDs with reduced size, as shown in the inset of figure 8(a)). The morphology of GQDs can also affect their optical properties. Several theoretical studies [218, 219] have reported the influence of the morphology of GQDs on their optical properties. Recently, Yang *et al* [220] reported an experimental study on the optical properties of triangular GQDs. Figures 8(b)–(c) show the TEM images of the triangular GQDs. In addition to the modulation of the fluorescence spectrum by controlling the size of the triangular GQDs, they found that the triangular GQDs had a significant influence on the fluorescence color purity. The optical properties of GQDs can also be affected by their edge effects. For example, different functional groups at the edges of GQDs can result in different optical properties. Theoretical studies reported by Geethalakshmi *et al* [221] suggested that it is unfavorable to obtain infrared fluorescence by increasing the size of GQDs to reduce their energy bandgap. Instead, the fluorescence of GQDs in the infrared band can be obtained

Table 1. Related property of GQDs prepared by top-down, bottom-up and chemical methods.

Methods	FQE (%)	Precursors	FL (ns)	PL (nm)	Size (nm)	DE	References	Pros	Cons	RM
Top-down	0.7/1.8	Graphite	0.45/2.95	328	20.7/49.8	—	[133]	Easy mass production, low cost, good crystallization, high purity and short period	Environmentally hazardous, poor uniformity, poor controllability and difficulty in functionalization	Graphite, carbon nanotubes or fullerenes are used as precursor materials, which are converted into GQDs through a series of cracking techniques, such as laser ablation, electrochemical electrolysis, explosion and electron beam etching, resulting in the change of size or dimension
	8.9	GO	3.16	Yellow	4.8	—	[135]			
	7.12/6.53	GF/MWCNTs	—	423	20	—	[136]			
	9.1	GF	9.8	450	6	N	[138]			
	8.6	Graphite	—	431	2.5–6	—	[139]			
	52.4	C_{60}	7.04	617	3.5	DAN	[141]			
	10 ± 3	Nitrogen-doped nanomesh graphene	—	458	3.18 ± 0.2	N	[140]			
	5	TBAP	—	450	8.6 ± 1.0	N	[149]			
Bottom-up	10.4	D-glucose	4.86	440	70	N	[160]	Good controllability, excellent performance, good uniformity, easy functionalization and eco-friendly	High cost, long period, low yield rate, aggregation and high power consumption	Using small organic molecules containing carbon rings, such as glucose, sucrose and pyridine, as precursor materials. GQDs are formed by polymerization using techniques, such as hydrothermal, microwave, solvothermal and plasma methods. This involves polymerization of materials to form GQDs with controllable size and morphology.
	38.7	CA + urea	—	400–525	3.5	N	[161]			
	24.2	*p*-phenylenediamine + DMF	—	Red	4.1	N	[163]			
	19.7	1,3,6-trinitropyrene + NaOH	—	Green	3.0	N	[163]			
	20.2	1,3,6-trinitropyrene + triethylamine	—	Blue	3.1	N	[163]			
	7.5	Glucose	1.61	590	4.1	N	[164]			
	7.1	Fructose + H_2SO_4	0.65–0.88	446	5.2	S	[165]			
	57.44	CA + MPA	—	460	4	S	[184]			
	60	Glucosamine	—	Near infrared	3.9	N + S	[185]			
	77	FA + Tris	—	380	1.95	—	[186]			
	31.43	$C_{16}H_{10}$	—	Blue	2.93	—	[187]			
	80	*o*-phenylenediamine	1.3	585	3.8	N	[188]			
	75	CA + ethylenediamine	12.86	Blue	1.04–4.81	B + N	[189]			
	68.1	CA + urea	—	Blue	4.2	N	[190]			
	18.9	D-glucose	6.4	550	5.4	—	[191]			
	1.5	Organosulfate		448	4.9	—	[192]			
	22.2	CA + urea		—	5–10	N	[193]			
	81	Salicylic acid	2.2	460	3.0	—	[194]			

(Continued.)

Table 1. (Continued.)

Chemistry	17.5	*p*-Benzoquinone	4.37	Yellow	20 ± 8	—	[172]	Easy to control, easy functionalization, low cost, high performance and wide selection of source materials	Complex reaction, long period, high power consumption and hostile environment	Carbon-based substances, such as methane, wood and organic macromolecules, are used as precursor sources to form precursor of GQDs through chemical reactions. GQDs are formed using top-down or bottom-up techniques, which involve changing the chemical of raw materials used as precursor.
	41.26	L- or D-oysteine	7.56	510	5–7	N + S	[174]			
	1.4	$C_{90}H_{30}$	—	Brown	3.14	—	[178]			
	11.76	Graphite	—	550	6.5	—	[179]			
	17.4	Graphite	—	475	3.78 ± 0.83	—	[195]			
	64	Graphite	—	475	19 ± 2.9	N	[196]			
	23.1	Graphite	—	Green	—	N	[197]			
	46	Graphite	7.2	Blue	1.84 ± 0.28	N	[198]			
	65	SCNWTs	8.1	400	4.8 ± 1.4	—	[199]			

Note: GO, graphene oxide; GF, graphite flakes; TBAP, tetrabutylammonium perchlorate; DAN, 2,3-diaminoaphthalene; CA, citric acid; DMF, dimethylformamide; MPA-3, mercaptopropionic acid; FA, folic acid; tris, tris(hydroxymethylamino methane); SCNWTs, single-walled carbon nanotubes; FQE, fluorescence quantum efficiency; FL, fluorescence lifetime; DE, doping element; RM, reaction mechanism.

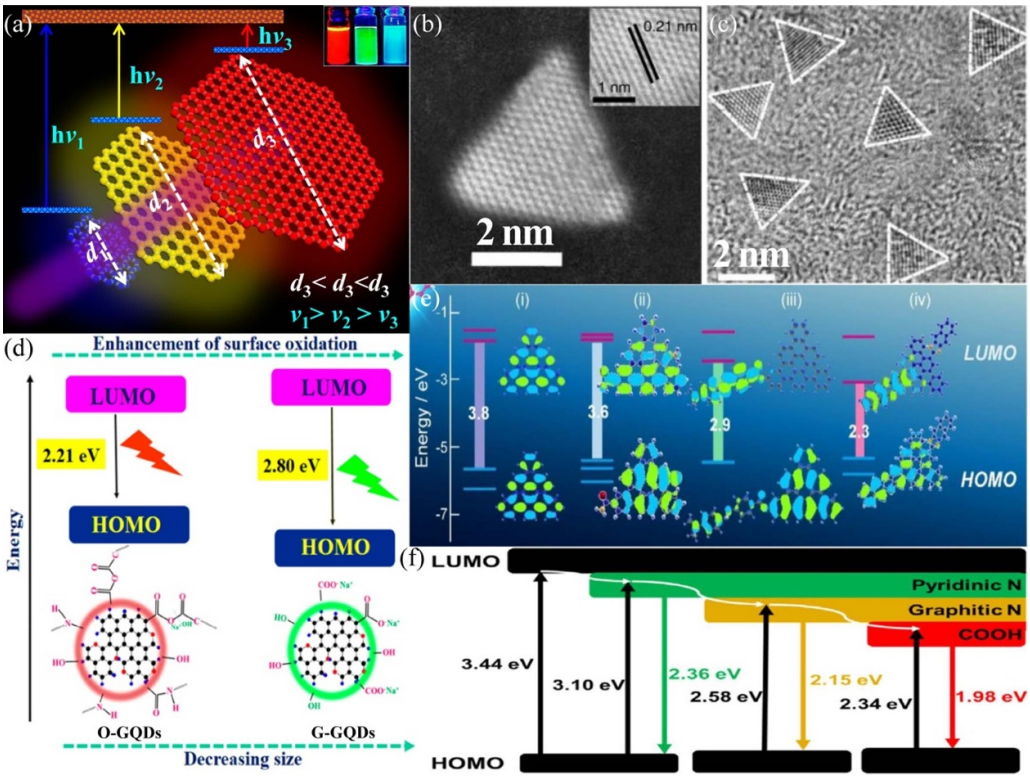

Figure 8. Optical properties of GQDs. (a) Schematic of the change of optical bandgap with different sizes of GQDs (inset: fluorescence of GQDs having different sizes). Reprinted with permission from [217]. Copyright (2019) American Chemical Society. (b) Synthesis route of the NBE-T-CQDs by solvothermal treatment of PG triangulogen. Typical aberration-corrected HAADF-STEM image of R-NBE-T-CQDs (inset: corresponding high-resolution image). (c) Wide-area TEM image of G-NBE-T-CQDs. The triangular projections are highlighted by white contour lines. Reproduced from [220]. CC BY 4.0. (d) Reasonable mechanism behind blue shift of O-CDs at pH 13. Reprinted with permission from [217] Copyright (2019) American Chemical Society. (e) Predicted energy level diagrams for graphene with different functional groups: i, H-GQDs; ii, NH_2-GQDs; iii, pMR-GQDs; iv, DAN-GQDs. The schematics show the chemical structures used for the theoretical calculations. The isosurface presents the HOMO and LUMO [224]. John Wiley & Sons.© 2020 The Chemical Society of Japan & Wiley-VCH Verlag GmbH & Co. KGaA, Weinheim. (f) Schematic of the possible energy levels of the PL-tunable GQDs. Reprinted from [231], © 2020 Elsevier B.V. All rights reserved.

through the action of the edge functional groups. This was demonstrated experimentally by Sahu *et al* [217] and Xiong *et al* [222]. They reported the influence of oxygen functional groups at the edges of GQDs on the fluorescence properties of GQDs. The fluorescence spectral range of GQDs can be influenced by their size and surface functional groups, as illustrated in the left diagram of figure 8(d). GQDs with different functional groups in solutions and films would result in a shift in their fluorescence peaks, as observed by Wang *et al* [223] and illustrated in the right diagram of figure 8(d). Figure 8(e) shows schematics illustrating the modulation of the optical energy bandgap of the GQDs functionalized with different functional groups. The energy bandgap of GQDs functionalized with H, NH_2, *p*MR and DAN functional groups can vary from 3.8 to 2.3 eV [224]. The degree of graphitization can influence the optical properties of GQDs, as reported by Wei *et al* [225]. They observed a reduction in the optical bandgap of GQDs (i.e. leading to a fluorescence redshift) as the degree of graphitization of GQDs increased. The optical properties of GQDs can also be affected by the introduction of heterogeneous atoms, such as elements from Group V and/or VI, into the GQDs [226–230]. The introduction of sulfur atoms into GQDs is commonly studied to determine their influence on the optical properties of GQDs. Recently, Fan *et al* [231] introduced two different elements, namely nitrogen and sulfur atoms, into GQDs and observed a change in their fluorescence properties, which were attributed to the impurity level produced by the heterogeneous atoms, as illustrated in figure 8(f). Other optical properties of GQDs have been studied recently, such as the stress of GQDs for optical modulation at infrared wavelengths [232], intrinsic GQDs exhibiting a single-photon emission phenomenon [233] and nonlinear optical properties of GQDs [234, 235]. An enhanced understanding of the optical properties of GQDs allows further exploration and development of GQD applications, particularly in integrated photonic devices [236].

3.2. *Thermal property*

The transformation between field and heat conduction can be observed in GQDs due to the quantum confinement of the nanomaterials. When energy is incident on the GQDs, electrons are confined within the GQDs, with their edges as boundaries.

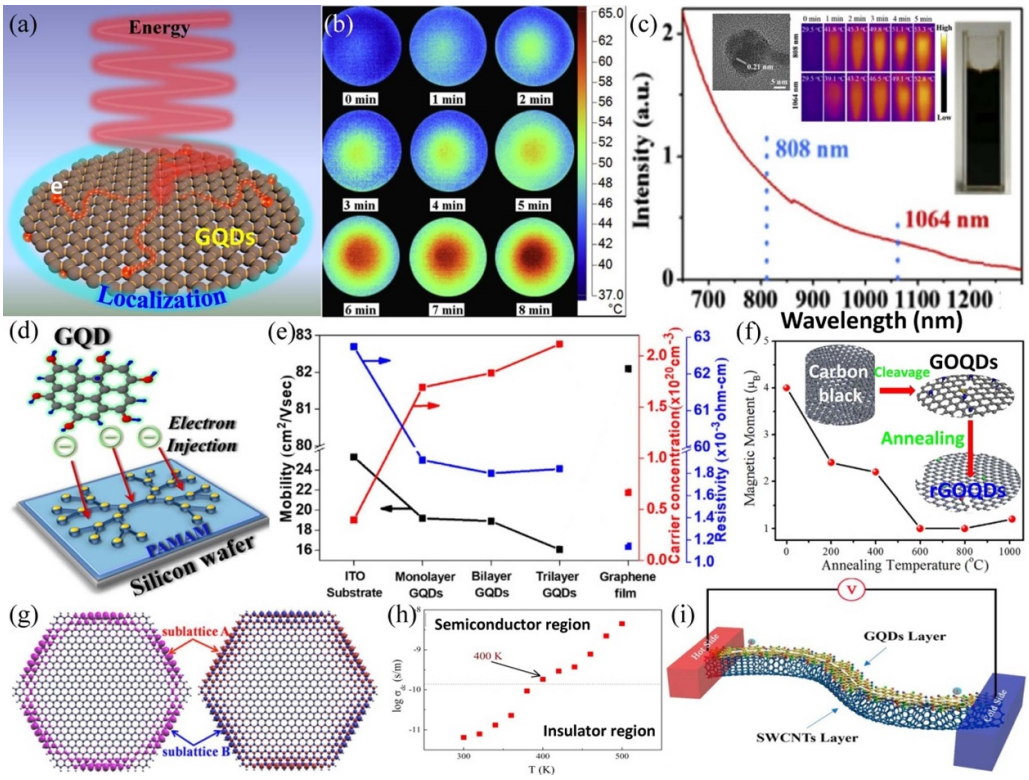

Figure 9. Other properties of GQDs. (a) Schematic of the photothermal conversion of GQDs. (b) Infrared thermal images of GQDs (100 μg ml^{-1}) under NIR irradiation (808 nm; 2 W cm^{-2}). Reprinted from [238], © 2020 Elsevier B.V. All rights reserved. (c) Optical absorption spectrum of GQDs in the NIR region from 650 to 1300 nm (inset: TEM image of GQDs (left), infrared thermographic images of GQD solutions filled in centrifuge tubes under continuous 808 and 1064 nm laser irradiation from 0 to 5 min (middle) and photograph of the solution (right)). Reprinted from [239], © 2020 Elsevier Ltd. All rights reserved. (d) Schematic of electron injection from GQDs into organic materials. Reprinted from [243], with permission from AIP Publishing. (e) Carrier mobility, concentration and resistivity for the ITO substrate, GQDs with different wet transfer numbers and graphene film. Reprinted from [244], © 2019 Elsevier B.V. All rights reserved. (f) Dependence of magnetic moment of GQDs on annealing temperature (inset: synthetic scheme of GQD samples). Reprinted from [245], © 2019 Elsevier B.V. All rights reserved. (g) Spin density isosurfaces of GQDs in antiferromagnetic (left) and ferromagnetic (right) couplings at the inter-edges. The red and blue isosurfaces represent the spin-up and spin-down states, respectively. Reproduced from [246]. CC BY 4.0. (h) Variation in dc conductivity of GQDs with temperature. Reprinted from [247] with permission from AIP Publishing. (i) Schemes of GQDs/SWCNTs. Reprinted with permission from [240]. Copyright (2020) American Chemical Society.

Because of the localized electrons and high electron mobility of the GQDs, the edges of the GQDs become charge aggregation regions that ease the transfer of charge in GQD-hybrid materials [237]. Li *et al* [238] found that GQDs can convert infrared light into heat energy. Figure 9(a) shows the photothermal conversion of the GQDs. The temperature of the GQD solution irradiated by the NIR laser was reported to change drastically within 8 min, as shown in figure 9(b). Shen *et al* [239] reported that GQDs with nitrogen-containing groups exhibited greater absorption effect to NIR band of 808 and 1064 nm, as shown in figure 9(c). When the nitrogen content of the GQDs was increased from 1.68 at. % to 4.3 at. %, the photothermal conversion efficiency increased from 43.6% to 81.3% under laser irradiation of 808 and 1064 nm. The temperature of the GQD solution increased rapidly in less than 5 min, as shown in figure 9(c). The morphology and solution of the GQDs are shown in figure 9(c). In addition, the coupling of GQDs with carbon nanotubes can improve the thermoelectric properties of carbon nanotubes, as demonstrated by Du *et al* [240]. They reported an improvement in the power factor and a reduction in the thermal conductivity of carbon nanotubes upon coupling of GQDs with carbon nanotubes, as shown in figure 9(i). The thermal conductivity of GQDs has attracted significant interest [208, 241, 242]. Studies include functionalization of GQDs and the preparation of soluble GQDs to enhance heat dissipation and thermal control in a solution.

3.3. Electronic property

To date, only a few experimental studies have been performed to study the electrical properties of GQDs because of the small size of the nanomaterials, ranging from a few nanometers to tens of nanometers. Recently, Lin *et al* [243] reported the effective injection of electrons from GQDs into organic compounds, as illustrated in figure 9(d). They performed steady-state and time-resolved photoluminescence techniques in their studies. To understand the electrical properties of materials, it is often necessary to study their electrical parameters, such as carrier mobility and resistivity. Fu and Lin [244] studied the carrier mobility, resistivity and carrier concentration of GQDs with different numbers of layers. They found that the electrical properties of GQDs were significantly influenced by the

number of layers; for example, GQDs with an increased number of layers would lead to a decline in their carrier mobility, which can be attributed to the interlayer coupling that influences the ability to transfer charge. Figure 9(e) shows a plot of several electrical parameters against the number of GQD layers. Interestingly, GQDs can be converted from insulators to semiconductors at a certain critical temperature, as discovered by Sinha *et al* [247]. They recorded a large change in the electrical conductivity of the GQDs when the temperature was approximately 400 K, as shown in figure 9(h). More recently, superconductivity has been reported in a new carbon material [248], which is of great interest to the scientific community. Although there are only a few studies on the electrical properties of GQDs [249, 250], this topic continues to attract the attention of many researchers, as it has significant implications for the use of GQDs in nanoelectronic devices.

3.4. Magnetic property

Owing to the high edge-to-area ratio of GQDs, a large number of spin-polarized edge states may exist that could theoretically generate attractive magnetic properties [251]. The magnetic properties of GQDs can be modulated by their morphology [252], size [253] and other external factors [254] due to the effect of localized electrons at the edge states. Sun *et al* [245] found that the magnetic properties of GQDs with oxygen-containing functional groups were significantly modulated by annealing temperature. For example, the magnetic moment of the GQDs decreased significantly when the annealing temperature increased and the oxygen content decreased, as shown in figure 9(f). The discovery of this phenomenon will enable the development of novel applications of GQDs in spin devices. By coupling antiferromagnetic and ferromagnetic with GQDs, Yang *et al* [246] found that the spin states at the edges of the GQDs experienced significant changes, suggesting that the magnetic properties of the GQDs were determined by the local electronic states at their edges, as illustrated in figure 9(g). Much of the research performed [255, 256] on the magnetic properties of GQDs is intended for the potential use of carbon materials in spin devices, which would benefit from the quantum confinement and edge effects of GQDs.

4. Functionalization

The many unique properties described in the preceding section are attributed to the quantum confinement and edge effects of the GQDs. To explore other functionalities of GQDs for novel applications or to improve their unique properties, the nanomaterials can be modified by means of functionalization, which either takes the form of doping or composite formation. Similar to their parent material (i.e. graphene), intrinsic GQDs have limited chemically active sites [257, 258] that restrict the performance of the nanomaterials, resulting in low fluorescence quantum efficiency and chemical catalytic activity. Doping is highly effective for GQDs due to their edge effect and can significantly improve the chemical activity of the nanomaterials. The large specific surface area of intrinsic GQDs makes them attractive for forming composites with other materials. GQDs can form composites with organic [259–261] and inorganic [262–266] materials. In this section, progress in the functionalization of GQDs over the past two years is discussed in detail.

4.1. Doping

Doping is an effective method to improve the properties of materials. Single-element [267–269] and multielement [270–272] doping of GQDs has been studied extensively. Nitrogen-doped GQDs [273–276] have been studied extensively and have three different carbon–nitrogen atomic combinations: graphitic nitrogen, pyridinic nitrogen and pyrrolic nitrogen. Interestingly, graphitic nitrogen had the greatest influence on the performance of the GQDs. Hence, the properties and performance of GQDs can be enhanced by doping them with heterogeneous atoms, as illustrated in figure 10(a). Controlled doping of GQDs and the ability to control their properties is of great importance. Kim *et al* [277] demonstrated the use of laser ablation technique in liquid to produce nitrogen-doped GQDs from carbon nano-onions in a mixed solution containing nitrogen. The nitrogen content in GQDs can be regulated by controlling the laser parameters and nitrogen concentration in the solution. This technique is illustrated in figure 10(b). Zhang *et al* [278] reported a simple, environmentally friendly, one-step method for preparing nitrogen-doped GQDs. This involved the opening of fullerenes using the microwave-activated nitrogen plasma technique, as illustrated in figure 10(c). The method produced crystalline nitrogen-doped GQDs, which exhibited blue fluorescence in a solution. Furthermore, the fluorescence intensity decreases when the concentration of iron ions in the solution increases; hence, the nitrogen-doped GQDs can be used in biosensing applications.

Chemical vapor deposition (CVD) is often used to prepare graphene films. However, Kumar *et al* [279] demonstrated the use of CVD to produce nitrogen-doped GQDs using chitosan as a carbon and nitrogen source. Chitosan was decomposed at high temperature into carbon compounds containing nitrogen, which were absorbed at the surface of copper foil. The nucleation of the compounds subsequently led to the formation of nitrogen-doped GQDs, as illustrated in figure 10(f). Doping of GQDs with nitrogen can effectively improve their optical properties, as demonstrated by Khan and Kim [281]. They found that the absorption spectra of nitrogen-doped GQDs would extend into the low-energy photon range, as shown in figure 10(f). Moreover, doping GQDs with nitrogen introduced more chemically active sites and enhanced the fluorescence quantum efficiency to 99%. Kuo *et al* [283] found that the fluorescence of nitrogen-doped GQDs could cover a wide spectrum range (e.g. from ultraviolet to NIR) when the size of the doped GQDs was regulated, hence indicating that the size-dependent fluorescence of GQDs is still significant. The doping of metallic elements in GQDs has recently received much attention. As shown in figure 10(g), isopropyl alcohol containing aluminum, gallium salt and nonmetallic boric acid were used to synthesize

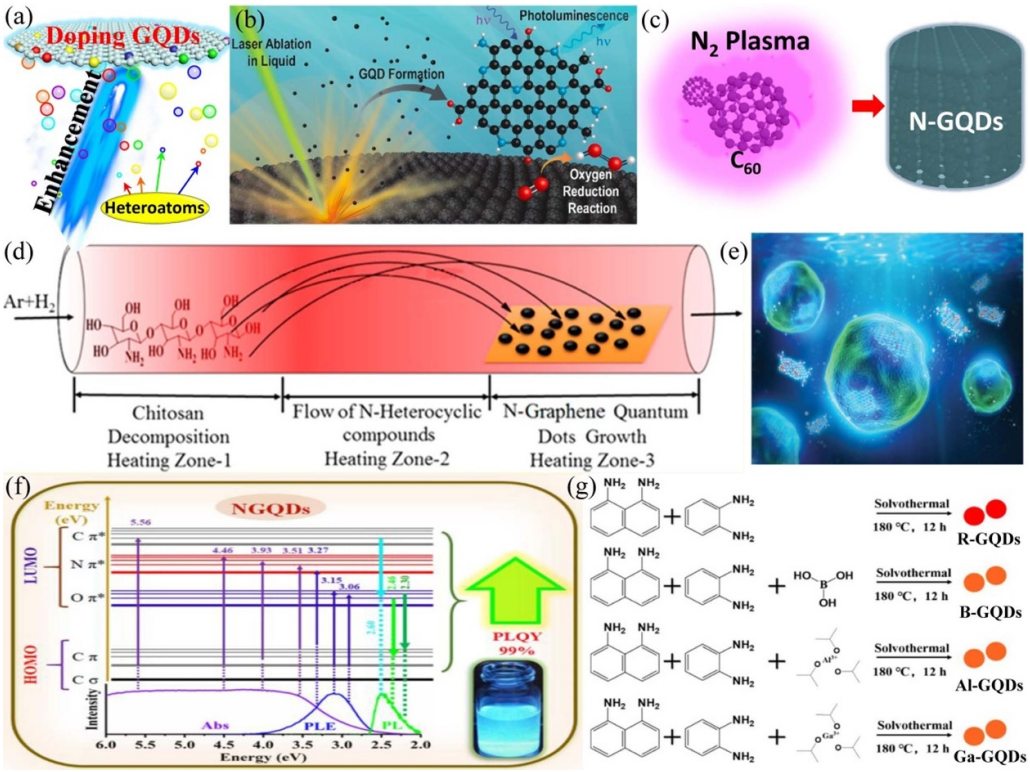

Figure 10. Doping of GQDs by heteroatoms. (a) Schematic of doping of GQDs with heteroatoms for enhancing their performance. (b) Schematic of controlled nitrogen doping of GQDs through laser ablation in aqueous solutions. Reprinted with permission from [277]. Copyright (2019) American Chemical Society. (c) Illustration of the nitrogen-doped GQD fabrication process. Reprinted with permission from [278]. Copyright (2018) American Chemical Society. (d) Schematic of the synthesis of nitrogen-doped GQDs by chemical vapor deposition. Reprinted with permission from [279]. Copyright (2018) American Chemical Society. (e) Schematic depicting nitrogen-and-iron-co-doped GQDs for the detection of ferric ions in biological fluids and cellular imaging. Reproduced from [280] with permission from the Royal Society of Chemistry. (f) Jablonski diagram (top) representing the energy levels of nitrogen-doped GQDs along with associated absorption, PLE and PL spectra (bottom) and optical image of nitrogen-doped GQD solution. Reprinted with permission from [281]. Copyright (2018) American Chemical Society. (g) Synthesis scheme of GQDs with different doping elements via solvothermal method. Reprinted from [282], © 2020 Elsevier B.V. All rights reserved.

aluminum-, gallium- and boron-doped GQDs, respectively [282]. These metal-doped GQDs demonstrated a significant improvement in their fluorescence quantum efficiency, which was due to the chemical bonds of carbon–nitrogen–metal–oxygen. Gao *et al* [280] reported on the synthesis of nitrogen-and-iron-co-doped GQDs using hydrothermal method. These GQDs were used for the detection of iron ions in biological samples and for cellular imaging, as shown in figure 10(e).

There has been a significant amount of research conducted on the subject of doping GQDs, which includes single-element doping with elements, such as sulfur [184, 284, 285], phosphorus [286], nitrogen [287], fluorine [288], boron [289] and silicon [290], as well as multielement doping with combinations, such as nitrogen–sulfur [291–296], nitrogen–phosphorus [297, 298], nitrogen–boron [299–301] and nitrogen–oxygen [302, 303]. To achieve better performance, multielement doping consisting of four elements has also been reported [304]. Recently, much progress has been made in the development of metal-doped GQDs. For example, the doping of GQDs with magnesium [305] and rare metal elements [306] has been studied for biological sensing and imaging applications. Furthermore, GQDs doped with selenium [307] have been explored for therapeutic applications, such as in the treatment of acute kidney injury. In summary, doping of GQDs [308–316] has been demonstrated to be an effective way to improve the performance of GQDs, which are beneficial for many applications.

4.2. Composite

GQDs can form composites with other materials, which can be inorganic [317–321] or organic [322–331], either to develop a novel material system with new properties or to enhance the properties of the secondary material, as illustrated in figure 11(a). For example, the edge effect of GQDs would facilitate charge transfer between two materials, leading to an enhancement in the performance of GQD composite materials. This section of the review provides a detailed description of the GQD composite materials.

4.2.1 Composite with organic materials. The formation of GQD composites with organic materials has several advantages. For example, GQDs can be embedded in organic

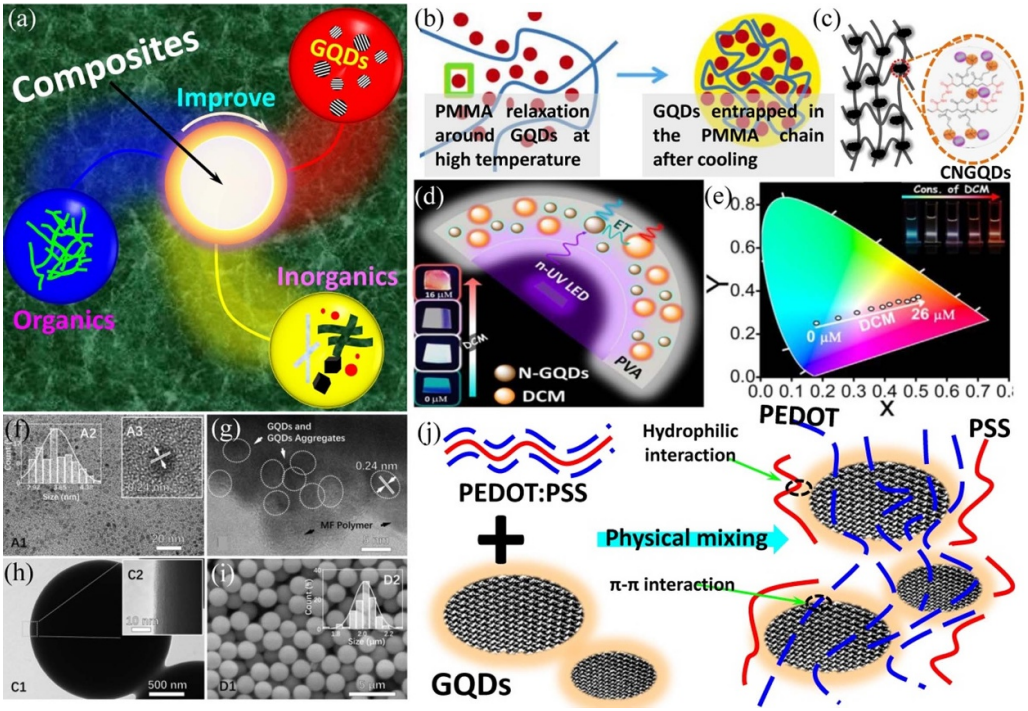

Figure 11. Composite of GQDs with other functional materials. (a) Schematic of the GQD composite with organic or inorganic materials to improve performance. (b) Illustrative representation of the formation and entrapment of CQDs within the PMMA structure. Reprinted from [332], © 2020 Elsevier Ltd. All rights reserved. (c) Chemical structure of the GQD: aerogel. Reprinted with permission from [333]. Copyright (2018) American Chemical Society. (d) Strategy for designing of F-WLED using DCM@N-GQDs$_{0.7}$ LD as the light emitter and n-UV light-emitting diode as the pumping source (inset: digital photograph of DCM@NGQDs$_{0.7}$ LD in the PVA matrix under UV radiation). (e) Variation of CIE color coordinates of the FRET-based LD system with different DCM concentrations. Reprinted from [334], © 2020 Elsevier Inc. All rights reserved. (f) High-resolution transmission electron microscope (HRTEM) images of GQDs (left inset: related size distribution). (g) Pulverized GQD–MF microspheres and (h) HRTEM images of the GQD–MF microspheres. (i) SEM image of the GQD–MF microspheres (inset: related size distribution). Reproduced from [335]. CC BY 4.0. (j) Scheme of assembly process of GQDs and PEDOT:PSS. Reproduced from [336]. CC BY 4.0.

materials, allowing for effective charge transfer. Moreover, the functional groups at the edge of the GQDs can form a strong and effective bond with the organic materials, thus easing the preparation of the GQD composites. Arthisree and Madhuri [337] prepared a composite film consisting of GQDs, polypropylene nitrile and polyaniline. The composite film was used to prepare a supercapacitor, which exhibited excellent performance of several orders of magnitude better than a film without the GQDs. The implementation of GQDs in polymer compounds can also improve the optical properties of the polymer, as demonstrated by Arthisree *et al* [338]. They prepared a composite of GQDs and polyvinyl butyral and reported an enhancement in the fluorescence spectrum of the GQD/polymer composite. This is due to the bonding of the GQD edge with hydroxyl and carboxyl groups in the polymer, leading to an increase in the number of chemical activity sites, which are favorable to the fluorescence performance of the composite. Using the bottom-up synthesis method, a composite of GQDs and polymer can be prepared using a one-step method. As shown in figure 11(b), Sarno *et al* [332] prepared a composite of GQDs and poly (methyl methacrylate) using oleic and citric acids via a one-step method. Traces of GQDs, acting as lubricant additives were found in the composite, which resulted in a remarkable improvement in the lubrication characteristics of the polymer. Such a GQD/polymer composite can therefore offer a new type of lubricant. He *et al* [335] reported the preparation of a white light-emitting device using a composite film of GQDs and melamine formaldehyde (MF). The GQDs were aggregated by encapsulation in the MF microsphere, and the concentration of the GQDs can effectively alter the fluorescence properties of the composite film. The TEM images of the GQD–MF microsphere are shown in figures 11(f)–(i).

In addition, polymers containing GQDs exhibit excellent thermoelectric properties. Du *et al* [336] reported on the synthesis of GQDs/PEDOT:PSS composite that significantly improved the thermoelectric properties of PEDOT:PSS and demonstrated 550% increase in power consumption factor compared to pure PEDOT:PSS. The assembly process of the GQDs and PEDOT:PSS is illustrated in figure 11(j). The stability of GQDs can be enhanced by developing a strong chemical bond with organic compounds. Martín–Pacheco *et al* [333] reported on the synthesis of GQD composite based on cationic covalent network, as depicted in figure 11(c). The polymeric network containing GQDs exhibited remarkable physical and optical stabilities, which are crucial for biosensing applications. The properties of the GQD composite could be influenced by both GQDs and organic compounds, as demonstrated by Pramanik *et al* [334]. They reported the preparation of white light-emitting luminescent composite

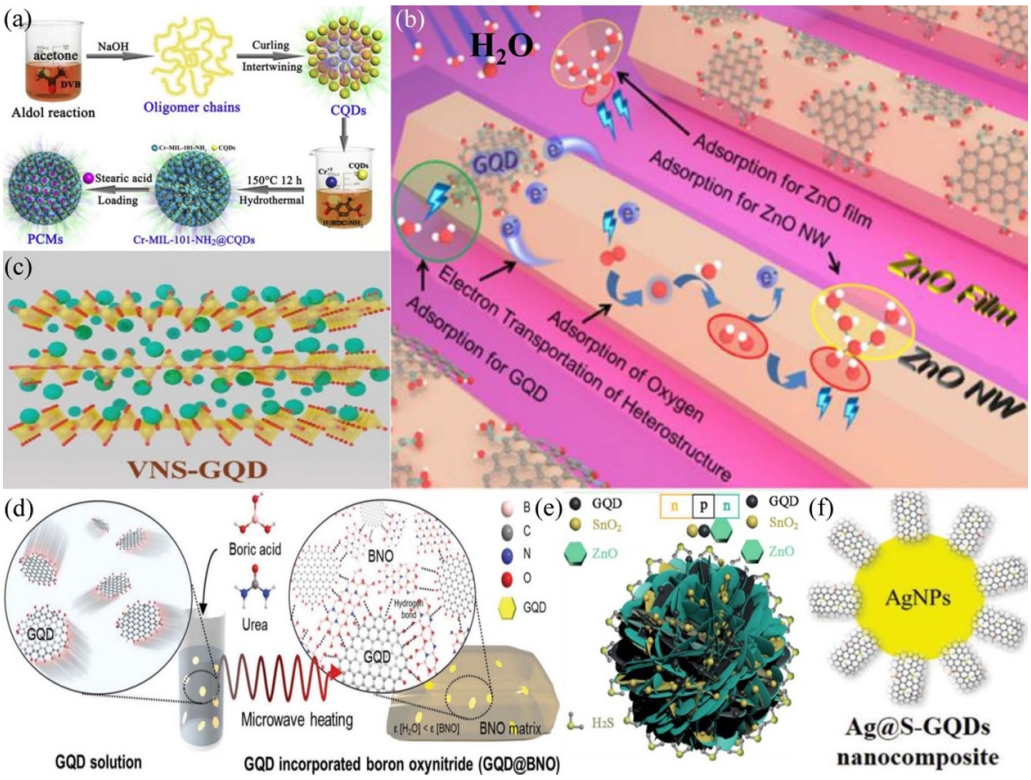

Figure 12. Composite of GQDs with various inorganic substances. (a) Schematic of the photoluminescence-functionalized composite PCMs. Reprinted from [348], © 2018 Published by Elsevier B.V. (b) Schematic of the adsorption mechanism of H_2O molecules on composite sensing layer. Reprinted with permission from [352]. Copyright (2020) American Chemical Society. (c) Synthesis scheme of interlayer-embedded GQDs endows V_2O_5 with the hydrothermal method. Reproduced from [361] with permission from the Royal Society of Chemistry. (d) Schematic of the fabrication of GQD@boron oxynitride by microwave heating [370]. John Wiley & Sons.© 2018 WILEY-VCH Verlag GmbH & Co. KGaA, Weinheim. (e) Schematic of the band configuration at the interface of the GQD−SnO_2/ZnO nanostructure in different atmospheres. Reprinted with permission from [353]. Copyright (2020) American Chemical Society. (f) Schematic of the structure of Ag@S-GQDs nanocomposite. Reproduced from [373] with permission from the Royal Society of Chemistry.

films by tuning the concentrations of GQDs and DCM dye, as illustrated in figures 11(d)–(e).

4.2.2 Composite with inorganic materials. Much research has been reported on the synthesis of GQD-based composites with different inorganic materials, which can enhance the properties of inorganic materials for specific applications. For example, there are reports on the preparation of GQD-based composites with inorganic materials in the form of flakes [339], layers [340], rods [341], nanowires [342], networks [343] and other shapes [344–347], resulting in a remarkable improvement in the properties of inorganic materials. Chen *et al* [348] demonstrated the integration of GQDs in a metal–organic framework to form a fluorescence-functionalized phase change material (PCM), which was excellent in thermal energy and fluorescence harvesting, as illustrated in figure 12(a). In addition, composites of GQDs and zinc oxide have been widely studied for applications in solar cells, photodetectors, photocatalysis and other fields [349–351]. Recently, Wu *et al* [352] developed a flexible wearable humidity sensor based on GQDs and zinc oxide nanowire composites. The formation of a p-n junction between the GQDs and zinc oxide nanowires and the large specific surface areas of the nanomaterials contributed to the ultrahigh sensitivity of the device, as illustrated in figure 12(b). In addition, Shao *et al* [353] prepared a highly selective and responsive gas sensor based on GQD-modified metal oxide materials, consisting of porous and layered structures of tin dioxide and zinc oxide nanomaterials forming n-p-n heterojunctions with p-type GQDs, as shown in figure 12(e). Furthermore, Ahmadi *et al* [354] prepared electrochemical and photoelectrochemical sensors based on nanocomposites of GQDs, titania and ceria for the detection of dopamine. Compared with the electrochemical sensor, the photoelectrochemical sensor exhibited a lower limit of detection, better sensitivity and a wider detection range. The use of GQD-based composites with inorganic materials in capacitors for energy storage applications has also attracted considerable attention [355–359]. GQDs have significant advantages for improving the performance of capacitors because of their large specific surface area and good electrical conductivity. Yun *et al* [360] prepared a 3D composite aerogel, comprising of GQDs, reduced graphene oxide (rGO) and porous iron oxide. The composite was used as an anode material for alkaline aqueous batteries, which demonstrated an ultrahigh specific capacity and excellent cycle performance, partly due to the good electrical conductivity of the GQDs. Furthermore, GQDs

play an important role in the future development of all solid-state capacitors, thereby circumventing the need for electrolytes in capacitors. Recently, Ganganboina *et al* [361] introduced GQDs between layers of vanadium oxide nanosheets to form nanocomposites of GQDs and vanadium oxide for use as anode electrodes in energy storage, as shown in figure 12(c). A small amount of GQDs can significantly improve the performance of energy storage batteries. Their work demonstrated the novel use of GQDs in developing nanocomposites with multilayers of two-dimensional materials for energy storage applications. The enhancement of the optical properties of GQD-based composites with inorganic materials has been reported by several groups [362–369]. Park *et al* [370] synthesized GQDs and boron oxynitride composite using a one-step microwave heating process, as illustrated in figure 12(d). The composite exhibited a high photoluminescence quantum yield (PL-QY) of up to 36.4%, which was eightfold higher than that of pristine GQD in water. Charge transfer between GQDs and titanium dioxide nanoplates in nanocomposites was studied by Murali *et al* [371]. The large specific surface area and edge effect of the GQDs would promote charge transfer between the two materials, which was used in gas sensing of nitric oxide. Cobalt/nickel-based capacitors can be found in many commercial applications; hence, improvement in their performance is of great commercial interest. Luo *et al* [372] reported on the synthesis of composites consisting of tremella-like $NiCo_2O_4$ coated with GQDs. The composite exhibited an excellent specific capacitance and energy density due to the abundant edge sites of the GQDs. GQD-based composites can also be used for antibacterial applications, as demonstrated by Kadian *et al* [373]. They prepared nanocomposites consisting of silver nanoparticles decorated with sulfur-doped GQDs, as shown in figure 12(f). The nanocomposites demonstrated good dispersion and stability with a significant improvement in antibacterial activity. Cyclic stability and thermal safety are of paramount importance in supercapacitors. Sun *et al* [374] coated the surface of cobalt–lithium nanoparticles with GQDs, thus forming a stable conductive layer at the surface of the nanoparticles. The thermal safety and cycling performance of the cobalt–lithium capacitors improved remarkably due to the excellent conductivity and stability and the large specific surface area of GQDs. Yuan *et al* [375] reported the synthesis of nanocomposite consisting of graphitic carbon nitride nanorods decorated with GQDs using a hydrothermal method, which allowed the formation of closely contacted nanorods and GQD interface. An improvement in the photocatalytic activity of the nanocomposite for the removal of antibiotics was observed compared to that of the pristine nanorods. GQDs decorated on the surface of multiwall carbon nanotubes were studied by Arumugasamy *et al* [376]. The nanocomposite was used in electrochemical sensor for the detection of dopamine. The incorporation of GQDs enhanced the electrocatalytic activity, sensitivity, selectivity and reproducibility of the sensor. The properties of inorganic materials have been shown to improve significantly upon incorporation of GQDs [377–390]. The excellent properties of the GQD-based composite materials could lead to many novel applications.

5. Applications

GQDs have many exciting applications in various fields due to their excellent properties and facile preparation techniques. The size dependence of GQDs on their optical and electronic properties has enabled the application of nanomaterials in the field of photoelectronics, such as broadband photodetectors [391], solar cells [273], white light-emitting diodes (LEDs) [141], fluorescent probes [110], lasers [167] and integrated optics [224]. As GQDs are members of the carbon family and have similar biological compatibility, especially GQDs in the nanometer regime, the nanomaterials have been explored for use in various biological applications, such as biomedicine [307], biological markers [98] and cancer treatment [111]. The ease of functionalization of GQDs has enabled them to find important applications in the field of agriculture for the removal of contaminants and detection of hazardous analytes, as well as agricultural nitrogen engineering using GQD-based nanocomposites [392]. The large specific surface area of GQDs has led to their utilization in various applications, such as in anticorrosion [393] and gas sensor [394]. In addition, Janus micromotors have been developed using modified GQDs to provide ultrafast detection of bacterial endotoxins [395]. In recent years, the characteristics and properties of GQDs have been studied extensively, which has brought benefits to many different fields of application. This section provides an overview of the different applications of GQDs, ranging from biomedical to energy applications.

5.1. Biomedical applications

GQDs have attracted considerable attention from researchers in the field of biomedicine due to their nanometer-scale size and biocompatibility [125, 396–404]. The nanometer-scale size of GQDs allows them to penetrate cells for diagnostic and therapeutic applications. Furthermore, the ease of functionalization of the edges of GQDs has led to the use of nanomaterials for drug delivery into cells, thereby improving the therapeutic effects of drugs. The remarkable thermal and electrical properties of GQDs allow the effective transformation of light energy into heat energy under NIR light irradiation, making them suitable for use in photothermal and photodynamic therapies. In addition, GQDs have been found to exhibit special properties that act as peroxidase or oxidase via electron transportation to convert certain biomolecules from normal species (e.g. H_2O_2 and $^3O_2$) to cytotoxic reactive oxygen species (ROS) (e.g. $^{\cdot}OH$ and $^1O_2$) upon light irradiation [237], thus promoting wound healing. The strong and broad fluorescence properties of GQDs have benefitted applications, such as bio-imaging [405, 406] and metal ion detection [407–412] in a variety of fields. Indeed, GQDs have many important applications in the biomedical field, ranging from diagnostics to treatment, as illustrated in figure 13(a).

5.1.1 Cancer cell and tumor therapy. Recently, Ruiyi *et al* [413] reported the use of GQDs functionalized with folic

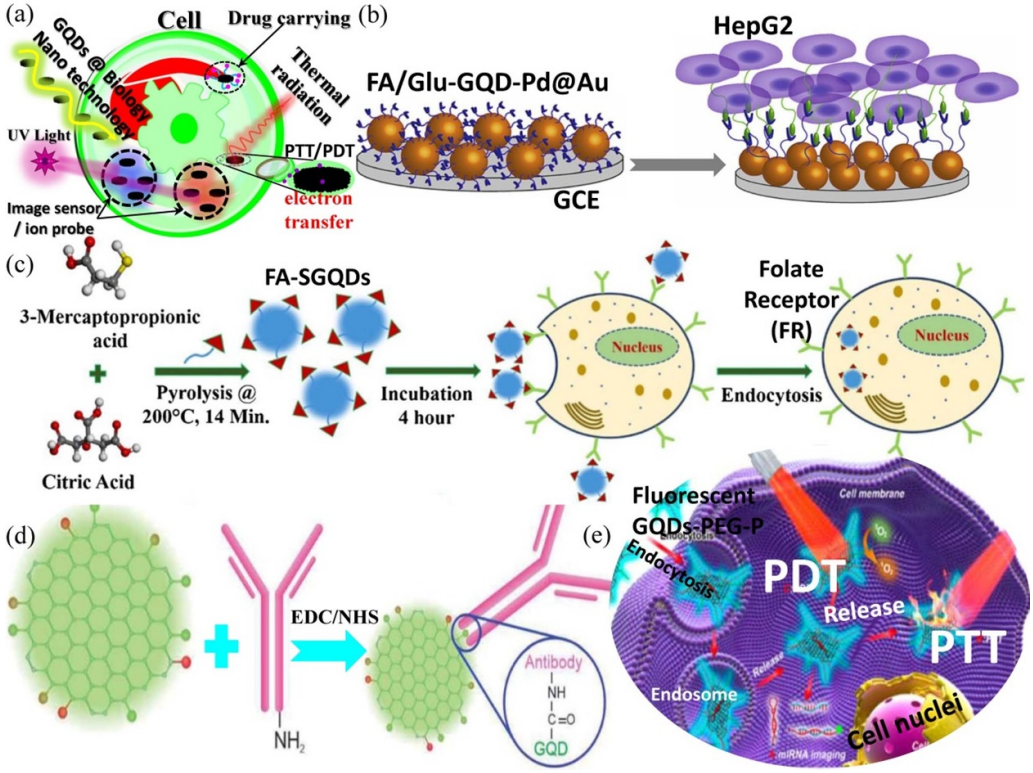

Figure 13. Biological applications of GQDs. (a) Bionanotechnology applications of GQDs, ranging from drug carriers and biotherapy to bioimaging and probe applications. (b) Schematic of the fabrication of an electrochemical sensing platform for cancer cells. Reprinted from [413], © 2020 Elsevier B.V. All rights reserved. (c) Schematic of the synthesis process of FA-SGQDs and their application in targeted bioimaging of FR overexpressed cancer cells. Reproduced from [414], with permission from Springer Nature. (d) Schematic of attaching anti-PSMA antibody on GQDs. Reproduced from [415] with permission from the Royal Society of Chemistry. (e) Theranostic platform for intracellular miRNA detection and combined photothermal therapy (PTT)/photodynamic therapy (PDT) [416]. John Wiley & Sons.© 2020 WILEY-VCH Verlag GmbH & Co. KGaA, Weinheim.

acid and glutamic acid in gold-coated palladium nanoparticles (acting as redox probes) for electrochemical detection of circulating cancer cells in human blood. Figure 13(b) shows the preparation process of the hybrid nanomaterials. The folic acid- and glutamic acid-functionalized GQDs would offer strong binding to cancer cells and provide reversible redox reactions that produce electrochemical signals upon binding. Such a hybrid significantly enhances the electrocatalytic activity and redox characteristics, leading to a low detection limit of two cells per milliliter. Kadian *et al* [414] prepared sulfur-doped GQDs functionalized with folic acid and used them as a fluorescent probe, which exhibited high quantum efficiency of 78%. The functionalized GQDs were capable of identifying folate receptor (FR)-positive and FR-negative cancer cells, as depicted in figure 13(c). The edge of the GQDs can be modified with antibodies specific to cancer-derived exosomes for medical diagnosis, as demonstrated by Barati *et al* [415]. Figure 13(d) shows a schematic of the GQDs immobilized with antibodies that can be used for the detection of exosomes. The ability to immobilize antibodies in GQDs will allow the future development of GQD-based immunosensors for the rapid detection of diseases. GQDs exhibit a high photothermal conversion efficiency under NIR light irradiation. This characteristic has enabled the development of photochromic nanoparticles for photoacoustic imaging-guided photothermal chemotherapy [416]. Once the GQDs enter cells, such as viral or cancer cells, the temperature of the GQDs increases upon irradiation with NIR light, resulting in selective cell death due to the elevated temperature, hence leading to biological therapy. This is the basic principle of photothermal therapy (PTT) using GQDs. In addition, functionalized GQDs, which exhibit high singlet oxygen generation, are suitable for use in photodynamic therapy (PDT). The production of singlet oxygen promotes the redox reaction in cells, thus causing rapid decay of cells. The mechanism of these two therapeutic strategies using GQDs for cancer treatment related to irradiation with light energy is shown in figure 13(e).

The use of GQDs to improve disease diagnosis and treatment has been demonstrated by several research groups [417–421]. Composites based on GQDs have also been studied by many researchers to further enhance their efficiency in biomedical applications. Recently, Zheng *et al* [422] prepared porous copper sulfide nanoparticles decorated with GQDs for controlled intracellular drug release. Anti-cancer drugs, such as doxorubicin, were embedded in the porous copper sulfide nanoparticles. Upon irradiation with NIR light, the drug was released due to an increase in temperature experienced by the nanocomposite of doxorubicin, GQDs and copper sulfide nanoparticles. Therefore, the nanocomposite provided a combination of PTT and chemotherapy for the treatment of

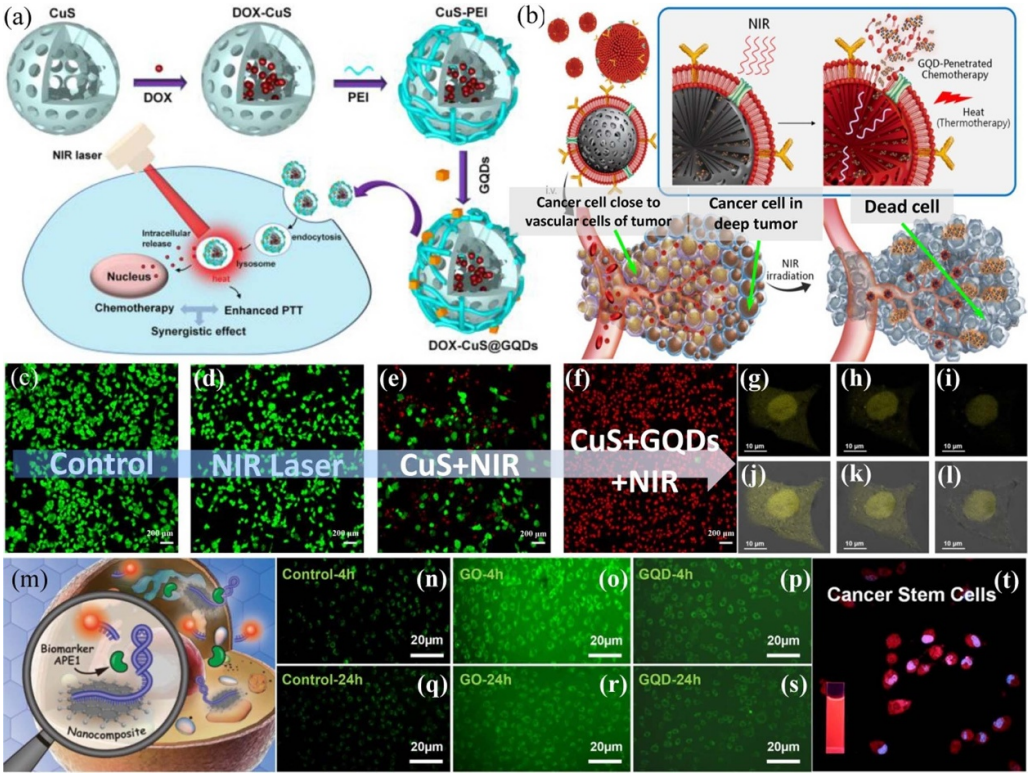

Figure 14. (a) Schematic representation of multifunctional DOX-CuS@GQDs NPs: fabrication process and illustration of controlled intracellular release and combined photothermal chemotherapy. (b) Schematic representation of targeted RBC-membrane-enveloped nanosponge-mediated tumor accumulation and drug/GQD penetration. Reprinted with permission from [423]. Copyright (2018) American Chemical Society. (c)–(f) Confocal images of MDA-MB-231 cells after different treatments and co-staining with calcein AM and PI; the green and red areas represent the regions of living and dead cells, respectively. Reproduced from [422], with permission from Springer Nature. (g)–(l) Confocal cell imaging (488 nm laser excitation) of HeLa cells with R-GQDs at different temperatures: 32 °C (g), (j), 37 °C (h), (k), and 42 °C (i), (l). (g), (h) and (i) are the fluorescence images of HeLa cells; (j), (k) and (l) are the merged (dark field merged with bright field) pictures. Reprinted with permission from [424]. Copyright (2020) American Chemical Society. (m) Schematic display of GQD-based nanocomposites for diagnosing cancer biomarker APE1 in living cells. Reprinted with permission from [425]. Copyright (2020) American Chemical Society. (n)–(s) Effects of nontoxic doses of GO-100 and GQDs-50 (15 μg ml^{-1}) on MMP. The cells were stained with rhodamine 123. Fluorescence microscopy images of MCF-7. Reprinted from [426], © 2020 Elsevier Ltd. All rights reserved. (t) Laser confocal scanning microscopy (LCSM) images of merged images of breast CSCs incubated with CSCNP-R-CQDs (200 μl 1 mg ml^{-1}) for 12 h and breast CSCs stained with DAPI (inset: photographs of the CSCNP-R-CQD aqueous solution under UV light (365 nm)). Reprinted with permission from [427]. Copyright (2020) American Chemical Society.

cancer, as illustrated in figure 14(a). Figures 14(c)–(f) show confocal images of cancer cells after different treatments. Sung *et al* [423] reported on the preparation of GQDs and docetaxel composite supported with red blood cell membrane. The nanocomposite served as a stealth agent and photolytic carrier, which could deliver drugs deep into the tumor tissue via the bloodstream. A combination of chemotherapy and photolytic effects from the GQD-based nanocomposite upon irradiation with NIR light effectively damaged and inhibited the tumor cells, as illustrated in figure 14(b). GQDs are often used as markers for biological imaging. Interestingly, the fluorescence properties of GQDs are not only dependent on their size and functional groups but also on their temperature, as discovered by Gao *et al* [424]. Figures 14(g)–(l) show the confocal images of HeLa cells with GQDs as fluorescent labels at different temperatures. Their work suggests that GQDs are suitable for use as biological thermoprobes and selective temperature detectors, hence adding new functionalities to GQD fluorescent probes. Early detection of cancer is important for the successful treatment of the disease. Much effort has been made to study the use of GQDs for cancer diagnosis. Zhang *et al* [425] designed and prepared nanocomposites of GQDs and single-molecule DNA as diagnostic probes to detect cellular apurinic/apyrimidinic endonuclease 1 (APE1), which has been identified as a predictive cancer biomarker. A large accumulative fluorescent signal in living cells can be generated by a small quantity of cellular APE1 through repeated enzyme catalytic circulation, as depicted in figure 14(m). The nanocomposite can also be used for the highly sensitive and specific detection of other APE1-dysregulated diseases. GQDs are attractive nanomaterials for application in the field of biotherapy due to their excellent biocompatibility and nontoxicity. The toxicity of GQDs and GO was studied by Hashemi *et al* [426]. They found that GQDs exhibited lower toxicity than GO, as the latter had a greater influence on the basal level of genes and mitochondrial membrane potential (MMP). Figures 14(n)–(s) show the fluorescence microscopy images of MCF-7 cells with nontoxic doses of GO and GQDs.

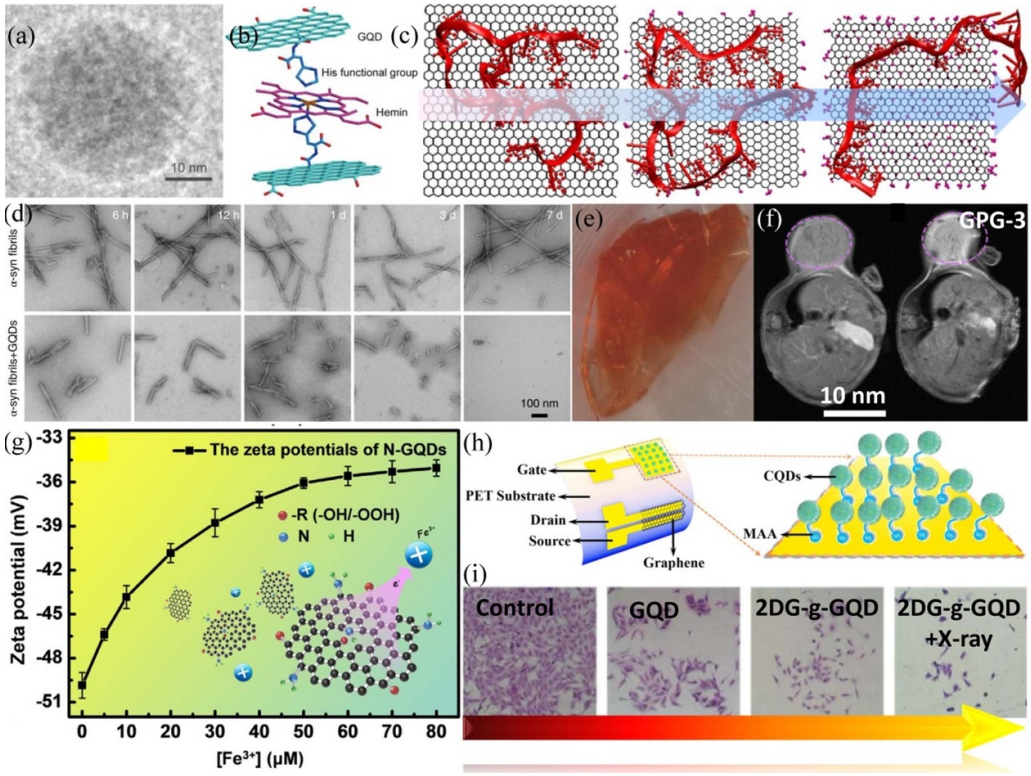

Figure 15. (a) Morphology of His-GQD/hemin, as recorded by TEM. (b) Proposed structure of His-GQD/hemin containing hemin, histidine functional groups and the hydrophobic basal plane of GQD. Reproduced from [428], with permission from Springer Nature. (c) Molecular dynamics simulations confirmed the dependency of A_{30} ssDNA adsorption on the GQD oxidation level. The final configurations of A_{30} ssDNA with GQD-0%, GQD-2% and GQD-17% (from left to right) for a 100 ns simulation. Reproduced from [429]. CC BY 4.0. (d) TEM images of preformed α-syn fibrils at various time points (6 and 12 h, and 1, 3 and 7 d) in the absence (top) and presence (bottom) of the GQDs. Reproduced from [430], with permission from Springer Nature. (e) Photograph of the doxorubicin-loaded CMC/GQDs. Reprinted from [433], © 2019 Elsevier B.V. All rights reserved. (f) An *in vivo* MRI of a nude mouse is shown (left) pre-injection, and then (right) 30 min post-injection with GP_6G-3 via the tail vein. The mouse was injected subcutaneously and imaged using a 7.0 T animal MRI scanner; the portion in the carmine circle was a tumor. Reprinted from [434], © 2020 Elsevier Ltd. All rights reserved. (g) The zeta potentials of nitrogen-doped GQDs toward different Fe^{3+} concentrations in the system. Reprinted from [439], © 2020 Elsevier B.V. All rights reserved. (h) Schematic of the Cu^{2+} ion sensor based on solution-gated graphene transistors. Reprinted with permission from [440]. Copyright (2020) American Chemical Society. (i) The invasion capacity was examined by transwell chamber assays after incubation with 2DG-g-GQD for 24 h. Reproduced from [441] with permission from the Royal Society of Chemistry.

By coating GQDs with anticancer drugs at their surface, nanomaterials can be used to deliver drugs to cancer cells to treat the disease. Recently, Fan *et al* [427] reported the preparation of GQDs loaded with doxorubicin (an anticancer drug) and found that the drug-loaded GQDs could penetrate cancer cells and cancer stem cells. The doxorubicin-loaded GQDs demonstrated remarkable therapeutic effects by killing cancer stem cells. Figure 14(t) shows a laser confocal scanning microscopy image of the drug-loaded GQDs in cancer stem cells. Over the last couple of years, there have been an increasing number of reports on the use of GQDs to treat cancer with some intriguing experimental results, thus bringing the possibility of curing cancer closer to reality.

5.1.2 Therapy for other diseases. GQDs have demonstrated a wide range of applications in the biological field due to their ease of functionalization and biocompatibility. Recently, Gong *et al* [428] designed and prepared an artificial enzyme consisting of histidine-functionalized GQDs and a hemin (His-GQDs/hemin) complex. Figures 15(a) and (b) show the TEM images and structure of the artificial enzyme, respectively. The His-GQDs/hemin complex, which can detect hydrogen peroxide and blood glucose, exhibited a relatively high catalytic performance and excellent acid resistance and can operate over a wide temperature range. The use of GQDs in the design of artificial enzymes provides an effective platform for practical applications. The functional groups of GQDs can significantly influence their optical and electrical properties. Landry *et al* [429] found that the degree of oxidation of GQDs has a remarkable effect on the adsorption of biopolymers, such as single-strand DNA (ssDNA). For example, the adsorption of ssDNA was weak at low-oxidized GQDs, whereas strong adsorption of ssDNA was observed in nonoxidized GQDs, as illustrated in figure 15(c). The intrinsic fluorescence of the GQDs was reduced dramatically when ssDNA was absorbed onto low-oxidized GQDs, suggesting that the GQD properties can be regulated by the polymer sequence and type. GQDs have also been shown to be effective in treating diseases, such as Alzheimer's disease [430], diabetes [431] and

mitochondrial dysfunction [432]. For example, aggregation and transmission of α-synuclein (α-syn) in the midbrain may be related to the pathogenesis of Parkinson's disease. Kwon *et al* [430] found that GQDs could inhibit fibrillization of α-syn and interact directly with mature fibrils to trigger disaggregation, as depicted in figure 15(d). Hence, GQDs can be potentially used to treat Parkinson's disease. GQDs have been studied for use as drug carriers due to their biocompatibility. Namazi *et al* [433] reported on the use of GQDs as cross-linker for carboxymethyl cellulose. The nanocomposite hydrogel was biocompatible and exhibited pH-sensitive swelling and degradation properties. It can be loaded with drugs, and the release of drugs can be triggered by the pH. Using doxorubicin as an example, the researchers investigated the drug delivery properties of the nanocomposite hydrogel, as shown in figure 15(e). Recently, GQDs were used as contrast agents in magnetic resonance imaging (MRI), as reported by Li *et al* [434]. They prepared Gd^{3+}-loaded polyethylene glycol-modified GQDs as contrast agent for MRI. They found that changing the localized superacid microenvironment of the nanocomposite can significantly improve its magnetic relaxivity, which was much higher than that of commercially available contrast agents, thus enhancing the performance of MRI, as shown in figure 15(f). Furthermore, the nanocomposite modified with folic acid was suitable for MRI-fluorescent dual-mode targeted tumor imaging with low biotoxicity, both *in vitro* and *in vivo*. The GQD-based contrast agent is of great interest in its applications in MRI, as it provides accurate monitoring and diagnosis of diseases. The use of GQDs as metal ion probes in biosensing applications has attracted much research interest [435–438]. Wang *et al* [439] prepared nitrogen-doped GQDs exhibiting yellow emission with high quantum yield. The doped GQDs were used to detect iron ions in natural water and potentially for intracellular iron ion detection. Complexation between iron ions and nitrogen-doped GQDs can significantly quench the fluorescence intensity of the doped GQDs, which is highly selective for iron ions, as illustrated in figure 15(g). Another example of the use of GQDs as metal ion probes was demonstrated by Fan *et al* [440]. They modified a solution-gated graphene transistor with GQDs, as shown in figure 15(h). A change in the electrical double-layer capacitance at the gate due to the interaction between copper ions and GQDs results in a change in the channel current. They found that copper ions exhibited excellent binding characteristics with GQDs, making the sensor highly sensitive and selective to copper ions. GQDs have significant therapeutic effects on tumors. In addition to the combined PTT, PDT and drug delivery therapy, GQDs also play an important role in tumor radiotherapy. Tung *et al* [441] reported on the use of GQDs grafted with 2-deoxy-D-glucose as radiosensitizer to treat osteosarcoma, which showed improvement in the therapeutic efficacy, as shown in figure 15(i). The improved therapeutic effect is due to a significant increase in oxidative stress response and DNA damage in osteosarcoma cells caused by the GQD complex, which selectively targets tumor cells. Therefore, the GQD complex has the potential to achieve low-dose high-precision radiotherapy treatment for osteosarcoma. In recent years, GQDs have been used in many applications in the biomedical field, such as biomedical imaging [442–446], immune probes [447], fluorescence probes [448–456], drug carriers [457, 458], sterilization [459–462], wound healing [463–465] and cancer treatment and diagnosis [421, 425, 433, 441]. The effectiveness of nanodrugs to different age groups has also been studied [466]. In summary, the excellent properties of GQDs will significantly impact the biomedical field in the near future, ranging from diagnosis to treatment of diseases.

5.2. Energy applications

GQDs have wide-ranging applications in the field of energy, which covers energy generation to consumption (as illustrated in figure 16(a)), because of their excellent properties and low-cost facile preparation methods. In energy generation, GQDs have been explored for use in solar photovoltaic devices [467–472] and hydrogen production from photo-hydrolysis of water [473–477]. In energy storage, GQDs have been used in the preparation of electrodes for supercapacitors due to their large specific surface areas and good electrical properties [478–482]. In terms of energy consumption, GQDs have been used to enhance the brightness and tailor the color of light-emitting devices due to their excellent optical properties [483–486]. Therefore, this review provides a detailed description of the applications of GQDs in the three aspects of energy generation, storage and consumption, especially the important research achievements in recent years.

Many efforts in the field of solar energy research have been directed toward achieving a high level of efficiency in the utilization of solar energy. In addition to achieving high solar energy conversion efficiency, researchers are investigating means to reduce the cost of solar energy utilization, store solar energy and improve the ability to capture solar energy. Recently, many research groups have studied the use of GQDs in solar cells [380, 491–505] and in solar hydrolytic hydrogen production [369, 506–514]. Both solar cells and solar hydrolytic hydrogen production provide clean sources of energy, and the former convert light energy directly into electricity; hence, it can be considered as an efficient means of solar energy utilization. GQDs can play a significant role in improving the performance of solar cells due to their remarkable electrical and optical properties. For example, Kim *et al* [281] found that GQDs exhibit a significant photon down-conversion effect, which is particularly significant when doped with nitrogen. The nitrogen-doped GQDs exhibited fluorescence quantum efficiency of 99% and large Stokes shift of 98 nm. When combining nitrogen-doped GQDs with copper indium gallium selenide (CIGS), the conversion efficiency of the thin-film solar cell reached 15.3%. The enhancement in performance was due to the photon down-conversion and light-trapping effect of the nitrogen-doped GQDs. Perovskite solar cells have attracted much research interest in recent years due to their many advantages, such as low cost and high conversion efficiency. Gan *et al* [276] used nitrogen-doped GQDs as functional semiconductor additives in perovskite thin films. The nitrogen active sites in the GQDs passivated the grain boundary trap states. The matching of the

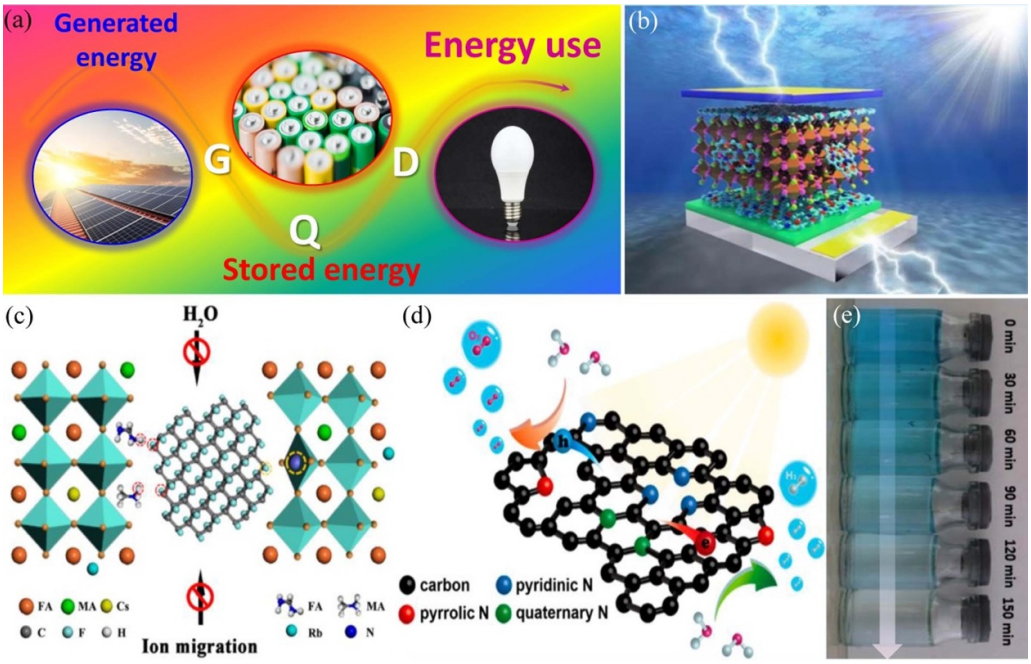

Figure 16. Energy applications of GQDs. (a) Schematic of the energy applications of GQDs from energy generation to energy storage to utilization. (b) Schematic of the engineered interfaces throughout the entire perovskite solar cell via the incorporation of N-and-S-co-doped GQDs. Reprinted with permission from [487]. Copyright (2020) American Chemical Society. (c) Schematic of the positive role of FGQDs in perovskite films. Reprinted with permission from [488]. Copyright (2020) American Chemical Society. (d) Schematic of nitrogen-doped GQDs for solar hydrogen production. Reprinted with permission from [489]. Copyright (2020) American Chemical Society. (e) Photographs of nitrogen-doped GQD solution under light irradiation at different times. Reprinted from [490], © 2020 Elsevier Ltd. All rights reserved.

energy structure of the GQDs at the grain boundary with that of the perovskite enabled charge transport at the grain boundaries. Furthermore, the n-type behavior of the nitrogen-doped GQDs significantly improved the electronic properties of the perovskite thin film, resulting in an improvement in charge transport as well as a reduction in interface recombination. The conversion efficiency of the solar cells was reported to be as high as 19.8%. Moreover, the solar cell exhibited stable performance without encapsulation due to the protected grain boundaries and the hydrophobicity of the modified film with the addition of nitrogen-doped GQDs. Chen *et al* [487] also studied the effect of adding GQDs to perovskite solar cells and found that GQDs have several functions, such as promoting crystal growth of perovskite, easing extraction of charge at cathode and anode interfaces, inducing defect passivation and inhibiting charge recombination. Upon introducing GQDs into Fe_2O_3-based perovskite solar cells (as shown in figure 16(b)), the conversion efficiency of the solar cells increased from 14% to 19.2%. The solar cells also demonstrated a significant improvement in durability, including humidity, ultraviolet light and temperature stabilities. To date, although the performance of most flexible solar cells is not as good as that of rigid solar cells, the wearable and portable nature of flexible solar cells has attracted much research effort, as they offer many exciting applications. Yang *et al* [488] found that fluorine-doped GQDs can effectively reduce defect density at the perovskite thin film by passivating the grain boundaries and surface, thus increasing the conversion efficiency of the solar cell to 20.40%. The perovskite solar cell with fluorine-doped GQDs exhibited excellent thermal and environmental stabilities, as it could prevent the invasion of external water molecules and the spread of ions outside the perovskite, as depicted in figure 16(c). A solar cell converts light energy into electrical energy, whereas a photodetector converts light energy into electrical signals. Although these two devices yield different results, the design of the solar cell is similar to that of a photovoltaic detector. Shin *et al* [515] reported the use of GQDs as hole transport layers in perovskite solar cells. They found that GQDs improved the crystallinity of the perovskite film and increased the work function of the hole transport layer, resulting in enhanced solar cell performance. They also suggest that GQDs in perovskite films, whether as solar cells or photodetectors, would have the same effect. To understand the passivation of grain boundary in a perovskite film using GQDs, Ma *et al* [516] added GQDs containing hydroxyl and carbonyl functional groups to a perovskite solution. The addition of GQDs led to an improvement in the photoluminescence intensity of the film and carrier lifetime, thereby suggesting a reduction in nonradiative recombination due to the passivation of the grain boundary at the film. Furthermore, the addition of GQDs increased the thickness of the perovskite film, resulting in an improved conversion efficiency of up to 18.24% for this solar cell. Silicon is currently the most widely used material for commercially available solar cells. The performance of silicon solar cells has almost reached its maximum efficiency due to the maturity of the silicon technology. However, researchers are still making relentless efforts to reduce the cost and increase the conversion efficiency of silicon solar

cells. Diao *et al* [517] reported the fabrication of heterojunction solar cells consisting of GQDs and silicon. The GQDs were used as the hole transport layer and electron-blocking layer. They separate the photogenerated electron–hole pairs and inhibit carrier recombination at the anode. These heterojunction solar cells could achieve a conversion efficiency of 12.35%. In recent years, much research effort has been devoted to studying the use of GQDs in solar cell applications. Table 2 provides a list of the GQD-based solar cells with their performance indicators.

GQDs have also been used to produce hydrogen using solar energy. Hydrogen can be used as a green energy source, and recent research has focused on methodologies to produce hydrogen efficiently. The key to efficient hydrogen production is to improve the catalytic performance of the photocatalyst. Huang *et al* [518] prepared a ternary composite photocatalyst that comprises BiOCl, GQDs and rGO. The GQDs significantly improved the photocatalytic performance by 8.4 times compared to pure BiOCl due to an enhancement in charge separation and injection. Compared with rGO, the GQDs demonstrated much better performance. The study found that the GQDs did not significantly enhance the light absorption and showed that the improvement in photocatalytic performance was not necessary due to an enhancement in optical absorption; however, the electrical properties of the composite were also of particular importance. GQDs doped with nitrogen exhibited remarkable optical and electrical properties, which could affect their photocatalytic performance. Tsai *et al* [489] found that C–N bond induced visible light absorption when GQDs were doped with nitrogen, as shown in figure 16(d). Moreover, an increase in the carrier lifetime and concentration was reported upon increasing the nitrogen concentration in the GQDs. Compared to intrinsic GQDs, the nitrogen-doped GQDs demonstrated an increase in photocatalytic hydrogen production efficiency due to an enhancement in charge dynamics and reaction kinetics and increased carrier concentration. This finding suggests that doping of GQDs is an effective way to improve their photocatalytic performance. The use of GQD-based composites, consisting of other photocatalytic materials, is another effective way to improve the efficiency of photocatalytic hydrogen production. Chang *et al* [519] demonstrated the use of GQDs in CdSe-sensitized TiO_2 nanorods to improve the photocatalytic efficiency for solar hydrogen production. It was found that the introduction of GQDs resulted in vectorial charge transfer and improved reaction kinetics. Importantly, the GQDs reduced the photoetching at CdSe, thereby ensuring the long-term stability of the electrode. In addition, Xue *et al* [520] prepared a CdS–GQD–titanate nanotube ternary nanocomposite for hydrogen production. The nanocomposite demonstrated remarkable photocatalytic performance due to its enhanced ability to capture visible light, longer lifetime of photogenerated carrier, faster interfacial charge transport rate and longer electron transport distance. In addition to improving the catalytic performance for the solar photolysis of water, GQDs can also perform photocatalytic hydrolysis of certain pollutants [521–524]. Dejpasand *et al* [490] prepared nitrogen-doped GQDs with a broad absorption spectrum and down-conversion effect. The photodegradation of methylene blue using nitrogen-doped GQDs under illumination was studied using energy states. Figure 16(e) shows the degradation of the methylene blue solution using nitrogen-doped GQDs under different illumination durations. Therefore, the aforementioned studies clearly indicate the important role of GQDs in improving the photocatalyic performance.

Energy storage is critical for the implementation of renewable energy. It is also important for mobile devices and electric vehicles. A battery is used to store electrical energy and has a device structure similar to that of a capacitor consisting of a dielectric material sandwiched between two electrodes to charge and discharge electric charges. Much research has been conducted on the development of environmentally friendly and low-cost capacitors that exhibit high energy densities and stabilities. Carbon was first used as an electrode material in lithium-ion batteries in the 1980s [525]. Subsequently, many groups have studied other forms of carbon materials, such as graphite, carbon nanotubes, graphene and GQDs, as electrode materials. Li *et al* [526] prepared nitrogen-doped GQDs onto a carbonized metal–organic framework (cMOF), which was used as an electrode material for supercapacitors. The nitrogen-doped GQDs played a vital role in improving the pseudocapacitive activity and surface wettability of the electrodes, leading to enhanced performance of the supercapacitor. Figure 17(a) shows the structure of the supercapacitor consisting of nitrogen-doped GQDs/cMOF as the anode and activated carbon as the cathode.

The low-cost, facile preparation of supercapacitor electrodes is of great commercial interest. Zhang *et al* [527] prepared composite electrodes consisting of porous wood carbon (PWC), MnO_2 and GQDs. After pyrolyzing natural wood to produce PWC, MnO_2 and GQDs were decorated on PWC using a facile hydrothermal method. A schematic of the PWC/MnO_2/GQDs composite electrode is shown in figure 17(b). The GQDs significantly promoted the transport of ions and protected MnO_2 from falling off from the surface of the PWC, leading to an improvement in the electrochemical performance of the electrodes and demonstrating good rate capability and cycling stability. GQD-modified composite materials have attracted much research interest for the development of low-cost high-performance energy storage devices. Qiu *et al* [528] reported the synthesis of histidine-functionalized GQD/layered double hydroxide (His-GQDs/LDH) composite using a microwave method. The composite exhibited flower ball-like structures and was used as the anode material. The large specific surface area and electrical conductivity of the composite resulted in high specific capacitance and remarkable cycling stability. They also produced a supercapacitor exhibiting excellent energy storage performance and cycling stability using the His-GQDs/LDH composite and active carbon as the positive and negative electrodes, respectively, as shown in figure 17(c). In addition to being used as electrode materials, GQDs can form composites with other materials for use as separators in capacitors because of their large specific surface area and small size. Pang *et al* [529] developed a separator coated with a composite of multiwall carbon nanotubes and nitrogen-doped GQDs and used it in Li–S batteries. This provided a physical

Table 2. Properties of GQD-based solar cells.

Device structure	Doped elements	Rigid/ flexible	Short-circuit current (mA cm^{-2})	Open-circuit voltage (V)	Fill factor (%)	External quantum efficiency (%)	Power conversion efficiency (%)	References
Gr/Mo/CIGS/CdS/ZnO/NGQDs/Ni-Al	N	Rigid	31.77	0.668	73.09	80 at 600 nm	15.31	[281]
N-GQDs PMMA/FTO/ZnO:Al/ZnO/CdS/CIGS/Au	N	Rigid	36.13	0.6592	67.91	—	16.13	[273]
NiO_x/GN-GQDs + PVK/PCBM/BCP/Ag	N	Rigid	23.4	1.06	80	95 at 500 nm	19.8	[276]
Glass/ITO/PANI-GQDs/Al	PANI	—	25.11	0.34	0.10	—	0.86	[323]
FTO/PEDOT:PSS/GQDs/PVK/PCBM/Ag	—	Flexible	21.41	1.002	75.31	—	16.15	[324]
ZnO/GQDs (DSSCs)	—	Rigid	12.2	0.68	63	—	5.27	[347]
TFSA-GR/MoS_2/P3HT:PCBM:GQDs/Al	—	Flexible	10.88	0.588	66.08	70 at 500 nm	4.23	[467]
FTO/TiO_2/GQDs/N719/Iodolyte (DSSCs)	—	Rigid	13.77	0.7	44	—	5.1	[470]
PEDOT:GQDs/porous Si/n-Si/TiO_2	—	Rigid	28.53	0.537	68.48	80 at 500 nm	10.49	[471]
Gr/GQDs/Si	—	Rigid	29.33	0.51	66.59	—	9.97	[472]
FTO/α-Fe_2O_3/N,S-GQDs/PVK/N,S-GQDs/Spiro-OMeTAD/Au	N,S	Rigid	23.6	1.047	79	—	19.2	[487]
Gr/GQDs/n-Si/In-Ga	—	Rigid	30.74	0.58	63	85 at 500 nm	12.35	[517]
FTO/S,N-GQDs-sensitized C-ZnO (DSSCs)	S,N	Rigid	1.84	0.36	45.28	—	0.293	[380]
ITO/SnO_2/SnO_2:GQDs/PVK	—	Rigid	24.4	1.11	78	90 at 550 nm	21.1	[491]
FTO/N-GQDs-N719/TiO_2/Pt/FTO (DSSCs)	N	Rigid	17.65	0.72	59	—	7.49	[492]
FTO/TiO_2-GQDs-N719/Pt/FTO (DSSCs)	—	Rigid	20.03	0.73	61	—	8.92	[493]
FTO/TiO_2-GQDs-Ulva/Pt/FTO (DSSCs)	—	Rigid	2.04	0.75	52	—	0.81	[494]
FTO/TiO_2/GQDs/PVK/Spiro-OMeTAD/Au	—	Rigid	21.92	0.97	67	82 at 400 nm	14.36	[495]
ITO/NiO_x/NiO_x:AGQDs/PVK/PCBM/BCP/Ag	Amino	Flexible	22.3	1.05	83.1	—	19.4	[496]
FTO/SnO_2:GQDs/PVK/Spiro-OMeTAD/Au	—	Flexible	23.5	1.08	77	90 at 500 nm	19.6	[497]
ITO/NiO/NiO:GQDs/PVK/PCBM/Ag	—	Rigid	20.22	1.08	77.15	—	16.97	[498]
In-Ga/Si/CNTs/GQDs/PVP/Ag	—	Rigid	35.58	0.598	70.22	90 at 700 nm	14.94	[499]
Glass/ITO/PEDOT:PSS/P3HT:PCBM:GQDs/Al	—	Rigid	18.9	0.55	32	—	3.32	[500]
FTO/ZnO:GQDs/PVK/Spiro-OMeTAD/Au	—	Rigid	24.7	1.02	70	—	17.63	[501]
ITO/TiO_2:GQDs/N719/Pt (DSSCs)	—	Flexible	14.32	0.68	53.2	—	5.18	[502]
GQDs/PVK	N	Rigid	24.7	0.81	43.8	—	8.77	[504]
GQDs/Si	N	Rigid	31.94	0.601	70	—	13.4	[505]

Note: PTAA, poly[bis(4-phenyl)(2,4,6-trimethylphenyl)amine]; PVK, perovskite; PANI, polyaniline; DSSCs, dye sensitized solar cells; CIGS, copper indium gallium selenide; TFSA-GR, bis-(trifluoromethanesulfonyl)-amide-doped graphene.

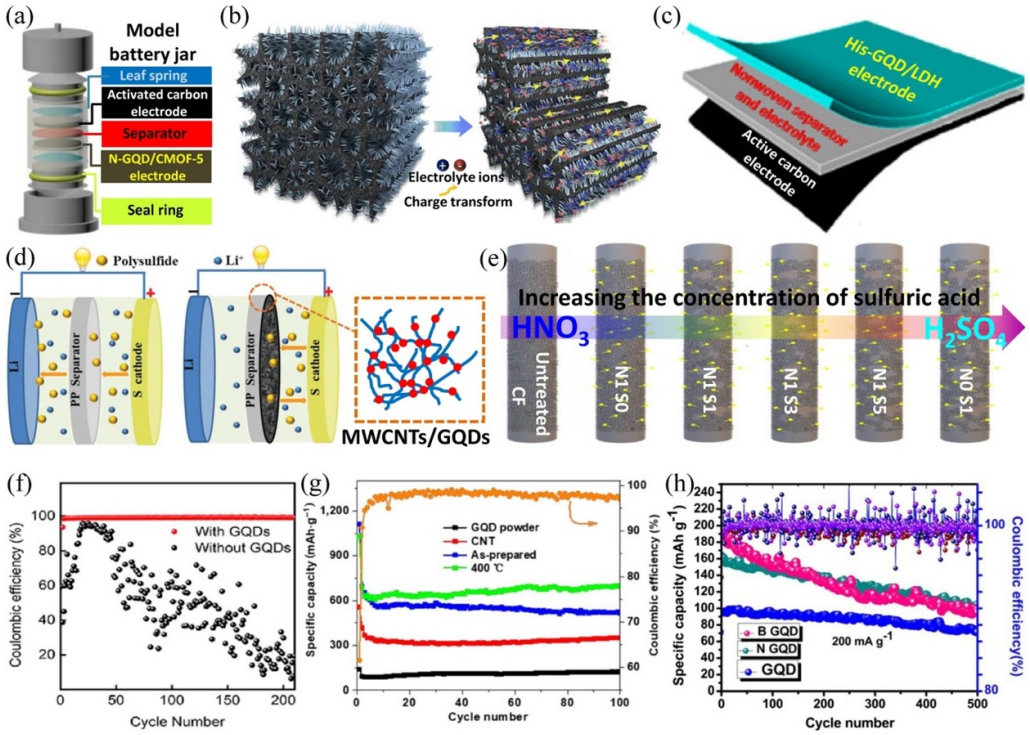

Figure 17. Applications of GQDs in energy storage batteries. (a) Schematic of asymmetric nitrogen-doped GQD/cMOF-5/AC supercapacitor. Reproduced from [526] with permission from the Royal Society of Chemistry. (b) Schematic of ions and charge transfer inside the PWC/MnO_2/GQDs electrode. Reprinted from [527], © 2020 Elsevier Ltd. All rights reserved. (c) Illustration of the composition of a supercapacitor. Reprinted from [528], © 2020 Elsevier Inc. All rights reserved. (d) Schematic representation of lithium–sulfur (Li–S) batteries employing a commercial PP separator and the MWCNT/NCQD-coated separator [529]. John Wiley & Sons.© 2018 WILEY-VCH Verlag GmbH & Co. KGaA, Weinheim. (e) Illustration of the generation of the hydrophilic group and GQDs on CF with different acid treatments. Reprinted with permission from [530]. Copyright (2020) American Chemical Society. (f) Cycling performances of the Li|Cu cells using electrolyte with and without GQDs at the current density of 1 mA cm^{-2} with 1 mAh cm^{-2} plating capacity in each cycle. Reprinted from [531], © 2019 Elsevier Ltd. All rights reserved. (g) Cycling performance at 100 mA g^{-1} for GQD powders, original CNTs, as-prepared and GQD@CNTs annealed at 400 °C. Reproduced from [532], Copyright © 2020, Tsinghua University Press and Springer-Verlag GmbH Germany, part of Springer Nature. (h) Cyclic stability curve of GQD, NGQD and BGQD. Reprinted from [533], © 2019 Elsevier B.V. All rights reserved.

barrier against polysulfide movement and chemical adsorption of polysulfides by the composite, as illustrated in figure 17(d). The composite-coated separator significantly improved the cycle life and anti-self-discharge performance of Li–S batteries. This development is important for practical applications of lithium-ion batteries. The use of GQD heterostructure electrodes can effectively improve the energy density of aqueous supercapacitors by increasing their potential window, as reported by Jia *et al* [534]. They found that heterostructure electrodes consisting of GQDs and MnO_2 provided good interfacial bonding via Mn–O–C bonds. Using the GQDs/MnO_2 electrodes, the potential window can be extended to 1.3 V (more than the theoretical value) due to a potential drop in the built-in electric field of the heterostructure. Flexible capacitors have attracted much interest in recent years [535, 536]. One of the key components is a flexible electrode material, and carbon fiber is known to be an ideal candidate. Hsiao and Lin [530] treated carbon fiber with a mixture of nitric acid and sulfuric acid at different ratios. They found that GQDs and functional groups were formed on the surface of the carbon fiber after acid treatments, as depicted in figure 17(e). At the same time, the treatment roughened the surface of carbon fiber. Both the formation of GQDs and roughening of the carbon fiber led to a large specific surface area at the electrode, which significantly increased the energy storage capacity of the flexible capacitors. GQDs can also be added to the electrolyte to regulate the electrochemical interface, thereby improving the performance of the capacitor. Hu *et al* [531] found that the addition of GQDs into the electrolyte would prevent the growth of dendrite in Li–S batteries containing high sulfur loading. The GQDs acted as heterogeneous sites for uniform nucleation and provided continuous regulation for dendrite-free lithium deposition under the control of an electric field and ion flux. This improved the cycling stability of the Li–S batteries, as demonstrated in figure 17(f). This study provides a solution to the inherent problems of the Li–S battery anode. A composite of GQDs and carbon nanotubes was explored for use as an electrode material for capacitors. Zhao *et al* [532] prepared a coaxial structure of GQD-coated carbon nanotubes as electrode material for energy storage of lithium ions. The GQDs were grafted onto 3D carbon nanotube frameworks to avoid agglomeration of the GQDs. These

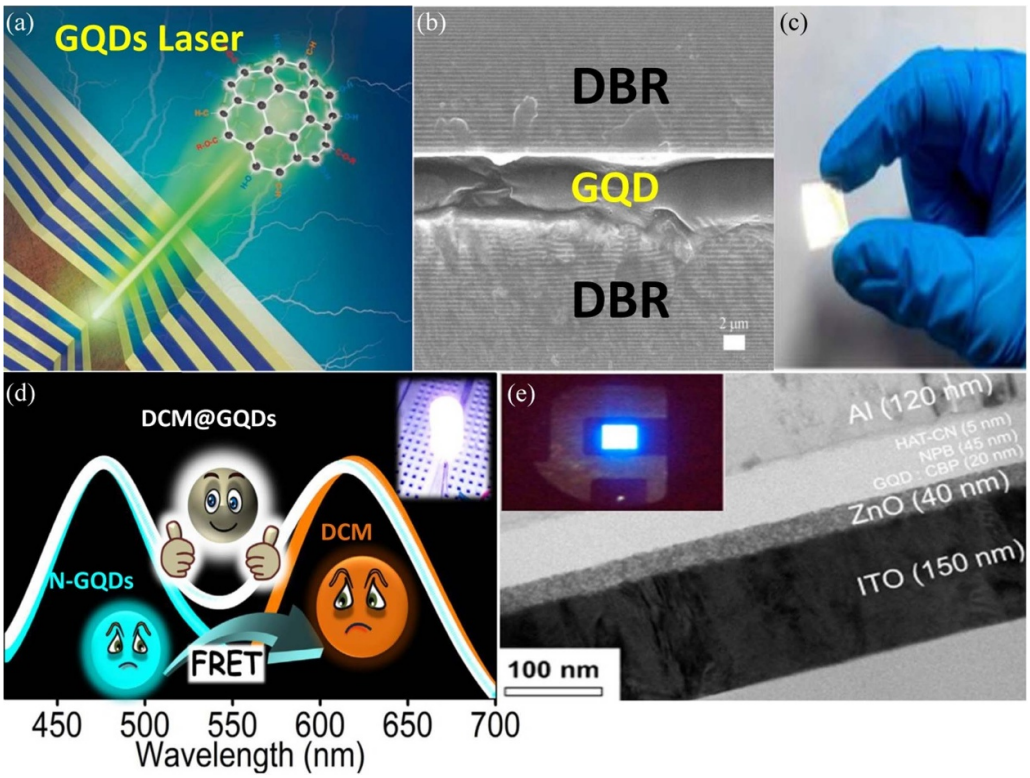

Figure 18. Applications of GQDs in light-emitting devices. (a) Schematic structure of the GQD-VCSEL, consisting of top and bottom dielectric Ta_2O_5/SiO_2 DBRs with synthesized GQDs sandwiched between them. (b) Cross-sectional SEM image of the fabricated GQD-VCSEL. (c) Photograph of the fabricated DBR under room light. Reprinted with permission from [167]. Copyright (2019) American Chemical Society. (d) Schematic of Förster resonance energy transfer (FRET)-assisted generation of white light in doped GQD-DCM dye luminescent duo (LD) system for fabrication of light-emitting LEDs (WLEDs) (inset: picture of WLEDs). Reprinted from [334], © 2020 Elsevier Inc. All rights reserved. (e) Cross-sectional TEM image of GQD–LEDs (inset: photograph of characteristic deep blue light emitted from the GQDs–LEDs at an applied voltage of 4.75 V). Reprinted with permission from [160]. Copyright (2019) American Chemical Society.

GQDs with oxygen functional groups provided enormous storage sites for lithium ions and were therefore responsible for the enhanced performance of the lithium-ion battery anode. Figure 17(g) shows the remarkable cycling performance and stability of the annealed GQD-coated carbon nanotubes as a lithium-ion battery anode. The introduction of impurities in GQDs can create defect states that have a significant effect on the properties of GQDs. Vijaya Kumar Saroja *et al* [533] reported that the edge defects of both GQDs and doped GQDs contributed to the improvement in the energy storage performance of the capacitors. As shown in figure 17(h), the GQDs doped with either nitrogen or boron atoms showed an improvement in the energy storage capacity with good cycling stability. The GQDs can improve the performance of capacitors when applied as electrodes, electrolytes and separators [537–549]. These strategies provide ideas for the development of new and improved capacitors.

Efficient energy use is an important topic in the field of energy application. Because of their unique optical properties, GQDs have been found to improve the performance of light-emitting devices. This is mainly due to the formation of a composite membrane that can be coated on the surface of monochrome LEDs. The fluorescence effect of the GQDs changes the wavelength of the light emitted from the LED. In recent years, GQDs have been used to develop light emitters that utilize the quantum confinement effect of the nanomaterials. White LEDs have been of great interest in the field of luminescence because of their energy-saving characteristic. Pramanik *et al* [334] reported the generation of white light using a combination of Förster resonance energy transfer and rare-earth-free luminescent material duo, as illustrated in figure 18(d). The white LEDs were prepared using composite colloids comprising nitrogen-doped GQDs and DCM dye. The energy gap can be regulated by nitrogen doping in GQDs, thereby tuning and widening the luminescence range of the dye.

Instead of using rare-earth material, Wang *et al* [550] found that chloride-doped GQDs can emit white light directly when under the irradiation of UV light. The chloride-doped GQDs were embedded in a silicon resin to form a composite film, which exhibited high transparency, flexibility, excellent optical stability and thermal stability. The film was attached directly to the LEDs to produce a white light. As the chlorine-doped GQDs were dispersed homogeneously within the film, the resultant natural white light was uniform without defects. These rare-earth-free white-luminescent chlorine-doped GQDs not only prevent the shortcomings of multicolor phosphors, but they also provide a green alternative

for producing light emitters. There are reports on the formation of other GQD-based composite films, whose optical properties can be regulated by adjusting the concentration of the doped GQDs. Wu *et al* [335] prepared GQDs encapsulated MF polymer microspheres. The emission wavelength was extended from blue to full visible range under UV irradiation, resulting in white-light luminescence. The luminescence properties were tunable by varying the doping concentration of the GQDs. A flexible thin film was formed by dispersing the GQD–MF microspheres in the polymer matrix and was used on LEDs to produce high-quality white-light emission and light diffusion. However, the aggregation of GQDs due to the interaction of π bonds often leads to photoluminescence quenching, thus limiting the performance of GQD-based light emitter devices. Recently, Park *et al* [370] incorporated GQDs with boron oxynitride (GQDs@BNO), which resulted in high PL-QY. The effective dispersion of GQDs in the BNO matrix significantly suppressed the aggregation of GQDs and therefore minimized photoluminescence quenching. An increase in the spontaneous emission rate of the GQDs was observed as the GQDs were surrounded by the BNO matrix having a high refractive index and enabled fluorescence energy transfer from the BNO donor with a larger bandgap to the GQD acceptor with a smaller bandgap, thus enhancing its electroluminescence activity. The optical properties of the GQDs are also influenced by the morphology of the nanomaterials. Lee *et al* [160] found that the edge states of GQDs have a significant role in their luminescence properties. They studied the relationship between the GQD crystalline size and their exciton lifetime by effectively controlling the morphology of the GQDs. Figure 18(e) shows the device structure of the GQD-based light-emitting device, which exhibited blue luminescence, as shown in the inset. Interestingly, the blue emission was not affected by the doping level of GQDs. In addition to LED, laser is also an important optoelectronic device, especially for optical communication. There are only a few reports on the use of GQDs in lasers because of the complexity of the structural design of lasers compared to that of LEDs. Lee *et al* [167] prepared a vertical optical cavity consisting of GQDs and distributed Bragg reflectors (DBRs). Figures 18(a) and (b) show the device structure of the GQD-based vertical-cavity surface-emitting laser. The design of the DBR provided a broad stopband that spectrally overlapped with the emitted GQDs and allowed high transmittance of light excitation in the UV region. An optical image of the fabricated DBR is shown in figure 18(c). The emission wavelength of the GQD-based laser was mainly concentrated in the green-light band. These results demonstrate that the GQDs can be used as optical gain materials.

In summary, GQDs can be used as fluorescent and light-emitting materials. Furthermore, the facile, low-cost and environmentally friendly preparation process for GQDs would allow widespread applications. GQDs have many important applications in the field of energy, ranging from energy generation to storage and utilization, because of their unique physical and chemical properties. The research and development of GQDs will continue to grow and find many novel applications in the field of energy.

5.3. Detector and sensor applications

The bandgap of GQDs can be modulated by means of size control and dopants, which can result in tunable spectral responses ranging from UV to NIR bands.

When GQDs form heterojunctions with other photoelectric materials, the quantum confinement effect of GQDs can reduce the recombination of electron–hole pairs, thereby increasing the exciton lifetime and resulting in a high gain. The photoelectric properties of GQDs are not affected by external compressive stress when coated on flexible substrates due to their small dimensions. Therefore, GQDs are suitable for the preparation of wideband, high detectivity and responsivity-flexible photodetectors. The large specific surface area and edge effect of GQDs make them attractive for use in gas sensors. In particular, GQDs with functional groups are highly selective to gas; thus, they are also suitable as the active layer in gas sensors. The excellent characteristics of GQDs could lead to high-performance photodetectors and gas sensors, in which the mechanism is based on the absorption of either incident photons or gases, causing a change in the electronic properties of the GQDs, as illustrated in figure 19(a). This section provides a review of the recent developments in GQD-based photodetectors and gas sensors.

There have been reports on the application of GQDs in photodetectors. However, the mechanism of charge transport in heterojunctions formed between GQDs and other materials, especially those of van der Waals heterojunctions, is still unclear. Shan *et al* [551] applied femtosecond pump–probe spectroscopy, two-phase electron injection model and modified rate equations to quantitatively solve the charge transfer rate at the interface of a mixed van der Waals GQD/MoS_2 heterostructure. A schematic of the device structure is shown in figure 19(b). Understanding the electron transfer and relaxation processes in the heterostructure would assist in developing methods to alter the optical performance of the device. They found that the cascaded relaxation of hot electrons in GQDs, due to the quantum confinement effect, can significantly influence the interfacial dynamics. This finding can be used to optimize the performance of photoelectric devices based on mixed-dimensional heterostructures. The use of graphene in photodetectors is limited because of its low optical absorption coefficient. Therefore, modifying graphene with materials having high absorption coefficients is an effective way to develop high-performance graphene-based photodetectors. Zhu *et al* [554] attached GQDs onto vertically oriented graphene (VOG), which was used to form a heterojunction with germanium. A photodetector consisting of GQDs/VOG/Ge with enhanced performance in the detection of NIR light was prepared. The improved properties of the photodetector were caused by the synergistic effect of the GQDs and VOG, which resulted in enhanced light absorption and increased electron transport. The modification of VOG with GQDs is an effective way to control the Fermi level of VOG, increase the internal electric field of the Schottky junction and promote the separation of photoinduced electron–hole pairs. Under 1550 nm light irradiation, the responsivity and detectivity of the prepared

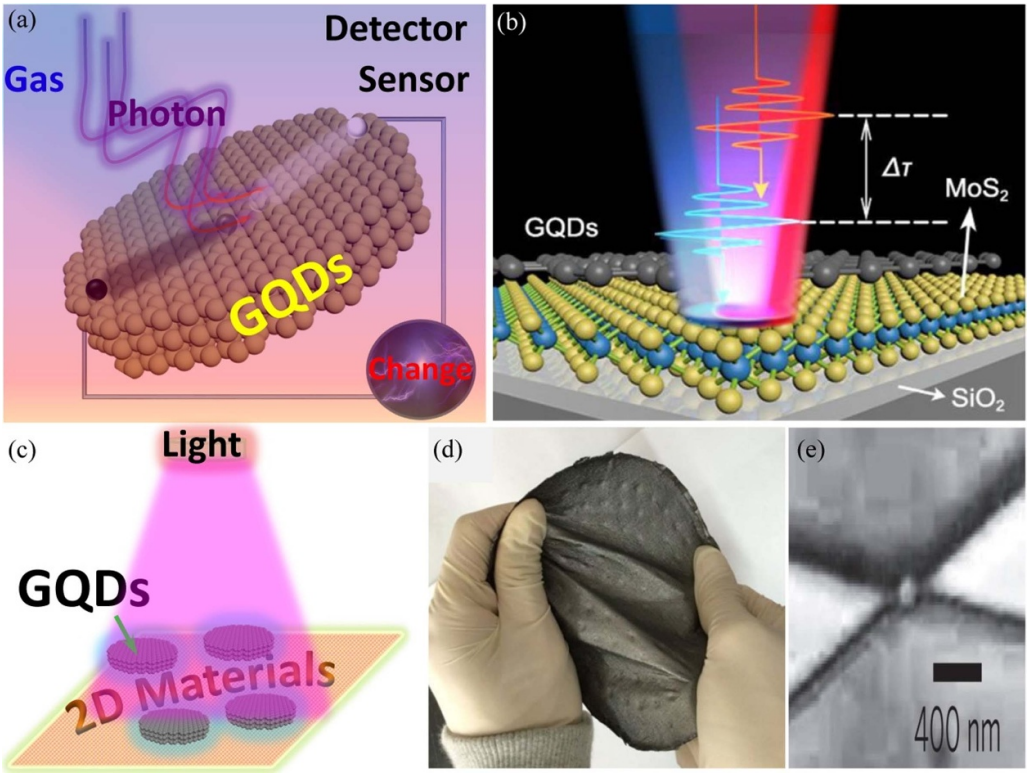

Figure 19. Applications of GQDs in photodetectors. (a) Schematic of photodetector and gas sensor based on GQDs. (b) Schematic of ultrafast pump–probe measurements in reflection configuration. The 400 nm pulse pumps the GQD/MoS_2 heterostructures, and the 650 nm probe arrives at the sample with a delay time of $\Delta\tau$. Reprinted from [551],© 2019 Elsevier Ltd. All rights reserved. (c) Schematic of the hybrid architecture of the GQD/two-dimensional material heterojunction photodetector. (d) Photograph of S,N–GQDs–rGO–cotton photodetector during twisting. Reproduced from [552], with permission from Springer Nature. (e) SEM image of a typical GQD. Reproduced from [553] with permission from Springer Nature.

devices were 1.06×10^6 A W^{-1} and 2.11×10^{14} cm $Hz^{1/2}$ W^{-1}, respectively. The use of plasmonic nanostructures is another effective way to improve the performance of photodetectors, especially in extending the response range of the detector. Thakur *et al* [555] directly synthesized gold nanoparticle/GQD nanohybrid using micro-plasmas and used it in photodetectors. Due to the plasmonic absorption of gold nanoparticles, the spectral response range of the photodetector was extended. The synergistic effect was attributed to the strong fluorescence quenching in AuNPs@GQDs combined with 2D graphene layer in the device, resulting in ultrahigh responsivity and detectivity of 10^3 A W^{-1} and 10^{13} Jones (1 Jones is equal to 1 cm $Hz^{1/2}W^{-1}$), respectively. Flexible photoelectric devices, especially wearable photoelectric detectors, have attracted much interest recently. Luo *et al* [552] prepared a flexible photodetector by spraying S-and-N-co-doped GQDs on rGO-coated cotton substrate, as shown in figure 19(d). The photodetector demonstrated high responsivity and detectivity of 0.2–1.25 A W^{-1} and 3.86×10^{10} Jones, respectively, in the broad wavelength range between UV and NIR. This can be attributed to the charge transfer between S,N-doped GQDs and rGO, resulting in the separation of the photogenerated carriers. The strong optical absorption of GQDs and the good conductivity of rGO are believed to contribute to the excellent performance of the flexible photodetector. Jang *et al* [556] reported a flexible deep UV photodetector based on GQDs sandwiched between two graphene layers on a polyethylene terephthalate substrate. The photodetector exhibited responsivity and detectivity of 0.1 A W^{-1} and 1.1×10^{13} Jones, respectively, when irradiated at a wavelength of 254 nm. Figure 19(c) shows a schematic of the photodetector based on multidimensional graphene structures. Further study on the use of a hybrid multidimensional nanostructures for photodetectors was conducted by Nguyen *et al* [378]. They prepared a high-performance photodetector based on 2D tungsten diselenide (WSe_2) coated with nitrogen-doped GQDs. The enhanced photoluminescence was due to the neutral exciton emission caused by the nitrogen-doped GQDs. In addition, the strong optical absorption of GQDs and effective charge transfer from the GQDs to 2D WSe_2 resulted in a 480% increase in photoresponsivity compared to the pristine 2D WSe_2 photodetector. It was found that the photogating effect has an important role in enhancing the performance of the multidimensional heterojunction photodetector. The luminescent downshifting effect of GQDs has been discovered for a long time. Kumbhakar *et al* [557] have taken the advantage of such an effect of graphene to improve the performance of photoconductive cells. More recently, Hasan *et al* [558] discovered that the optical properties of nitrogen-doped GQDs can change upon exposure to short- (254 nm), medium- (302 nm) and long-wave (365 nm) UV irradiation, resulting in a reduction in absorption from 200 to 320 nm and improvement beyond

320 nm. The UV treatment of the nitrogen-doped GQDs would lead to the quenching of blue and NIR fluorescence along with a substantial increase in green/yellow emission; hence, this phenomenon can be used as a potential UV sensing mechanism. The change in the optical properties was mainly attributed to the increase in the size of the nitrogen-doped GQDs driven by free radicals and the decrease in their functional groups. As the GQDs exhibit strong absorption and high sensitivity to UV radiation, they can find potential applications in UV photodetectors. In addition to their response to high-energy ultraviolet and visible bands, GQDs have also been explored for use in detecting the NIR band. El Fatimy *et al* [553] prepared GQD bolometers that demonstrated excellent performance at temperatures of up to 77 K. This is attributed to the quantum confinement of GQDs that resulted in a remarkably high variation in electrical resistance with temperature. This is also due to the intrinsic properties of graphene; for example, light absorption in graphene causes a large change in electron temperature, making graphene suitable for hot-electron bolometers in the terahertz frequency range, as shown in figure 19(e). Recently, there has been much research interest and activities in the development of GQD-based photodetectors [559–564], especially in areas, such as the use of GQD composite materials, array-type photodetectors [565], broadband detection and terahertz detectors [566]. Table 3 provides a list of the recently developed GQD-based photodetectors and their performance indicators.

GQDs have also been studied for use in gas sensors because of their zero-dimensional properties and large specific surface areas. Arunragsa *et al* [569] prepared a room-temperature ammonia gas sensor by functionalizing the edges of GQDs with hydroxyl (OH) and deposited the functionalized GQDs onto nickel interdigitated electrode, as shown in figure 20(a). The results obtained from both experimental and theoretical studies showed that the hydroxyl functional group was the main factor affecting the sensitivity and selectivity of the sensor in detecting ammonia gas, which suggests that edge functionalization of GQDs is an effective way to obtain high-performance gas sensors with excellent selectivity to target gas. Composite materials based on GQDs have been studied to improve the selectivity of gas sensors. Shao *et al* [353] loaded ZnO nanosheets with GQDs and SnO_2 nanoparticles in the preparation of a highly selective gas sensor for the detection of H_2S. The resultant gas sensor exhibited high response speed, quick response/recovery time and excellent selectivity toward H_2S, as illustrated in figure 20(b). The heterojunction between p-type GQDs and n-type SnO_2 and ZnO widened the resistance variation upon gas adsorption. Another example of using GQD-based composite materials to improve the selectivity of gas sensors was demonstrated by Purbia *et al* [570], who prepared a gas sensor based on a nitrogen-doped GQDs/SnO_2 quantum dot heterostructure for the detection of NO_2. The improved sensitivity and selectivity of the sensor can be attributed to the enhanced electron transfer between SnO_2 and the nitrogen-doped GQDs, as well as the preferential absorption of NO_2 on the GQDs. Furthermore, the 0D heterostructure provided a large specific surface area, more active sites and a better nanoscale interface, thereby improving the performance of the gas sensor. Increasing the specific surface area and electron transfer characteristics of sensing materials is a way to improve the performance of gas sensors. Lv *et al* [319] reported the modification of a three-dimensional ordered macroporous In_2O_3 with nitrogen-doped GQDs. Figures 20(c)–(f) show the SEM images of the GQD/In_2O_3 composites. The formation of a heterojunction between the three-dimensional ordered macroporous In_2O_3 and nitrogen-doped GQDs, as well as the nitrogen doping in GQDs, are believed to play vital roles in improving the sensitivity, selectivity, response/recovery time and stability of NO_2 gas sensors. The mechanism of the gas sensor is illustrated in figure 20(g). As demonstrated, GQDs have shown great potential for the development of high-performance gas sensors due to their high specificity and ease of functionalization.

5.4. Other applications

Many novel applications of GQDs are still being explored and developed, as the nanomaterials are still in the early stages of research. For example, there are reports on the application of GQDs in corrosion resistance [571–574] because GQDs tend to form complexes with other substances. Jiang *et al* [575] prepared a composite coating of nitrogen-doped GQDS and polymethyltrimethoxysilane (PMTMS) on the surface of magnesium alloy. Because of the chemical bonding of nitrogen-doped GQDs with the Mg substrate and PMTMS, the corrosion resistance performance of the composite coating was enhanced remarkably, as shown in figure 21(a). Interestingly, GQDs also have potential applications in agriculture. Xu *et al* [576] found that GQDs can be used as catalysts for the absorption of water and nutrients, as they would significantly increase the specific surface area of epidermis cells at the root surface, hence promoting plant growth. They also discovered that the size of the GQDs has an effect on plant growth; for example, large GQDs neither promoted nor inhibited plant growth, whereas GQDs with a size of 10 nm promoted plant growth, as shown in figure 21(c). Based on both experimental and theoretical studies, the mechanism by which GQDs promote plant growth is illustrated in figure 21(b). GQDs have also been explored in the preparation of micro-motor, as demonstrated by Maria-Hormigos *et al* [577] and shown in figures 20(d)–(g). Other applications of GQDs are in fuel cells as previously reported [265]. Mohamad Nor *et al* [578] prepared a proton exchange membrane for fuel cell application using cross-linked highly sulfonated polyphenylsulfone (SPPSU) membrane that comprised of GQDs. Because of the cross-linking of GQDs and SPPSU after annealing at 180 °C, the proton conductivity of the cross-linked membrane was higher than that of the pristine SPPSU membrane. Furthermore, the cross-linked membrane also exhibited excellent dimensional stability. The schematic of the proton-conductive membrane is shown in figure 21(h). In addition, there are reports on the applications of GQDs as catalysts in a new type of fuels [579, 580], which can address challenges relating to energy shortage and environmental pollution. There are many other novel applications of GQDs [581], which are of great interest. Indeed, GQDs have

Table 3. List of recent GQD-based photodetectors and their performance indicators.

Device structure	Detected wavelength (nm)	Response time (rise/fall time) (ms)	Detectivity (cm $Hz^{1/2}$ W^{-1})	Responsivity (A W^{-1})	Operating temperature (K)	Rigid/flexible	References
ZnO/GQDs/ZnO	385	0.37	1.54×10^{14}	89.3	RT	Rigid	[351]
WSe2/N-GQDs	405	—	—	2578	RT	Rigid	[378]
GQDs/VOG/Ge	1550	0.051/0.054	2.11×10^{14}	1.06×10^{6}	RT	Rigid	[554]
Au@GQDs/Gr	325–808	65/53	5.1×10^{13}	4535	—	Rigid	[553]
S,N-GQDs/rGO	300–808	—	3.86×10^{10}	0.2–1.25	—	Flexible	[555]
Gr/GQDs/Gr	256	24/17	1.1×10^{13}	0.11	RT	Flexible	[556]
CdS/N-GQDs@PVA	395	—	9×10^{13}	3	—	Rigid	[557]
N-GQDs	254–365	—	1.03×10^{11}	0.59	—	Rigid	[558]
GQDs	THz	—	—	1×10^{10} VW^{-1}	6	Rigid	[553]
N-GQDs	1550	0.05/0.053	1.3×10^{10}	0.058	—	Rigid	[559]
GQDs/n-Si	300–1100	—	—	3.5	—	Rigid	[560]
ZnO/GQDs	365	—	3.5×10^{7}	0.14	RT	Rigid	[563]
GQDs	1064	—	—	0.96×10^{-3}	533	Rigid	[565]
GQDs	THz	—	—	—	0.17	Rigid	[566]
ZnO/GQDs/Poly-TPD	365	$0.37 \times 10^{-3}/0.78 \times 10^{-3}$	2×10^{11}	0.56	—	Rigid	[567]
GQDs/ZnO/GaN	200–800	159/68.7	7×10^{11}	3.2×10^{3}	—	Rigid	[568]

Note: PVA, poly(vinyl alcohol); poly-TPD, poly(*NN′-bis*-4-butylphenyl-*N*,*N′*-bisphenyl)benzidine.

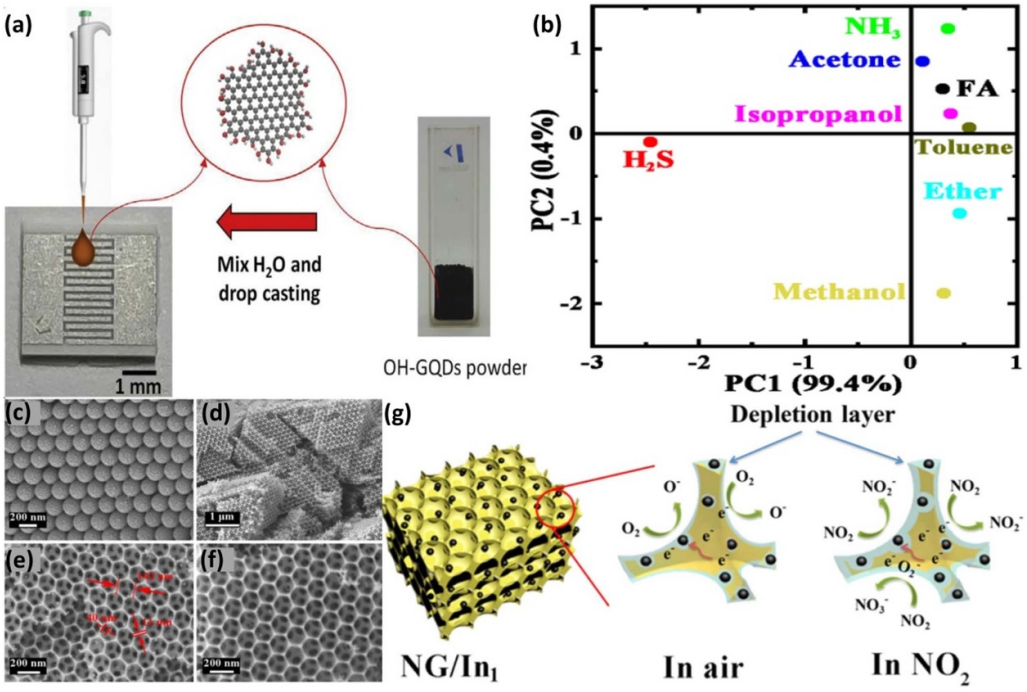

Figure 20. Applications of GQDs in gas sensors. (a) Schematic of the fabrication process of OH-GQD gas sensors. Reprinted from [569], © 2020 Elsevier B.V. All rights reserved. (b) Pattern recognition based on the principal component analysis method to show the selectivity of the GQD−SnO_2/ZnO sensor. Reprinted with permission from [353]. Copyright (2020) American Chemical Society. (c–f) SEM images of (c) PS microspheres, (d), (e), (f) three-dimensional ordered macroporous In_2O_3 under different magnifications and (g) N-GQDs/In_1. Reprinted with permission from [319]. Copyright (2020) American Chemical Society.

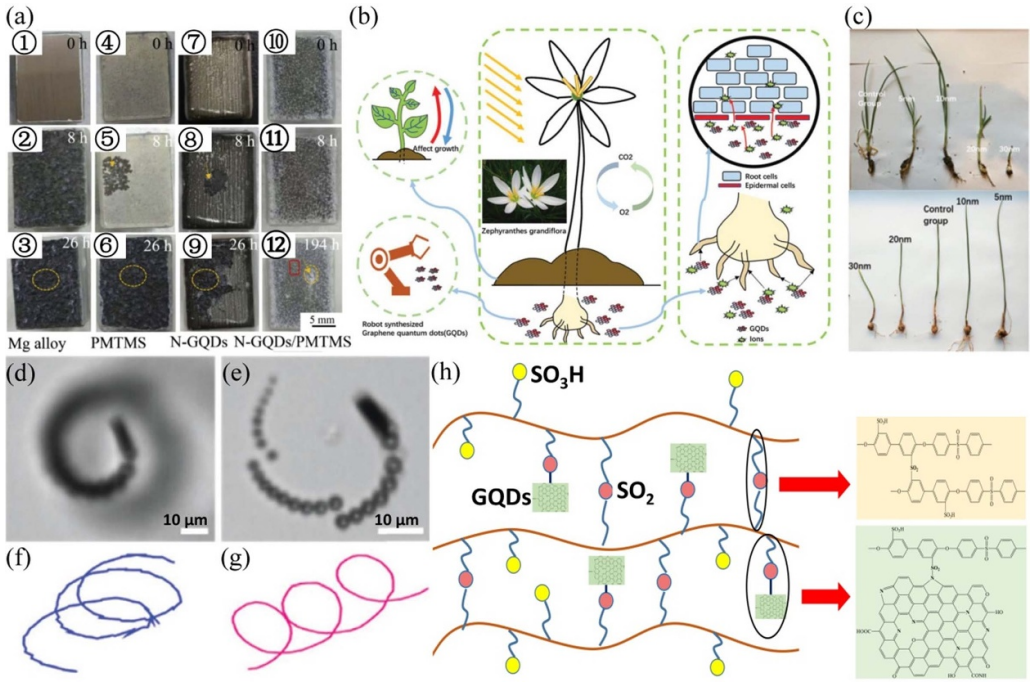

Figure 21. Other applications of GQDs. (a) Surface morphologies of the samples with different coatings before and after immersion tests in 3.5 wt% NaCl. Bare Mg alloy (①), PMTMS (④), N-GQDs (⑦) and N-GQDs/PMTMS specimens (⑩); (②, ⑤, ⑧, ⑪) corresponding specimens of (①, ④, ⑦, ⑩) after immersing 8 h; bare Mg alloy (③), PMTMS (⑥) and N-GQD (⑨) specimens after immersing 26 h; N-GQD/PMTMS specimen after immersing 194 h (⑫). Reprinted from [575], © 2019 Elsevier Ltd. All rights reserved. (b) Mechanism of the influence of GQDs on the growth of *Zephyranthes grandiflora* with ions and GQDs attached to the surfaces of the epidermal cells. (c) Photographs of (top) shallots and (bottom) *Zephyranthes. grandiflora* treated with GQDs having dimensions of 5, 10, 20 and 30 nm. Reproduced from [576] with permission from the Royal Society of Chemistry. (d)–(g) Time-lapse images (taken from Video S3, ESI†) and the corresponding trajectories of GQD micromotors moving in 1% and 2% peroxide solutions. Reproduced from [577] with permission from the Royal Society of Chemistry. (h) Schematic of cross-linked GQDs with high SPPSU as proton exchange membranes for fuel cell applications. Reprinted from [578], © 2020 Hydrogen Energy Publications LLC. Published by Elsevier Ltd. All rights reserved.

many important and wide-ranging applications that warrant our attention.

6. Conclusions

The essential properties of GQDs include quantum confinement and edge effects. While GQDs inherit many properties of graphene, they also exhibit strong fluorescence characteristics, strong optical absorption and excellent solubility. As an emerging member of the carbon material family, GQDs have many advantages over other carbon materials, such as biocompatibility, low toxicity and environmental friendliness. In this review, the unique properties of zero-dimensional GQDs are described in detail and compared to those of different low-dimensional carbon materials. From the perspective of GQD preparation, there are many different preparation methods of GQDs, which can be divided into three main categories: top-down, bottom-up and chemical methods. These methods were compared according to the size, functionalization, cost of production and other aspects of GQDs. The electrical, optical, magnetic, thermal and other properties of GQDs were also discussed in detail. Some of these properties can be controlled by the functionalization of GQDs, which has attracted much attention and has therefore been an important part of this review. This includes the introduction of impurity atoms and the formation of composites with other substances to modify the properties of GQDs. The excellent properties of GQDs and their composite materials have led to numerous exciting and wide-ranging applications in many different fields, such as biomedicine, energy, optoelectronics, agriculture and other emerging areas. The widespread applications of GQDs demonstrate their great variety of functionalities. As researchers continue to discover new properties of GQDs, novel applications based on the nanomaterials will continue to emerge. This review on the recent development of GQDs provides an important insight into the future research directions and applications of GQDs. It also provides a summary of recent research achievements of GQDs.

7. Future perspectives

The rapid development of GQDs is mainly due to their many potential applications in a wide variety of fields, such as biomedicine, sensors, optoelectronics, agriculture, environmental protection and robotics. In this section, future research directions and applications of GQDs are highlighted based on their unique characteristics and functions. The preparation technique of GQDs is the key to their application. Unlike other quantum dots, GQDs are nontoxic; hence, they have great potential for important applications in biomedical and

environmental protection. However, many preparation techniques for GQDs require the use of toxic chemical reagents. Therefore, further research on the preparation of GQDs using green and environmentally friendly techniques is crucial for the future application of GQDs. The application of GQDs in optoelectronics is still in its initial stage. At present, the application of GQDs in optoelectronics has two main problems: ability to prepare high-quality GQD films and ability to broaden the response wavelength of GQDs without losing their quantum confinement effect. To overcome the aforementioned problems, there is a need to perform in-depth research on the edge and quantum confinement effects of GQDs. In addition, only a few studies have investigated the electrical and magnetic properties of GQDs. Further research on GQDs can effectively develop more applications in emerging fields, such as the application of GQDs in solar cells and energy generation.

Acknowledgments

This work was supported by the National Natural Science Foundation of China (Grant Nos. 61106098, 51201150 and 11374250), Key Project of Applied Basic Research of Yunnan Province, China (Grant No. 2012FA003), PolyU Grant (1-ZVGH) and Research Grants Council of Hong Kong (Project Nos. PolyU 153030/15P and PolyU 153271/16P).

ORCID iD

Libin Tang https://orcid.org/0000-0002-7174-2963

References

[1] Novoselov K S, Geim A K, Morozov S V, Jiang D, Zhang Y, Dubonos S V, Grigorieva I V and Firsov A A 2004 Electric field effect in atomically thin carbon films *Science* **306** 666–9
[2] Novoselov K S, Fal′ko V I, Colombo L, Gellert P R, Schwab M G and Kim K 2012 A roadmap for graphene *Nature* **490** 192–200
[3] Zhang Y, Tan Y-W, Stormer H L and Kim P 2005 Experimental observation of the quantum Hall effect and Berry's phase in graphene *Nature* **438** 201–4
[4] Balandin A A, Ghosh S, Bao W, Calizo I, Teweldebrhan D, Miao F and Lau C N 2008 Superior thermal conductivity of single-layer graphene *Nano Lett.* **8** 902–7
[5] Lee C, Wei X, Kysar J W and Hone J 2008 Measurement of the elastic properties and intrinsic strength of monolayer graphene *Science* **321** 385–8
[6] Geim A K and Novoselov K S 2007 The rise of graphene *Nat. Mater.* **6** 183–91
[7] Castro Neto A H, Guinea F, Peres N M R, Novoselov K S and Geim A K 2009 The electronic properties of graphene *Rev. Mod. Phys.* **81** 109–62
[8] Geim A K 2009 Graphene: status and prospects *Science* **324** 1530–4
[9] Kroto H W, Heath J R, O'Brien S C, Curl R F and Smalley R E 1985 C60: buckminsterfullerene *Nature* **318** 162–3
[10] Kunz G F 1884 Five brazilian diamonds *Science* **3** 649–50
[11] Gao J, Niu J, Qin S and Wu X 2016 Ultradeep diamonds originate from deep subducted sedimentary carbonates *Sci. China Earth Sci.* **60** 207–17
[12] Szunerits S and Boukherroub R 2007 Different strategies for functionalization of diamond surfaces *J. Solid State Electrochem.* **12** 1205–18
[13] Wu B R 2007 Structural and vibrational properties of the 6H diamond: first-principles study *Diam. Relat. Mater.* **16** 21–28
[14] Chen X, Huang G, Tan Y, Yu Y, Guo H and Xu X 2018 Percent reduction in transverse rupture strength of metal matrix diamond segments analysed via discrete-element simulations *Materials* **11** 1048
[15] Wang X-G and Smith J R 2001 Copper/diamond adhesion and hydrogen termination *Phys. Rev. Lett.* **87** 186103
[16] Gracio J J, Fan Q H and Madaleno J C 2010 Diamond growth by chemical vapour deposition *J. Phys. D: Appl. Phys.* **43** 374017
[17] Shibata T, Kitamoto Y, Unno K and Makino E 2000 Micromachining of diamond film for MEMS applications *J. Microelectromech. Syst.* **9** 47–51
[18] Robertson J 2002 Diamond-like amorphous carbon *Mater. Sci. Eng.* R **37** 129–281
[19] Jian-Bing Z, Yan-Hui W and Liang D 2017 Recent progress in diamond-based electrocatalysts for fuel cells *J. Inorg. Mater.* **32** 673–80
[20] Mochalin V N, Shenderova O, Ho D and Gogotsi Y 2011 The properties and applications of nanodiamonds *Nat. Nanotechnol.* **7** 11–23
[21] Huang Q *et al* 2014 Nanotwinned diamond with unprecedented hardness and stability *Nature* **510** 250–3
[22] Vetter J 2014 60 years of DLC coatings: historical highlights and technical review of cathodic arc processes to synthesize various DLC types, and their evolution for industrial applications *Surf. Coat. Technol.* **257** 213–40
[23] Robertson J 1991 Hard amorphous (diamond-like) carbon *Prog. Solid State Chem.* **21** 199–333
[24] Shakun A, Vuorinen J, Hoikkanen M, Poikelispää M and Das A 2014 Hard nanodiamonds in soft rubbers: past, present and future–a review *Composites* A **64** 49–69
[25] Robertson J 1992 Properties of diamond-like carbon *Surf. Coat. Technol.* **50** 185–203
[26] Wang L, Xia Y, Zhang M, Fang Z and Shi W 2004 The influence of deposition conditions on the dielectric properties of diamond films *Semicond. Sci. Technol.* **19** L35–L8
[27] Wang Z L, Li J J, Sun Z H, Li Y L, Luo Q, Gu C Z and Cui Z 2007 Effect of grain size and pores on the dielectric constant of nanocrystalline diamond films *Appl. Phys. Lett.* **90** 133118
[28] Grill A 1999 Electrical and optical properties of diamond-like carbon *Thin Solid Films* **355** 189–93
[29] Demichelis F, Pirri C F and Tagliaferro A 1992 Evaluation of the $[C(sp^3)]/[C(sp^2)]$ ratio in diamondlike films through the use of a complex dielectric constant *Phys. Rev.* B **45** 14364–70
[30] Volksen W, Miller R D and Dubois G 2010 Low dielectric constant materials *Chem. Rev.* **110** 56–110
[31] Iijima S 1991 Helical microtubles of graphitic carbon *Nature* **354** 56–58
[32] Horton M, Hong H, Li C, Shi B, Peterson G P and Jin S 2010 Magnetic alignment of Ni-coated single wall carbon nanotubes in heat transfer nanofluids *J. Appl. Phys.* **107** 104320
[33] Baughman R H, Zakhidov A A and de Heer W A 2002 Carbon nanotubes—the route toward applications *Science* **297** 787–92
[34] Thess A *et al* 1996 Crystalline ropes of metallic carbon nanotubes *Science* **273** 483–7

[35] De Volder M F L, Tawfick S H, Baughman R H and Hart A J 2013 Carbon nanotubes: present and future commercial applications *Science* **339** 535–9

[36] Wilder Jeroen W G, Venema L C, Rinzler A G, Smalley R E and Dekker C 1998 Electronic structure of atomically resolved carbon nanotubes *Nature* **391** 59–62

[37] Bachilo S M, Strano M S, Kittrell C, Hauge R H, Smalley R E and Weisman R B 2002 Structure-assigned optical spectra of single-walled carbon nanotubes *Science* **298** 2361–6

[38] Sfeir M Y *et al* 2006 Optical spectroscopy of individual single-walled carbon nanotubes of defined chiral structure *Science* **312** 554–6

[39] Strano M S 2003 Probing chiral selective reactions using a revised kataura plot for the interpretation of single-walled carbon nanotube spectroscopy *J. Am. Chem. Soc.* **125** 16148–53

[40] O'Connell M J, Eibergen E E and Doorn S K 2005 Chiral selectivity in the charge-transfer bleaching of single-walled carbon-nanotube spectra *Nat. Mater.* **4** 412–8

[41] Cambré S, Schoeters B, Luyckx S, Goovaerts E and Wenseleers W 2010 Experimental observation of single-file water filling of thin single-wall carbon nanotubes down to chiral index (5,3) *Phys. Rev. Lett.* **104** 207401

[42] Bachtold A, Strunk C, Salvetat J-P, Bonard J-M, Forró L, Nussbaumer T and Schönenberger C 1999 Aharonov–Bohm oscillations in carbon nanotubes *Nature* **397** 673–5

[43] Lebedeva O S, Lebedev N G and Lyapkosova I A 2020 Effect of isomorphic impurities on the elastic conductivity of chiral carbon nanotubes *Russ. J. Phys. Chem.* A **94** 1647–56

[44] Takakura A, Beppu K, Nishihara T, Fukui A, Kozeki T, Namazu T, Miyauchi Y and Itami K 2019 Strength of carbon nanotubes depends on their chemical structures *Nat. Commun.* **10** 3040

[45] Sam A, K. V P and Sathian S P 2019 Water flow in carbon nanotubes: the role of tube chirality *Phys. Chem. Chem. Phys.* **21** 6566–73

[46] Gifford B J, Saha A, Weight B M, He X, Ao G, Zheng M, Htoon H, Kilina S, Doorn S K and Tretiak S 2019 Mod(n-m,3) dependence of defect-State emission bands in aryl-functionalized carbon nanotubes *Nano Lett.* **19** 8503–9

[47] Novoselov K S, Geim A K, Morozov S V, Jiang D, Katsnelson M I, Grigorieva I V, Dubonos S V and Firsov A A 2005 Two-dimensional gas of massless Dirac fermions in graphene *Nature* **438** 197–200

[48] Volovik G E and Pudalov V M 2016 Graphite on graphite *JETP Lett.* **104** 880–2

[49] Zhu J, Wang X, Guo L, Wang Y, Wang Y, Yu M and Lau K-T 2007 A graphite foam reinforced by graphite particles *Carbon* **45** 2547–50

[50] Chattopadhyay J, Mukherjee A, Hamilton C E, Kang J, Chakraborty S, Guo W, Kelly K F, Barron A R and Billups W E 2008 Graphite epoxide *J. Am. Chem. Soc.* **130** 5414–5

[51] Hu Y *et al* 2020 An ultraviolet photoelectron spectroscopy study on bandgap broadening of epitaxial graphene on SiC with surface doping *Carbon* **157** 340–9

[52] Craciun M F, Russo S, Yamamoto M and Tarucha S 2011 Tuneable electronic properties in graphene *Nano Today* **6** 42–60

[53] Zhao X-J *et al* 2019 Molecular bilayer graphene *Nat. Commun.* **10** 10

[54] Jung W R, Choi J H, Lee N, Shin K, Moon J-H and Seo Y-S 2012 Reduced damage to carbon nanotubes during ultrasound-assisted dispersion as a result of supercritical-fluid treatment *Carbon* **50** 633–6

[55] Zhang H W, Zhang Z Q and Wang L 2009 Molecular dynamics simulations of electrowetting in double-walled carbon nanotubes *Curr. Appl. Phys.* **9** 750–4

[56] Park D, Kim Y H and Lee J K 2003 Synthesis of carbon nanotubes on metallic substrates by a sequential combination of PECVD and thermal CVD *Carbon* **41** 1025–9

[57] Han M Y, Özyilmaz B, Zhang Y and Kim P 2007 Energy band-gap engineering of graphene nanoribbons *Phys. Rev. Lett.* **98** 206805

[58] Aigner S, Pietra L D, Japha Y, Entin-Wohlman O, David T, Salem R, Folman R and Schmiedmayer J 2008 Chemically derived, ultrasmooth graphene nanoribbon semiconductors *Science* **319** 1226–9

[59] Son Y-W, Cohen M L and Louie S G 2006 Energy gaps in graphene nanoribbons *Phys. Rev. Lett.* **97** 216803

[60] Son Y-W, Cohen M L and Louie S G 2006 Half-metallic graphene nanoribbons *Nature* **444** 347–9

[61] Lu J P and Yang W 1994 Shape of large single- and multiple-shell fullerenes *Phys. Rev.* B **49** 11421–4

[62] Pinto Y, Fowler P W, Mitchell D and Avnir D 1998 Continuous chirality analysis of model stone-wales rearrangements in fullerenes *J. Phys. Chem.* B **102** 5776–84

[63] Rašović I 2016 Water-soluble fullerenes for medical applications *Mater. Sci. Technol.* **33** 777–94

[64] Krätschmer W 2011 The story of making fullerenes *Nanoscale* **3** 2485

[65] Varma C M, Zaanen J and Raghavachari K 1991 Superconductivity in the fullerenes *Science* **254** 989–92

[66] Qian Z, Ma J, Shan X, Shao L, Zhou J, Chen J and Feng H 2013 Surface functionalization of graphene quantum dots with small organic molecules from photoluminescence modulation to bioimaging applications: an experimental and theoretical investigation *RSC Adv.* **3** 14571

[67] Ahmed S R, Kumar S, Ortega G A, Srinivasan S and Rajabzadeh A R 2021 Target specific aptamer-induced self-assembly of fluorescent graphene quantum dots on palladium nanoparticles for sensitive detection of tetracycline in raw milk *Food Chem.* **346** 128893

[68] Mirzakhani M, Zarenia M, Ketabi S A, da Costa D R and Peeters F M 2016 Energy levels of hybrid monolayer-bilayer graphene quantum dots *Phys. Rev.* B **93** 165410

[69] Häusler W and Egger R 2009 Artificial atoms in interacting graphene quantum dots *Phys. Rev.* B **80**

[70] Ryu J, Lee E, Lee S and Jang J 2014 Fabrication of graphene quantum dot-decorated graphene sheets via chemical surface modification *Chem. Commun.* **50** 15616–8

[71] Fan X 2015 Graphene: a promising two-dimensional support for heterogeneous catalysts *Front. Mater.* **1** 39

[72] Galvão N, Vasconcelos G, Pessoa R, Machado J, Guerino M, Fraga M, Rodrigues B, Camus J, Djouadi A and Maciel H 2018 A novel method of synthesizing graphene for electronic device applications *Materials* **11** 1120

[73] Yang J, Hu P and Yu G 2019 Perspective of graphene-based electronic devices: graphene synthesis and diverse applications *APL Mater.* **7** 20901

[74] Zhang X, Wang Y, Luo G and Xing M 2019 Two-dimensional graphene family material: assembly, biocompatibility and sensors applications *Sensors* **19** 2966

[75] Dai B, Fu L, Zou Z, Wang M, Xu H, Wang S and Liu Z 2011 Rational design of a binary metal alloy for chemical vapour deposition growth of uniform single-layer graphene *Nat. Commun.* **2** 522

[76] Bourdo S E, Al Faouri R, Sleezer R, Nima Z A, Lafont A, Chhetri B P, Benamara M, Martin B, Salamo G J and

Biris A S 2017 Physicochemical characteristics of pristine and functionalized graphene *J. Appl. Toxicol.* **37** 1288–96
[77] Cao M-S, Wang X-X, Cao W-Q and Yuan J 2015 Ultrathin graphene: electrical properties and highly efficient electromagnetic interference shielding *J. Mater. Chem.* C **3** 6589–99
[78] Ago H, Fukamachi S, Endo H, Solís-Fernández P, Mohamad Yunus R, Uchida Y, Panchal V, Kazakova O and Tsuji M 2016 Visualization of grain structure and boundaries of polycrystalline graphene and two-dimensional materials by epitaxial growth of transition metal dichalcogenides *ACS Nano* **10** 3233–40
[79] Cao Y, Fatemi V, Fang S, Watanabe K, Taniguchi T, Kaxiras E and Jarillo-Herrero P 2018 Unconventional superconductivity in magic-angle graphene superlattices *Nature* **556** 43–50
[80] Lu X *et al* 2019 Superconductors, orbital magnets and correlated states in magic-angle bilayer graphene *Nature* **574** 653–7
[81] Kerelsky A *et al* 2019 Maximized electron interactions at the magic angle in twisted bilayer graphene *Nature* **572** 95–100
[82] Konstantatos G, Badioli M, Gaudreau L, Osmond J, Bernechea M, de Arquer F P G, Gatti F and Koppens F H L 2012 Hybrid graphene–quantum dot phototransistors with ultrahigh gain *Nat. Nanotechnol.* **7** 363–8
[83] Liu C-H, Chang Y-C, Norris T B and Zhong Z 2014 Graphene photodetectors with ultra-broadband and high responsivity at room temperature *Nat. Nanotechnol.* **9** 273–8
[84] Sun Z, Liu Z, Li J, a G-A, Lau S-P and Yan F 2012 Infrared photodetectors based on CVD-grown graphene and PbS quantum dots with ultrahigh responsivity *Adv. Mater.* **24** 5878–83
[85] Yang K, Zhang S, Zhang G, Sun X, Lee S-T and Liu Z 2010 Graphene in mice: ultrahigh in vivo tumor uptake and efficient photothermal therapy *Nano Lett.* **10** 3318–23
[86] Lee H *et al* 2016 A graphene-based electrochemical device with thermoresponsive microneedles for diabetes monitoring and therapy *Nat. Nanotechnol.* **11** 566–72
[87] Shen H, Zhang L, Liu M and Zhang Z 2012 Biomedical applications of graphene *Theranostics* **2** 283–94
[88] Pumera M 2011 Graphene in biosensing *Mater. Today* **14** 308–15
[89] Zhang Y, Ali S F, Dervishi E, Xu Y, Li Z, Casciano D and Biris A S 2010 Cytotoxicity effects of graphene and single-wall carbon nanotubes in neural phaeochromocytoma-derived PC12 cells *ACS Nano* **4** 3181–6
[90] Chen Y, Tan C, Zhang H and Wang L 2015 Two-dimensional graphene analogues for biomedical applications *Chem. Soc. Rev.* **44** 2681–701
[91] Tian P, Tang L, Teng K S, Xiang J and Lau S P 2019 Recent advances in graphene homogeneous p–n junction for optoelectronics *Adv. Mater. Technol.* **4** 1900007
[92] Li L, Zhang D, Deng J, Fang J and Gou Y 2020 Review—preparation and application of graphene-based hybrid materials through electrochemical exfoliation *J. Electrochem. Soc.* **167** 086511
[93] Chen Y, Gong X-L and Gai J-G 2016 Progress and challenges in transfer of large-area graphene films *Adv. Sci.* **3** 1500343
[94] Lin L, Peng H and Liu Z 2019 Synthesis challenges for graphene industry *Nat. Mater.* **18** 520–4
[95] Liao L and Duan X 2012 Graphene for radio frequency electronics *Mater. Today* **15** 328–38
[96] Ponomarenko L A, Schedin F, Katsnelson M I, Yang R, Hill E W, Novoselov K S and Geim A K 2008 Chaotic dirac billiard in graphene quantum dots *Science* **320** 356–8
[97] Pan D, Zhang J, Li Z and Wu M 2010 Hydrothermal route for cutting graphene sheets into blue-luminescent graphene quantum dots *Adv. Mater.* **22** 734–8
[98] Li Y, Zhao Y, Cheng H, Hu Y, Shi G, Dai L and Qu L 2012 Nitrogen-doped graphene quantum dots with oxygen-rich functional groups *J. Am. Chem. Soc.* **134** 15–18
[99] Peng J *et al* 2012 Graphene quantum dots derived from carbon fibers *Nano Lett.* **12** 844–9
[100] Tang L *et al* 2012 Deep ultraviolet photoluminescence of water-soluble self-passivated graphene quantum dots *ACS Nano* **6** 5102–10
[101] Tian P, Tang L, Teng K S and Lau S P 2018 Graphene quantum dots from chemistry to applications *Mater. Today Chem.* **10** 221–58
[102] Shen J, Zhu Y, Yang X and Li C 2012 Graphene quantum dots: emergent nanolights for bioimaging, sensors, catalysis and photovoltaic devices *Chem. Commun.* **48** 3686
[103] Yan Y, Gong J, Chen J, Zeng Z, Huang W, Pu K, Liu J and Chen P 2019 Recent advances on graphene quantum dots: from chemistry and physics to applications *Adv. Mater.* **31** 1808283
[104] Haque E, Kim J, Malgras V, Reddy K R, Ward A C, You J, Bando Y, Hossain M S A and Yamauchi Y 2018 Recent advances in graphene quantum dots: synthesis, properties, and applications *Small Methods* **2** 1800050
[105] Bacon M, Bradley S J and Nann T 2013 Graphene quantum dots *Part. Part. Syst. Charact.* **31** 415–28
[106] Li L, Wu G, Yang G, Peng J, Zhao J and Zhu J-J 2013 Focusing on luminescent graphene quantum dots: current status and future perspectives *Nanoscale* **5** 4015–39
[107] Sun H, Wu L, Wei W and Qu X 2013 Recent advances in graphene quantum dots for sensing *Mater. Today* **16** 433–42
[108] Du Y and Guo S 2016 Chemically doped fluorescent carbon and graphene quantum dots for bioimaging, sensor, catalytic and photoelectronic applications *Nanoscale* **8** 2532–43
[109] Gan Z, Xu H and Hao Y 2016 Mechanism for excitation-dependent photoluminescence from graphene quantum dots and other graphene oxide derivates: consensus, debates and challenges *Nanoscale* **8** 7794–807
[110] Liu Q, Guo B, Rao Z, Zhang B and Gong J R 2013 Strong two-photon-induced fluorescence from photostable, biocompatible nitrogen-doped graphene quantum dots for cellular and deep-tissue imaging *Nano Lett.* **13** 2436–41
[111] Iannazzo D, Pistone A, Salamò M, Galvagno S, Romeo R, Giofré S V, Branca C, Visalli G and Di Pietro A 2017 Graphene quantum dots for cancer targeted drug delivery *Int. J. Pharm.* **518** 185–92
[112] Zheng B, Chen Y, Li P, Wang Z, Cao B, Qi F, Liu J, Qiu Z and Zhang W 2017 Ultrafast ammonia-driven, microwave-assisted synthesis of nitrogen-doped graphene quantum dots and their optical properties *Nanophotonics* **6** 259–67
[113] Zhu S, Song Y, Wang J, Wan H, Zhang Y, Ning Y and Yang B 2017 Photoluminescence mechanism in graphene quantum dots: quantum confinement effect and surface/edge state *Nano Today* **13** 10–14
[114] Niu X, Li Y, Shu H and Wang J 2016 Revealing the underlying absorption and emission mechanism of nitrogen doped graphene quantum dots *Nanoscale* **8** 19376–82
[115] Qian F, Li X, Tang L, Lai S K, Lu C and Lau S P 2016 Potassium doping: tuning the optical properties of graphene quantum dots *AIP Adv.* **6** 75116

[116] Sierański K and Szatkowski J 2015 Substitutional impurity in the graphene quantum dots *Physica* E **73** 40–44
[117] Li L-L, Liu K-P, Yang G-H, Wang C-M, Zhang J-R and Zhu J-J 2011 Fabrication of graphene–quantum dots composites for sensitive electrogenerated chemiluminescence immunosensing *Adv. Funct. Mater.* **21** 869–78
[118] Geng X *et al* 2010 Aqueous-processable noncovalent chemically converted graphene-quantum dot composites for flexible and transparent optoelectronic films *Adv. Mater.* **22** 638–42
[119] Zhou Y, Qu Z-B, Zeng Y, Zhou T and Shi G 2014 A novel composite of graphene quantum dots and molecularly imprinted polymer for fluorescent detection of paranitrophenol *Biosens. Bioelectron.* **52** 317–23
[120] Liu W, Yan X, Chen J, Feng Y and Xue Q 2013 Novel and high-performance asymmetric micro-supercapacitors based on graphene quantum dots and polyaniline nanofibers *Nanoscale* **5** 6053–62
[121] Pan D, Jiao J, Li Z, Guo Y, Feng C, Liu Y, Wang L and Wu M 2015 Efficient separation of electron–hole pairs in graphene quantum dots by TiO_2 heterojunctions for dye degradation *ACS Sustain. Chem. Eng.* **3** 2405–13
[122] Zhou X, Ma P, Wang A, Yu C, Qian T, Wu S and Shen J 2015 Dopamine fluorescent sensors based on polypyrrole/graphene quantum dots core/shell hybrids *Biosens. Bioelectron.* **64** 404–10
[123] Kaur M, Kaur M and Sharma V K 2018 Nitrogen-doped graphene and graphene quantum dots: a review onsynthesis and applications in energy, sensors and environment *Adv. Colloid Interface Sci.* **259** 44–64
[124] Chakravarty D, Erande M B and Late D J 2015 Graphene quantum dots as enhanced plant growth regulators: effects on coriander and garlic plants *J. Sci. Food Agric.* **95** 2772–8
[125] Iravani S and Varma R S 2020 Green synthesis, biomedical and biotechnological applications of carbon and graphene quantum dots. A review *Environ. Chem. Lett.* **18** 703–27
[126] El Fatimy A, Nath A, Kong B D, Boyd A K, Myers-Ward R L, Daniels K M, Jadidi M M, Murphy T E, Gaskill D K and Barbara P 2018 Ultra-broadband photodetectors based on epitaxial graphene quantum dots *Nanophotonics* **7** 735–40
[127] Chu X, Wang J, Zhang J, Dong Y, Sun W, Zhang W and Bai L 2017 Preparation and gas-sensing properties of SnO_2/graphene quantum dots composites via solvothermal method *J. Mater. Sci.* **52** 9441–51
[128] Zeng Z, Chen S, Tan T T Y and Xiao F-X 2018 Graphene quantum dots (GQDs) and its derivatives for multifarious photocatalysis and photoelectrocatalysis *Catal. Today* **315** 171–83
[129] Lawal A T 2019 Graphene-based nano composites and their applications. A review *Biosens. Bioelectron.* **141** 111384
[130] Kundu S, Yadav R M, Narayanan T N, Shelke M V, Vajtai R, Ajayan P M and Pillai V K 2015 Synthesis of N, F and S co-doped graphene quantum dots *Nanoscale* **7** 11515–9
[131] Bak S, Kim D and Lee H 2016 Graphene quantum dots and their possible energy applications: a review *Curr. Appl. Phys.* **16** 1192–201
[132] Geng D, Wang H, Wan Y, Xu Z, Luo B, Xu J and Yu G 2015 Direct top-down fabrication of large-area graphene arrays by an in situ etching method *Adv. Mater.* **27** 4195–9
[133] Jovanović S P, Marković Z M, Syrgiannis Z, Dramićanin M D, Arcudi F, Parola V L, Budimir M D and Marković B M T 2017 Enhancing photoluminescence of graphene quantum dots by thermal annealing of the graphite precursor *Mater. Res. Bull.* **93** 183–93
[134] Luo P, Guan X, Yu Y and Li X 2017 New insight into electrooxidation of graphene into graphene quantum dots *Chem. Phys. Lett.* **690** 129–32
[135] Zhao Y, Wu X, Sun S, Ma L, Zhang L and Lin H 2017 A facile and high-efficient approach to yellow emissive graphene quantum dots from graphene oxide *Carbon* **124** 342–7
[136] Lin L and Zhang S 2012 Creating high yield water soluble luminescent graphene quantum dots via exfoliating and disintegrating carbon nanotubes and graphite flakes *Chem. Commun.* **48** 10177
[137] Lu J, Yeo P S E, Gan C K, Wu P and Loh K P 2011 Transforming C60 molecules into graphene quantum dots *Nat. Nanotechnol.* **6** 247–52
[138] Kang S, Jeong Y K, Ryu J H, Son Y, Kim W R, Lee B, Jung K H and Kim K M 2020 Pulsed laser ablation based synthetic route for nitrogen-doped graphene quantum dots using graphite flakes *Appl. Surf. Sci.* **506** 144998
[139] Alidad F, Navik R, Gai Y and Zhao Y 2018 Production of pristine graphene quantum dots from graphite by a shear-mixer in supercritical CO_2 *Chem. Phys. Lett.* **710** 64–69
[140] Yang F *et al* 2020 Nitrogen-doped graphene quantum dots prepared by electrolysis of nitrogen-doped nanomesh graphene for the fluorometric determination of ferric ions *Microchim. Acta* **187** 1–10
[141] Chen Y-X, Lu D, Wang G-G, Huangfu J, Wu Q-B, Wang X-F, Liu L-F, Ye D-M, Yan B and Han J 2020 Highly efficient orange emissive graphene quantum dots prepared by acid-free method for white LEDs *ACS Sustain. Chem. Eng.* **8** 6657–66
[142] Kang S, Jeong Y K, Jung K H, Son Y, Choi S-C, An G S, Han H and Kim K M 2019 Simple preparation of graphene quantum dots with controllable surface states from graphite *RSC Adv.* **9** 38447–53
[143] Ten K A, Aulchenko V M, Lukjanchikov L A, Pruuel E R, Shekhtman L I, Tolochko B P, Zhogin I L and Zhulanov V V 2009 Application of introduced nano-diamonds for the study of carbon condensation during detonation of condensed explosives *Nucl. Instrum. Methods Phys. Res.* A **603** 102–4
[144] Ramezani H and Mansoori G A 2007 *Nature* 44–47
[145] Xu K and Xue Q 2007 Deaggregation of ultradispersed diamond from explosive detonation by a graphitization–oxidation method and by hydroiodic acid treatment *Diam. Relat. Mater.* **16** 277–82
[146] Abdullahi I M, Langenderfer M, Shenderova O, Nunn N, Torelli M D, Johnson C E and Mochalin V N 2020 Explosive fragmentation of luminescent diamond particles *Carbon* **164** 442–50
[147] He Z, Huang H, Jiang R, Mao L, Liu M, Chen J, Deng F, Zhou N, Zhang X and Wei Y 2020 Click multiwalled carbon nanotubes: a novel method for preparation of carboxyl groups functionalized carbon quantum dots *Mater. Sci. Eng.* C **108** 110376
[148] Qiang R, Hou K, Wang J and Yang S 2020 Smooth and dense graphene quantum dots-based lubricating coatings prepared by electrophoretic deposition *Appl. Surf. Sci.* **509** 145338
[149] Chu K, Adsetts J R, He S, Zhan Z, Yang L, Wong J M, Love D A and Ding Z 2020 Electrogenerated chemiluminescence and electroluminescence of N-doped graphene quantum dots fabricated from an electrochemical exfoliation process in nitrogen-containing electrolytes *Chem. Eur. J.* **26** 15892–900
[150] Hadad C *et al* 2020 Graphene quantum dots: from efficient preparation to safe renal excretion *Nano Res.* **14** 674–83
[151] Xu H, Zhou S, Fang W and Fan Y 2020 Synthesis of N-doped graphene quantum dots from bulk N-doped

carbon nanofiber film for fluorescence detection of Fe^{3+} and ascorbic acid *Fuller. Nanotub. Carbon Nanostruct.* **29** 218–26
[152] Jia J, Sun Y, Zhang Y, Liu Q, Cao J, Huang G, Xing B, Zhang C, Zhang L and Cao Y 2020 Facile and efficient fabrication of bandgap tunable carbon quantum dots derived from anthracite and their photoluminescence properties *Front. Chem.* **8** 183
[153] Lin T-C, Lee S-C and Cheng H-H 2004 Silicon–germanium spherical quantum dot infrared photodetectors prepared by the combination of bottom-up and top-down technologies *J. Vac. Sci. Technol.* B **22** 109
[154] Shi M, Dong L, Zheng S, Hou P, Cai L, Zhao M, Zhang X, Wang Q, Li J and Xu K 2019 "Bottom-up" preparation of MoS_2 quantum dots for tumor imaging and their in vivo behavior study *Biochem. Biophys. Res. Commun.* **516** 1090–6
[155] Hang D-R, Sun D-Y, Chen C-H, Wu H-F, Chou M M C, Islam S E and Sharma K H 2019 Facile bottom-up preparation of WS_2-based water-soluble quantum dots as luminescent probes for hydrogen peroxide and glucose *Nanoscale Res. Lett.* **14** 271
[156] Ahmad P *et al* 2019 Fabrication of hexagonal boron nitride quantum dots via a facile bottom-up technique *Ceram. Int.* **45** 22765–8
[157] Wu J *et al* 2015 Defect-free self-catalyzed GaAs/GaAsP nanowire quantum dots grown on silicon substrate *Nano Lett.* **16** 504–11
[158] Gong J, Steinsultz N and Ouyang M 2016 Nanodiamond-based nanostructures for coupling nitrogen-vacancy centres to metal nanoparticles and semiconductor quantum dots *Nat. Commun.* **7** 11820
[159] Li R, Tang L, Zhao Q, Ly T H, Teng K S, Li Y, Hu Y, Shu C and Lau S P 2019 In_2S_3 quantum dots: preparation, properties and optoelectronic application *Nanoscale Res. Lett.* **14** 161
[160] Lee S H, Kim D Y, Lee J, Lee S B, Han H, Kim Y Y, Mun S C, Im S H, Kim T-H and Park O O 2019 Synthesis of single-crystalline hexagonal graphene quantum dots from solution chemistry *Nano Lett.* **19** 5437–42
[161] Gu S, Hsieh C-T, Gandomi Y A, Chang J-K, Li J, Li J, Zhang H, Guo Q, Lau K C and Pandey R 2019 Microwave growth and tunable photoluminescence of nitrogen-doped graphene and carbon nitride quantum dots *J. Mater. Chem.* C **7** 5468–76
[162] Yang J-S, Chang Y-C, Huang Q-H, Lai Y-Y and Chiang W-H 2020 Microplasma-enabled nanocarbon assembly for the diameter-selective synthesis of colloidal graphene quantum dots *Chem. Commun.* **56** 10365–8
[163] Zhao J, Zheng Y, Pang Y, Chen J, Zhang Z, Xi F and Chen P 2020 Graphene quantum dots as full-color and stimulus responsive fluorescence ink for information encryption *J. Colloid Interface Sci.* **579** 307–14
[164] Tang L, Ji R, Li X, Teng K S and Lau S P 2013 Energy-level structure of nitrogen-doped graphene quantum dots *J. Mater. Chem.* C **1** 4908
[165] Li X, Lau S P, Tang L, Ji R and Yang P 2014 Sulphur doping: a facile approach to tune the electronic structure and optical properties of graphene quantum dots *Nanoscale* **6** 5323–8
[166] Li X, Lau S P, Tang L, Ji R and Yang P 2013 Multicolour light emission from chlorine-doped graphene quantum dots *J. Mater. Chem.* C **1** 7308
[167] Lee Y-J, Yeh T-W, Zou C, Yang Z-P, Chen J-W, Hsu P-L, Shen J-L, Chang C-C, Sheu J-K and Lin L Y 2019 Graphene quantum dot vertical cavity surface-emitting lasers *ACS Photonics* **6** 2894–901
[168] Gao S, Tang L, Xiang J, Ji R, Lai S K, Yuan S and Lau S P 2017 Facile preparation of sulphur-doped graphene quantum dots for ultra-high performance ultraviolet photodetectors *New J. Chem.* **41** 10447–51
[169] Zuo W, Tang L, Xiang J, Ji R, Luo L, Rogée L and Ping Lau S 2017 Functionalization of graphene quantum dots by fluorine: preparation, properties, application, and their mechanisms *Appl. Phys. Lett.* **110** 221901
[170] Zhao J, Tang L, Xiang J, Ji R, Yuan J, Zhao J, Yu R, Tai Y and Song L 2014 Chlorine doped graphene quantum dots: preparation, properties, and photovoltaic detectors *Appl. Phys. Lett.* **105** 111116
[171] Zhao J, Tang L, Xiang J, Ji R, Hu Y, Yuan J, Zhao J, Tai Y and Cai Y 2015 Fabrication and properties of a high-performance chlorine doped graphene quantum dot based photovoltaic detector *RSC Adv.* **5** 29222–9
[172] Liu M L, Yang L, Li R S, Chen B B, Liu H and Huang C Z 2017 Large-scale simultaneous synthesis of highly photoluminescent green amorphous carbon nanodots and yellow crystalline graphene quantum dots at room temperature *Green Chem.* **19** 3611–7
[173] Lee N E, Lee S Y, Lim H S, Yoo S H and Cho S O 2020 A novel route to high-quality graphene quantum dots by hydrogen-assisted pyrolysis of silicon carbide *Nanomaterials* **10** 277
[174] Li F, Li Y, Yang X, Han X, Jiao Y, Wei T, Yang D, Xu H and Nie G 2018 Highly fluorescent chiral N-S-doped carbon dots from cysteine: affecting cellular energy metabolism *Angew. Chem., Int. Ed.* **57** 2377–82
[175] Kapoor S, Jha A, Ahmad H and Islam S S 2020 Avenue to large-scale production of graphene quantum dots from high-purity graphene sheets using laboratory-grade graphite electrodes *ACS Omega* **5** 18831–41
[176] Xu L, Cheng C, Yao C and Jin X 2020 Flexible supercapacitor electrode based on lignosulfonate-derived graphene quantum dots/graphene hydrogel *Org. Electron.* **78** 105407
[177] Chai X, He H, Fan H, Kang X and Song X 2019 A hydrothermal-carbonization process for simultaneously production of sugars, graphene quantum dots, and porous carbon from sugarcane bagasse *Bioresour. Technol.* **282** 142–7
[178] Yuan B, Sun X, Yan J, Xie Z, Chen P and Zhou S 2016 $C_{96}H_{30}$ tailored single-layer and single-crystalline graphene quantum dots *Phys. Chem. Chem. Phys.* **18** 25002–9
[179] Deka M J, Dutta A and Chowdhury D 2018 Tuning the wettability and photoluminescence of graphene quantum dots via covalent modification *New J. Chem.* **42** 355–62
[180] Choi Y, Bae S, Kim B-S and Ryu J 2021 Atomically-dispersed cobalt ions on polyphenol-derived nanocarbon layers to improve charge separation, hole storage, and catalytic activity of water-oxidation photoanodes *J. Mater. Chem.* A **9** 13874–82
[181] Osella S and Knippenberg S 2018 Environmental effects on the charge transfer properties of Graphene quantum dot based interfaces *Int. J. Quantum Chem.* **119**
[182] Noor N F M , Badri M A S, Salleh M M and Umar A A 2018 Synthesis of white fluorescent pyrrolic nitrogen-doped graphene quantum dots *Opt. Mater.* **83** 306–14
[183] Li J, Zhang X, Jiang J, Wang Y, Jiang H, Zhang J, Nie X and Liu B 2019 Systematic assessment of the Ttoxicity and potential mechanism of graphene derivatives in vitro and in vivo *Toxicol. Sci.* **167** 269–81
[184] Kadian S, Manik G, Kalkal A, Singh M and Chauhan R P 2019 Effect of sulfur doping on fluorescence and quantum yield of graphene quantum dots: an experimental and theoretical investigation *Nanotechnology* **30** 435704
[185] Hasan M T, Gonzalez-Rodriguez R, Ryan C, Faerber N, Coffer J L and Naumov A V 2018 Photo- and electroluminescence from nitrogen-doped and

nitrogen-sulfur codoped graphene quantum dots *Adv. Funct. Mater.* **28** 1804337
[186] Zhang Q, Deng S, Liu J, Zhong X, He J, Chen X, Feng B, Chen Y and Ostrikov K 2018 Cancer-targeting graphene quantum dots: fluorescence quantum yields, stability, and cell selectivity *Adv. Funct. Mater.* **29** 1–11
[187] Li N, Than A, Chen J, Xi F, Liu J and Chen P 2018 Graphene quantum dots based fluorescence turn-on nanoprobe for highly sensitive and selective imaging of hydrogen sulfide in living cells *Biomater. Sci.* **6** 779–84
[188] Bian H, Wang Q, Yang S, Yan C, Wang H, Liang L, Jin Z, Wang G and Liu S 2019 Nitrogen-doped graphene quantum dots for 80% photoluminescence quantum yield for inorganic γ-$CsPbI_3$ perovskite solar cells with efficiency beyond 16% *J. Mater. Chem.* A **7** 5740–7
[189] Yang P, Su J, Guo R, Yao F and Yuan C 2019 B,N-co-doped graphene quantum dots as fluorescence sensor for detection of Hg^{2+} and F^- ions *Anal. Methods* **11** 1879–83
[190] Gu S, Hsieh C-T, Ashraf Gandomi Y, Li J, Yue X X and Chang J-K 2019 Tailoring fluorescence emissions, quantum yields, and white light emitting from nitrogen-doped graphene and carbon nitride quantum dots *Nanoscale* **11** 16553–61
[191] Gogoi S, Devi R, Dutta H S, Bordoloi M and Khan R 2019 Ratiometric fluorescence response of a dual light emitting reduced carbon dot/graphene quantum dot nanohybrid towards As(III) *J. Mater. Chem.* C **7** 10309–17
[192] Yang J-S, Pai D Z and Chiang W-H 2019 Microplasma-enhanced synthesis of colloidal graphene quantum dots at ambient conditions *Carbon* **153** 315–9
[193] Gu S, Hsieh C-T, Yuan C-Y, Ashraf Gandomi Y, Chang J-K, Fu C-C, Yang J-W and Juang R-S 2020 Fluorescence of functionalized graphene quantum dots prepared from infrared-assisted pyrolysis of citric acid and urea *J. Lumin.* **217** 116774
[194] Zhu J *et al* 2017 Green, rapid, and universal preparation approach of graphene quantum dots under ultraviolet irradiation *ACS Appl. Mater. Interfaces* **9** 14470–7
[195] Zhang J, Ma Y-Q, Li N, Zhu J-L, Zhang T, Zhang W and Liu B 2016 Preparation of graphene quantum dots and their application in cell imaging *J. Nanomater.* **2016** 1–9
[196] Sapkota B, Benabbas A, Lin H-Y G, Liang W, Champion P and Wanunu M 2017 Peptide-decorated tunable-fluorescence graphene quantum dots *ACS Appl. Mater. Interfaces* **9** 9378–87
[197] Fang B-Y, Li C, Song Y-Y, Tan F, Cao Y-C and Zhao Y-D 2018 Nitrogen-doped graphene quantum dot for direct fluorescence detection of Al^{3+} in aqueous media and living cells *Biosens. Bioelectron.* **100** 41–48
[198] Su J, Zhang X, Tong X, Wang X, Yang P, Yao F, Guo R and Yuan C 2020 Preparation of graphene quantum dots with high quantum yield by a facile one-step method and applications for cell imaging *Mater. Lett.* **271** 127806
[199] Tachi S, Morita H, Takahashi M, Okabayashi Y, Hosokai T, Sugai T and Kuwahara S 2019 Quantum yield enhancement in graphene quantum dots via esterification with benzyl alcohol *Sci. Rep.* **9** 14115
[200] Ma Q, Tu T A O, Wang L I, Li H-O, Lin Z-R, Xiao M and Guo G-P 2012 Substrate modulated graphene quantum dots *Mod. Phys. Lett.* B **26** 1250162
[201] Choudhary R P, Shukla S, Vaibhav K, Pawar P B and Saxena S 2015 Optical properties of few layered graphene quantum dots *Mater. Res. Express* **2** 095024
[202] Luo Y, Li M, Sun L, Xu Y, Hu G, Tang T, Wen J and Li X 2017 Tuning the photoluminescence of graphene quantum dots by co-doping of nitrogen and sulfur *J. Nanopart. Res.* **19** 1–9
[203] Lin L, Rong M, Luo F, Chen D, Wang Y and Chen X 2014 Luminescent graphene quantum dots as new fluorescent materials for environmental and biological applications *TRAC Trends Anal. Chem.* **54** 83–102
[204] Kalita H, Harikrishnan V and Aslam M 2013 The transport behavior of graphene quantum dots pp 304–5
[205] Güçlü A D, Potasz P, Hawrylak P, Ihm J and Cheong H 2011 Optical properties of graphene quantum dots with fractionally filled degenerate shell of zero energy states pp 771–2
[206] Yamijala S S R K C, Bandyopadhyay A and Pati S K 2014 Electronic properties of zigzag, armchair and their hybrid quantum dots of graphene and boron-nitride with and without substitution: a DFT study *Chem. Phys. Lett.* **603** 28–32
[207] Qi B-P, Hu H, Bao L, Zhang Z-L, Tang B, Peng Y, Wang B-S and Pang D-W 2015 An efficient edge-functionalization method to tune the photoluminescence of graphene quantum dots *Nanoscale* **7** 5969–73
[208] Ettefaghi E, Ghobadian B, Rashidi A, Najafi G, Khoshtaghaza M H and Pourhashem S 2017 Preparation and investigation of the heat transfer properties of a novel nanofluid based on graphene quantum dots *Energy Convers. Manage.* **153** 215–23
[209] Cheng W-J, Liang G, Wu P, Zhao S-H, Jia T-Q, Sun Z-R and Zhang S-A 2018 Up-conversion luminescence tuning in Er^{3+}-doped ceramic glass by femtosecond laser pulse at different laser powers *Chin. Phys.* B **27** 123201
[210] Zhang Y, Luo L, Li K, Li W and Hou Y 2018 Reversible up-conversion luminescence modulation based on UV-VIS light-controlled photochromism in Er^{3+} doped Sr_2SnO_4 *J. Mater. Chem.* C **6** 13148–56
[211] Ge K, Zhang C, Sun W, Liu H, Jin Y, Li Z, Liang X-J, Jia G and Zhang J 2016 Up-conversion Y_2O_3:Yb^{3+},Er^{3+} hollow spherical drug carrier with improved degradability for cancer treatment *ACS Appl. Mater. Interfaces* **8** 25078–86
[212] Zhou J, Chen G, Wu E, Bi G, Wu B, Teng Y, Zhou S and Qiu J 2013 Ultrasensitive polarized up-conversion of Tm^{3+}–Yb^{3+} doped β-$NaYF_4$ single nanorod *Nano Lett.* **13** 2241–6
[213] Bai L, Xue N, Zhao Y, Wang X, Lu C and Shi W 2018 Dual-mode emission of single-layered graphene quantum dots in confined nanospace: anti-counterfeiting and sensor applications *Nano Res.* **11** 2034–45
[214] Li M, Chen T, Gooding J J and Liu J 2019 Review of carbon and graphene quantum dots for sensing *ACS Sens.* **4** 1732–48
[215] Zheng X T, Ananthanarayanan A, Luo K Q and Chen P 2014 Glowing graphene quantum dots and carbon dots: properties, syntheses, and biological applications *Small* **11** 1620–36
[216] Tang L, Ji R, Tian P, Kong J and Xiang J 2017 Functionalization of graphene by size and doping control and its optoelectronic applications *Proc. SPIE* **10177** 101770B
[217] Kumari R, Pal K, Karmakar P and Sahu S K 2019 pH-Responsive Mn-doped carbon dots for white-light-emitting diodes, fingerprinting, and bioimaging *ACS Appl. Nano Mater.* **2** 5900–9
[218] Pohle R, Kavousanaki E G, Dani K M and Shannon N 2018 Symmetry and optical selection rules in graphene quantum dots *Phys. Rev.* B **97** 115404
[219] Bugajny P, Szulakowska L, Jaworowski B and Potasz P 2017 Optical properties of geometrically optimized graphene quantum dots *Physica* E **85** 294–301
[220] Yuan F *et al* 2018 Engineering triangular carbon quantum dots with unprecedented narrow bandwidth emission for multicolored LEDs *Nat. Commun.* **9** 2249

[221] Geethalakshmi K R, Ng T Y and Crespo-Otero R 2016 Tunable optical properties of OH-functionalised graphene quantum dots *J. Mater. Chem.* C **4** 8429–38

[222] Ding H, Yu S-B, Wei J-S and Xiong H-M 2015 Full-color light-emitting carbon dots with a surface-state-controlled luminescence mechanism *ACS Nano* **10** 484–91

[223] Wang J *et al* 2018 Langmuir–Blodgett self-assembly of ultrathin graphene quantum dot films with modulated optical properties *Nanoscale* **10** 19612–20

[224] Tetsuka H 2019 Nitrogen-functionalized graphene quantum dots: a versatile platform for integrated optoelectronic devices *Chem. Rec.* **20** 429–39

[225] Wei S, Yin X, Li H, Du X, Zhang L, Yang Q and Yang R 2020 Multi-color fluorescent carbon dots: graphitized sp^2 conjugated domains and surface state energy level co-modulate band gap rather than size effects *Chem. Eur. J.* **26** 8129–36

[226] Feng J, Dong H, Pang B, Shao F, Zhang C, Yu L and Dong L 2018 Theoretical study on the optical and electronic properties of graphene quantum dots doped with heteroatoms *Phys. Chem. Chem. Phys.* **20** 15244–52

[227] Li W *et al* 2020 White luminescent single-crystalline chlorinated graphene quantum dots *Nanoscale Horiz.* **5** 928–33

[228] Feng J, Dong H, Pang B, Chen Y, Yu L and Dong L 2019 Tuning the electronic and optical properties of graphene quantum dots by selective boronization *J. Mater. Chem.* C **7** 237–46

[229] Wang G, Guo Q, Chen D, Liu Z, Zheng X, Xu A, Yang S and Ding G 2018 Facile and highly effective synthesis of controllable lattice sulfur-doped graphene quantum dots via hydrothermal treatment of durian *ACS Appl. Mater. Interfaces* **10** 5750–9

[230] Feng J, Guo Q, Liu H, Chen D, Tian Z, Xia F, Ma S, Yu L and Dong L 2019 Theoretical insights into tunable optical and electronic properties of graphene quantum dots through phosphorization *Carbon* **155** 491–8

[231] Gao D, Zhang Y, Liu A, Zhu Y, Chen S, Wei D, Sun J, Guo Z and Fan H 2020 Photoluminescence-tunable carbon dots from synergy effect of sulfur doping and water engineering *Chem. Eng. J.* **388** 124199

[232] Qi F and Jin G 2013 Strain sensing and far-infrared absorption in strained graphene quantum dots *J. Appl. Phys.* **114** 073509

[233] Zhao S *et al* 2018 Single photon emission from graphene quantum dots at room temperature *Nat. Commun.* **9** 3470

[234] Deb J, Paul D and Sarkar U 2020 Density functional theory investigation of nonlinear optical properties of T-graphene quantum dots *J. Phys. Chem.* A **124** 1312–20

[235] Shafraniuk S E 2019 Unconventional electromagnetic properties of the graphene quantum dots *Phys. Rev.* B **100** 075404

[236] Ghandchi M, Darvish G and Moravvej-Farshi M K 2020 Properties of bilayer graphene quantum dots for integrated optics: an ab initio study *Photonics* **7** 78

[237] Yu Y, Mei L, Shi Y, Zhang X, Cheng K, Cao F, Zhang L, Xu J, Li X and Xu Z 2020 Ag-conjugated graphene quantum dots with blue light-enhanced singlet oxygen generation for ternary-mode highly-efficient antimicrobial therapy *J. Mater. Chem.* B **8** 1371–82

[238] Wang C, Chen Y, Xu Z, Chen B, Zhang Y, Yi X and Li J 2020 Fabrication and characterization of novel cRGD modified graphene quantum dots for chemo-photothermal combination therapy *Sens. Actuators* B **309** 127732

[239] Geng B, Shen W, Fang F, Qin H, Li P, Wang X, Li X, Pan D and Shen L 2020 Enriched graphitic N dopants of carbon dots as F cores mediate photothermal conversion in the NIR-II window with high efficiency *Carbon* **162** 220–33

[240] Yao J-A, Peng X-X, Liu Z-K, Zhang Y-F, Fu P, Li H, Lin Z-D and Du F-P 2020 Enhanced thermoelectric properties of bilayer-like structural graphene quantum dots/single-walled carbon nanotubes hybrids *ACS Appl. Mater. Interfaces* **12** 39145–53

[241] Sedaghat F and Yousefi F 2019 Synthesizes, characterization, measurements and modeling thermal conductivity and viscosity of graphene quantum dots nanofluids *J. Mol. Liq.* **278** 299–308

[242] Amiri A, Shanbedi M and Dashti H 2017 Thermophysical and rheological properties of water-based graphene quantum dots nanofluids *J. Taiwan Inst. Chem. Eng.* **76** 132–40

[243] Lin T N, Inciong M R, Santiago S R, Kao C W, Shu G W, Yuan C T, Shen J L, Yeh J M and Chen-Yang Y W 2016 Electron injection from graphene quantum dots to poly(amido amine) dendrimers *Appl. Phys. Lett.* **108** 161904

[244] Fu W X and Lin J F 2019 Electrical and optical properties of the specimens with graphene quantum dots prepared by different number of wet transfer *Diam. Relat. Mater.* **99** 107527

[245] Sun Y, Pan H, Zheng Y, Zhang K, Fu L, Chen J, Zhang W and Tang N 2020 The effect of thermal annealing on the magnetic properties of graphene oxide quantum dots *Appl. Surf. Sci.* **501** 144234

[246] Hu W, Huang Y, Qin X, Lin L, Kan E, Li X, Yang C and Yang J 2019 Room-temperature magnetism and tunable energy gaps in edge-passivated zigzag graphene quantum dots *npj 2D Mater. Appl.* **3** 17

[247] Tripathi H S, Mukherjee R, Rudra M, Sutradhar R, Kumar R A and Sinha T P 2019 Insulator to semiconductor transition in graphene quantum dots *AIP Conf. Proc.* **2162** 020088

[248] Snider E, Dasenbrock-Gammon N, McBride R, Debessai M, Vindana H, Vencatasamy K, Lawler K V, Salamat A and Dias R P 2020 Room-temperature superconductivity in a carbonaceous sulfur hydride *Nature* **586** 373–7

[249] Yang H, Yuan W, Luo J and Zhu J 2019 Modulation of magnetic and electrical properties of bilayer grapheme quantum dots using rotational stacking faults *Chin. Phys.* B **28** 78106

[250] Darehdor M A, Roknabadi M R and Shahtahmassebi N 2019 Effects of phonon scattering on the electron transport and photocurrent of graphene quantum dot structures *Eur. Phys. J.* B **92**

[251] Sun Y, Zheng Y, Pan H, Chen J, Zhang W, Fu L, Zhang K, Tang N and Du Y 2017 Magnetism of graphene quantum dots *npj Quantum Mater.* **2**

[252] Nascimento J S, da Costa D R, Zarenia M, Chaves A and Pereira J M 2017 Magnetic properties of bilayer graphene quantum dots in the presence of uniaxial strain *Phys. Rev.* B **96**

[253] Das R, Dhar N, Bandyopadhyay A and Jana D 2016 Size dependent magnetic and optical properties in diamond shaped graphene quantum dots: a DFT study *J. Phys. Chem. Solids* **99** 34–42

[254] Cheng S, Yu J, Ma T and Peres N M R 2015 Strain-induced edge magnetism at the zigzag edge of a graphene quantum dot *Phys. Rev.* B **91** 075410

[255] Espinosa-Ortega T, Luk'yanchuk I A and Rubo Y G 2013 Magnetic properties of graphene quantum dots *Phys. Rev.* B **87** 205434

[256] Tan Z B, Cox D, Nieminen T, Lähteenmäki P, Golubev D, Lesovik G B and Hakonen P J 2015 Cooper pair splitting by means of graphene quantum dots *Phys. Rev. Lett.* **114** 096602

[257] Guo T, Wang L, Sun S, Wang Y, Chen X, Zhang K, Zhang D, Xue Z and Zhou X 2019 Layered MoS_2@graphene

functionalized with nitrogen-doped graphene quantum dots as an enhanced electrochemical hydrogen evolution catalyst *Chin. Chem. Lett.* **30** 1253–60
[258] Singh S K, Takeyasu K and Nakamura J 2018 Active sites and mechanism of oxygen reduction reaction electrocatalysis on nitrogen-doped carbon materials *Adv. Mater.* **31** 1804297
[259] Seibert J R, Keleş Ö, Wang J and Erogbogbo F 2019 Infusion of graphene quantum dots to modulate thermal conductivity and dynamic mechanical properties of polymers *Polymer* **185** 121988
[260] Ashraf A, Carter-Fenk K, Herbert J M, Farooqi B A, Farooq U and Ayub K 2019 Interaction of graphene quantum dots with oligothiophene: a comprehensive theoretical study *J. Phys. Chem.* C **123** 29556–70
[261] Safaie B, Youssefi M and Rezaei B 2018 Rheological behavior of polypropylene/carbon quantum dot nanocomposites: the effects of particles size, particles/matrix interface adhesion, and particles loading *Polym. Bull.* **76** 4335–54
[262] Velumani A, Sengodan P, Arumugam P, Rajendran R, Santhanam S and Palanisamy M 2020 Carbon quantum dots supported ZnO sphere based photocatalyst for dye degradation application *Curr. Appl. Phys.* **20** 1176–84
[263] Jamila G S, Sajjad S, Leghari S A K and Long M 2020 Nitrogen doped carbon quantum dots and GO modified WO_3 nanosheets combination as an effective visible photo catalyst *J. Hazard. Mater.* **382** 121087
[264] Cirone J, Ahmed S R, Wood P C and Chen A 2019 Green synthesis and electrochemical study of cobalt/graphene quantum dots for efficient water splitting *J. Phys. Chem.* C **123** 9183–91
[265] Gizem Güneştekin B, Medetalibeyoglu H, Atar N and Lütfi Yola M 2020 Efficient direct-methanol fuel cell based on graphene quantum dots/multi-walled carbon nanotubes composite *Electroanalysis* **32** 1977–82
[266] Shahbazi-Alavi H, Kareem Abbas A and Safaei-Ghomi J 2020 Sonosynthesis of pyranochromenes and biscoumarins catalyzed by Co_3O_4/NiO@GQDs@SO_3H nanocomposite *Nanocomposites* **6** 56–65
[267] Wang H, Zhang B, Zhao F and Zeng B 2018 One-pot synthesis of N-graphene quantum dot-functionalized I-BiOCl Z-scheme cathodic materials for "signal-off" photoelectrochemical sensing of chlorpyrifos *ACS Appl. Mater. Interfaces* **10** 35281–8
[268] Fan X and Fan Z 2019 Determination of thiourea by on–off fluorescence using nitrogen-doped graphene quantum dots *Anal. Lett.* **52** 2028–40
[269] Xie N *et al* 2020 Manipulation of 3D nanocarbon hybrids toward synthesis of N-doped graphene quantum dots with high photoluminescence quantum yield *J. Lumin.* **219** 116827
[270] Montejo-Alvaro F, Oliva J, Herrera-Trejo M, Hdz-García H M and Mtz-Enriquez A I 2019 DFT study of small gas molecules adsorbed on undoped and N-, Si-, B-, and Al-doped graphene quantum dots *Theor. Chem. Acc.* **138** 37
[271] Freitag N M *et al* 2018 Large tunable valley splitting in edge-free graphene quantum dots on boron nitride *Nat. Nanotechnol.* **13** 392–7
[272] Kang G-S, Lee S, Yeo J-S, Choi E-S, Lee D C, Na S-I and Joh H-I 2019 Graphene quantum dots with nitrogen and oxygen derived from simultaneous reaction of solvent as exfoliant and dopant *Chem. Eng. J.* **372** 624–30
[273] Khan F, Ahmad V, Alshahrani T, Al-Rasheidi M, Alanazi A M, Irshad K, Zahir M H and Kim J H 2023 Influence of synthesis parameters of N-doped graphene quantum dots and polymer composite layer on the performance of CIGS solar cells *Opt. Mater.* **135** 113251
[274] Wang C, Pan C, Wei Z, Wei X, Yang F and Mao L 2020 Bionanosensor based on N-doped graphene quantum dots coupled with CoOOH nanosheets and their application for in vivo analysis of ascorbic acid *Anal. Chim. Acta* **1100** 191–9
[275] Algarra M, Moreno V, Lázaro-Martínez J M, Rodríguez-Castellón E, Soto J, Morales J and Benítez A 2020 Insights into the formation of N doped 3D-graphene quantum dots. Spectroscopic and computational approach *J. Colloid Interface Sci.* **561** 678–86
[276] Gan X, Yang S, Zhang J, Wang G, He P, Sun H, Yuan H, Yu L, Ding G and Zhu Y 2019 Graphite-N doped graphene quantum dots as semiconductor additive in perovskite solar cells *ACS Appl. Mater. Interfaces* **11** 37796–803
[277] Calabro R L, Yang D-S and Kim D Y 2019 Controlled nitrogen doping of graphene quantum dots through laser ablation in aqueous solutions for photoluminescence and electrocatalytic applications *ACS Appl. Nano Mater.* **2** 6948–59
[278] Zheng H, Zheng P, Zheng L, Jiang Y, Wu Z, Wu F, Shao L, Liu Y and Zhang Y 2018 Nitrogen-doped graphene quantum dots synthesized by C_{60}/nitrogen plasma with excitation-independent blue photoluminescence emission for sensing of ferric ions *J. Phys. Chem.* C **122** 29613–9
[279] Kumar S, Aziz S T, Girshevitz O and Nessim G D 2018 One-step synthesis of N-doped graphene quantum dots from chitosan as a sole precursor using chemical vapor deposition *J. Phys. Chem.* C **122** 2343–9
[280] Gao X X, Zhou X, Ma Y F, Wang C P and Chu F X 2018 A fluorometric and colorimetric dual-mode sensor based on nitrogen and iron co-doped graphene quantum dots for detection of ferric ions in biological fluids and cellular imaging *New J. Chem.* **42** 14751–6
[281] Khan F and Kim J H 2018 N-functionalized graphene quantum dots with ultrahigh quantum yield and large stokes shift: efficient downconverters for CIGS solar cells *ACS Photonics* **5** 4637–43
[282] Yuan K, Zhang X, Li X, Qin R, Cheng Y, Li L, Yang X, Yu X, Lu Z and Liu H 2020 Great enhancement of red emitting carbon dots with B/Al/Ga doping for dual mode anti-counterfeiting *Chem. Eng. J.* **397** 125487
[283] Kuo W-S, Shen X-C, Chang C-Y, Kao H-F, Lin S-H, Wang J-Y and Wu P-C 2020 Multiplexed graphene quantum dots with excitation-wavelength-independent photoluminescence, as two-photon probes, and in ultraviolet–near infrared bioimaging *ACS Nano* **14** 11502–9
[284] Sangam S *et al* 2018 Sustainable synthesis of single crystalline sulphur-doped graphene quantum dots for bioimaging and beyond *Green Chem.* **20** 4245–59
[285] Kharangarh P R, Umapathy S and Singh G 2018 Thermal effect of sulfur doping for luminescent graphene quantum dots *ECS J. Solid State Sci. Technol.* **7** M29–M34
[286] Guo Z, Wu H, Li M, Tang T, Wen J and Li X 2020 Phosphorus-doped graphene quantum dots loaded on TiO_2 for enhanced photodegradation *Appl. Surf. Sci.* **526** 146724
[287] Gu S, Hsieh C-T, Tsai Y-Y, Ashraf Gandomi Y, Yeom S, Kihm K D, Fu C-C and Juang R-S 2019 Sulfur and nitrogen co-doped qraphene quantum dots as a fluorescent quenching probe for highly sensitive detection toward mercury ions *ACS Appl. Nano Mater.* **2** 790–8
[288] Zuo G, Xie A, Pan X, Su T, Li J and Dong W 2018 Fluorine-doped cationic carbon dots for efficient gene delivery *ACS Appl. Nano Mater.* **1** 2376–85
[289] Wang H, Revia R, Mu Q, Lin G, Yen C and Zhang M 2020 Single-layer boron-doped graphene quantum dots for contrast-enhanced *in vivo* T_1-weighted MRI *Nanoscale Horiz.* **5** 573–9

[290] Du F, Zeng Q, Lai Z, Cheng Z and Ruan G 2019 Silicon doped graphene quantum dots combined with ruthenium(III) ions as a fluorescent probe for turn-on detection of triclosan *New J. Chem.* **43** 12907–15
[291] Wang X-F, Wang G-G, Li J-B, Liu Z, Zhao W-F and Han J-C 2018 Towards high-powered remote WLED based on flexible white-luminescent polymer composite films containing S, N co-doped graphene quantum dots *Chem. Eng. J.* **336** 406–15
[292] Majumder T, Dhar S, Chakraborty P, Debnath K and Mondal S P 2019 S,N co-doped graphene quantum dots decorated C-doped ZnO nanotaper photoanodes for solar cells applications *Nano* **14** 1950012
[293] Ouyang Z, Lei Y, Chen Y, Zhang Z, Jiang Z, Hu J and Lin Y 2019 Preparation and specific capacitance properties of sulfur,nitrogen co-doped graphene quantum dots *Nanoscale Res. Lett.* **14** 219
[294] Schroer Z S *et al* 2019 Nitrogen–sulfur-doped graphene quantum dots with metal ion-resistance for bioimaging *ACS Appl. Nano Mater.* **2** 6858–65
[295] Zheng L, Zhang J, Hu Y H and Long M 2019 Enhanced photocatalytic production of H_2O_2 by Nafion coatings on S,N-codoped graphene-quantum-dots-modified TiO_2 *J. Phys. Chem.* C **123** 13693–701
[296] Boonta W, Talodthaisong C, Sattayaporn S, Chaicham C, Chaicham A, Sahasithiwat S, Kangkaew L and Kulchat S 2020 The synthesis of nitrogen and sulfur co-doped graphene quantum dots for fluorescence detection of cobalt(II) ions in water *Mater. Chem. Front.* **4** 507–16
[297] Xu Y, Wang S, Hou X, Sun Z, Jiang Y, Dong Z, Tao Q, Man J and Cao Y 2018 Coal-derived nitrogen, phosphorus and sulfur co-doped graphene quantum dots: a promising ion fluorescent probe *Appl. Surf. Sci.* **445** 519–26
[298] Omer K M, Tofiq D I and Hassan A Q 2018 Solvothermal synthesis of phosphorus and nitrogen doped carbon quantum dots as a fluorescent probe for iron(III) *Microchim. Acta* **185** 466
[299] Wang L, Jana J, Chung J S, Choi W M and Hur S H 2022 Designing an intriguingly fluorescent N, B-doped carbon dots based fluorescent probe for selective detection of NO_2^- ions *Spectrochim. Acta* A **268** 120657
[300] Liu Z, Mo Z, Niu X, Yang X, Jiang Y, Zhao P, Liu N and Guo R 2020 Highly sensitive fluorescence sensor for mercury(II) based on boron- and nitrogen-co-doped graphene quantum dots *J. Colloid Interface Sci.* **566** 357–68
[301] Liu Z, Mo Z, Liu N, Guo R, Niu X, Zhao P and Yang X 2020 One-pot synthesis of highly fluorescent boron and nitrogen co-doped graphene quantum dots for the highly sensitive and selective detection of mercury ions in aqueous media *J. Photochem. Photobiol.* A **389** 112255
[302] Li Z, Cao L, Qin P, Liu X, Chen Z, Wang L, Pan D and Wu M 2018 Nitrogen and oxygen co-doped graphene quantum dots with high capacitance performance for micro-supercapacitors *Carbon* **139** 67–75
[303] Xu L, Dun X, Zou J, Li Y, Jia M, Cui L, Gao J and Jin X 2018 Graphene hydrogel decorated with N,O co-doped carbon dots for flexible supercapacitor electrodes *J. Electrochem. Soc.* **165** A2217–A24
[304] Zhang Y, Zhao J, Sun H, Zhu Z, Zhang J and Liu Q 2018 B, N, S, Cl doped graphene quantum dots and their effects on gas-sensing properties of Ag-$LaFeO_3$ *Sens. Actuators* B **266** 364–74
[305] Han Y, Chen Y, Wang N and He Z 2018 Magnesium doped carbon quantum dots synthesized by mechanical ball milling and displayed Fe^{3+} sensing *Mater. Technol.* **34** 336–42
[306] Hasan M T, Gonzalez-Rodriguez R, Lin C-W, Campbell E, Vasireddy S, Tsedev U, Belcher A M and Naumov A V 2020 Rare-earth metal ions doped graphene quantum dots for near-IR in vitro/in vivo/ex vivo imaging applications *Adv. Opt. Mater.* **8** 2000897
[307] Rosenkrans Z T *et al* 2020 Selenium-doped carbon quantum dots act as broad-spectrum antioxidants for acute kidney injury management *Adv. Sci.* **7** 2000420
[308] Zhang L, Wang J, Fang G, Deng J and Wang S 2020 A molecularly imprinted polymer capped nitrogen-doped graphene quantum dots system for sensitive determination of tetracycline in animal-derived food *Chemistry Select* **5** 839–46
[309] Faraji M, Derakhshi P, Tahvildari K and Yousefian Z 2018 High performance Fe and N-codoped graphene quantum dot supported Pd_3Co catalyst with synergistically improved oxygen reduction activity and great methanol tolerance *Solid State Sci.* **83** 152–60
[310] Wang G *et al* 2019 Green preparation of lattice phosphorus doped graphene quantum dots with tunable emission wavelength for bio-imaging *Mater. Lett.* **242** 156–9
[311] Peng J, Zhao Z, Zheng M, Su B, Chen X and Chen X 2020 Electrochemical synthesis of phosphorus and sulfur co-doped graphene quantum dots as efficient electrochemiluminescent immunomarkers for monitoring okadaic acid *Sens. Actuators* B **304** 127383
[312] Jiang L, Ding H, Lu S, Geng T, Xiao G, Zou B and Bi H 2020 Photoactivated fluorescence enhancement in F,N-doped carbon dots with piezochromic behavior *Angew. Chem., Int. Ed. Engl.* **59** 9986–91
[313] Long P, Feng Y, Cao C, Li Y, Han J, Li S, Peng C, Li Z and Feng W 2018 Self-protective room-temperature phosphorescence of fluorine and nitrogen codoped carbon dots *Adv. Funct. Mater.* **28** 1800791
[314] Liu Y, Wu P, Wu X, Ma C, Luo S, Xu M, Li W and Liu S 2020 Nitrogen and copper (II) co-doped carbon dots for applications in ascorbic acid determination by non-oxidation reduction strategy and cellular imaging *Talanta* **210** 120649
[315] Wang N, Zheng A-Q, Liu X, Chen J-J, Yang T, Chen M-L and Wang J-H 2018 Deep eutectic solvent-assisted preparation of nitrogen/chloride-doped carbon dots for intracellular biological sensing and live cell imaging *ACS Appl. Mater. Interfaces* **10** 7901–9
[316] Kaewprom C, Areerob Y, Oh W-C, Ameta K L and Chanthai S 2020 Simultaneous determination of Hg(II) and Cu(II) in water samples using fluorescence quenching sensor of N-doped and N,K co-doped graphene quantum dots *Arabian J. Chem.* **13** 3714–23
[317] Li Y, Chen S, Lin D, Chen Z and Qiu P 2020 A dual-mode nanoprobe for the determination of parathion methyl based on graphene quantum dots modified silver nanoparticles *Anal. Bioanal. Chem.* **412** 5583–91
[318] Wang W, Wang S, Lv J, Zhao M, Zhang M, He G, Fang C, Li L and Sun Z 2018 Enhanced photoresponse and photocatalytic activities of graphene quantum dots sensitized Ag/TiO_2 thin film *J. Am. Ceram. Soc.* **101** 5469–76
[319] Lv Y-K, Li Y-Y, Zhou R-H, Pan Y-P, Yao H-C and Li Z-J 2020 N-doped graphene quantum dot-decorated three-dimensional ordered macroporous In_2O_3 for NO_2 sensing at low temperatures *ACS Appl. Mater. Interfaces* **12** 34245–53
[320] Mahato M K, Govind C, Karunakaran V, Nandy S, Sudakar C and Prasad E 2019 Enhanced charge transport and excited-state charge-transfer dynamics in a colloidal mixture of CdTe and graphene quantum dots *J. Phys. Chem.* C **123** 20512–21
[321] Park Y J, Ko K B, Lee K S, Seo T H, Hong C-H, Cuong T V and Son D I 2020 Solution processed graphene quantum

dots decorated ZnO nanoflowers for mediating photoluminescence *Appl. Surf. Sci.* **510** 145407
[322] Sung S, Park J H, Wu C and Kim T W 2020 Biosynaptic devices based on chicken egg albumen:graphene quantum dot nanocomposites *Sci. Rep.* **10** 1255
[323] Gebreegziabher G G, Asemahegne A S, Ayele D W, Mani D, Narzary R, Sahu P P and Kumar A 2019 Polyaniline–graphene quantum dots (PANI–GQDs) hybrid for plastic solar cell *Carbon Lett.* **30** 1–11
[324] Li W, Cheng N, Cao Y, Zhao Z, Xiao Z, Zi W and Sun Z 2020 Boost the performance of inverted perovskite solar cells with PEDOT:PSS/graphene quantum dots composite hole transporting layer *Org. Electron.* **78** 105575
[325] Sarabiyan Nejad S, Rezaei M and Bagheri M 2019 Polyurethane/nitrogen-doped graphene quantum dot (N-GQD) nanocomposites: synthesis, characterization, thermal, mechanical and shape memory properties *Polym.-Plast. Technol. Mater.* **59** 398–416
[326] Li L 2020 Biomemristic behavior for water-soluble chitosan blended with graphene quantum dot nanocomposite *Nanomaterials* **10** 559
[327] Liang Y, Li C, Li S, Su B, Hu M Z, Gao X and Gao C 2020 Graphene quantum dots (GQDs)-polyethyleneimine as interlayer for the fabrication of high performance organic solvent nanofiltration (OSN) membranes *Chem. Eng. J.* **380** 122462
[328] Vandana M *et al* 2020 Effect of different gel electrolytes on conjugated polymer- graphene quantum dots based electrode for solid state hybrid supercapacitors *Polym.-Plast. Technol. Mater.* **59** 2068–75
[329] Zhao J *et al* 2020 Graphene quantum dot reinforced electrospun carbon nanofiber fabrics with high surface area for ultrahigh rate supercapacitors *ACS Appl. Mater. Interfaces* **12** 11669–78
[330] Sarkar N, Sahoo G and Swain S K 2020 Graphene quantum dot decorated magnetic graphene oxide filled polyvinyl alcohol hybrid hydrogel for removal of dye pollutants *J. Mol. Liq.* **302** 112591
[331] Li S, Li C, Song X, Su B, Mandal B, Prasad B, Gao X and Gao C 2019 Graphene quantum dots-doped thin film nanocomposite polyimide membranes with enhanced solvent resistance for solvent-resistant nanofiltration *ACS Appl. Mater. Interfaces* **11** 6527–40
[332] Sarno M, Mustafa W A A, Senatore A and Scarpa D 2020 One-step "green" synthesis of dispersable carbon quantum dots/poly (methyl methacrylate) nanocomposites for tribological applications *Tribol. Int.* **148** 106311
[333] Martín-Pacheco A, Del Río Castillo A E, Martín C, Herrero M A, Merino S, García Fierro J L, Díez-Barra E and Vázquez E 2018 Graphene quantum dot–aerogel: from nanoscopic to macroscopic fluorescent materials sensing polyaromatic compounds in water *ACS Appl. Mater. Interfaces* **10** 18192–201
[334] Pramanik A, Biswas S, Tiwary C S, Kumbhakar P, Sarkar R and Kumbhakar P 2020 Forster resonance energy transfer assisted white light generation and luminescence tuning in a colloidal graphene quantum dot-dye system *J. Colloid Interface Sci.* **565** 326–36
[335] Wu Y, Zhang H, Pan A, Wang Q, Zhang Y, Zhou G and He L 2018 White-light-emitting melamine-formaldehyde microspheres through polymer-mediated aggregation and encapsulation of graphene quantum dots *Adv. Sci.* **6** 1801432
[336] Du F-P, Cao N-N, Zhang Y-F, Fu P, Wu Y-G, Lin Z-D, Shi R, Amini A and Cheng C 2018 PEDOT:PSS/graphene quantum dots films with enhanced thermoelectric properties via strong interfacial interaction and phase separation *Sci. Rep.* **8** 6441
[337] Arthisree D and Madhuri W 2020 Optically active polymer nanocomposite composed of polyaniline, polyacrylonitrile and green-synthesized graphene quantum dot for supercapacitor application *Int. J. Hydrog. Energy* **45** 9317–27
[338] Arthisree D L, Sumathi R R and Joshi G 2018 Effect of graphene quantum dots on photoluminescence property of polyvinyl butyral nanocomposite *Polym. Adv. Technol.* **30** 790–8
[339] Chen Z, Wang D, Wang X and Yang J 2020 Preparation and formaldehyde sensitive properties of N-GQDs/SnO_2 nanocomposite *Chin. Chem. Lett.* **31** 2063–6
[340] Hu J, Lei Y, Yuan M, Lin Y, Jiang Z, Ouyang Z, Du P and Wu Y 2020 Enhanced photoelectric performance of GQDs anchored WO_3 with a 'dot-on-nanoparticle' structure *Mater. Res. Express* **7** 075602
[341] Ou O, Lyu L and Sun L 2019 Facet-dependent interfacial charge transfer in TiO_2/nitrogen-doped graphene quantum dots heterojunctions for visible-light driven photocatalysis *Catalysts* **9** 345
[342] Zare Pirhaji J, Moeinpour F, Mirhoseini Dehabadi A and Yasini Ardakani S A 2020 Experimental study and modelling of effective parameters on removal of Cd(II) from water by halloysite/graphene quantum dots magnetic nanocomposite as an adsorbent using response surface methodology *Appl. Organomet. Chem.* **34** e5640
[343] Shao S, Kim H W, Kim S S, Chen Y and Lai M 2020 NGQDs modified nanoporous TiO_2/graphene foam nanocomposite for excellent sensing response to formaldehyde at high relative humidity *Appl. Surf. Sci.* **516** 145932
[344] Sun X, Li H-J, Ou N, Lyu B, Gui B, Tian S, Qian D, Wang X and Yang J 2019 Visible-light driven TiO_2 photocatalyst coated with graphene quantum dots of tunable nitrogen doping *Molecules* **24** 344
[345] Zhou Z, Zhao P, Wang C, Yang P, Xie Y and Fei J 2020 Ultra-sensitive amperometric determination of quercetin by using a glassy carbon electrode modified with a nanocomposite prepared from aminated graphene quantum dots, thiolated β-cyclodextrin and gold nanoparticles *Microchim. Acta* **187**
[346] Ramachandran P, Lee C Y, Doong R-A, Oon C E, Kim Thanh N T and Lee H L 2020 A titanium dioxide/nitrogen-doped graphene quantum dot nanocomposite to mitigate cytotoxicity: synthesis, characterisation, and cell viability evaluation *RSC Adv.* **10** 21795–805
[347] Ur R M, Xie F, Li Y and Wei M 2019 ZnO nanosheets encapsulating graphene quantum dots with enhanced performance for dye-sensitized solar cell *J. Electroanal. Chem.* **840** 160–4
[348] Chen X, Gao H, Yang M, Xing L, Dong W, Li A, Zheng H and Wang G 2019 Smart integration of carbon quantum dots in metal-organic frameworks for fluorescence-functionalized phase change materials *Energy Storage Mater.* **18** 349–55
[349] Alam S, Sahu T K, Gogoi D, Peela N R and Qureshi M 2020 Bio-template assisted hierarchical ZnO superstructures coupled with graphene quantum dots for enhanced water oxidation kinetics *Sol. Energy* **199** 39–46
[350] Mousavi S S, Sajad B and Majlesara M H 2019 Fast response ZnO/PVA nanocomposite-based photodiodes modified by graphene quantum dots *Mater. Des.* **162** 249–55
[351] Mousavi S S, Kazempour A, Efafi B, Ara M H M and Sajad B 2019 Effects of graphene quantum dots interlayer on performance of ZnO-based photodetectors *Appl. Surf. Sci.* **493** 1187–94
[352] Wu J, Yin C, Zhou J, Li H, Liu Y, Shen Y, Garner S, Fu Y and Duan H 2020 Ultrathin glass-based flexible, transparent, and ultrasensitive surface acoustic wave

humidity sensor with ZnO nanowires and graphene quantum dots *ACS Appl. Mater. Interfaces* **12** 39817–25
[353] Shao S, Chen X, Chen Y, Zhang L, Kim H W and Kim S S 2020 ZnO nanosheets modified with graphene quantum dots and SnO_2 quantum nanoparticles for room-temperature H_2S sensing *ACS Appl. Nano Mater.* **3** 5220–30
[354] Ahmadi N, Bagherzadeh M and Nemati A 2020 Comparison between electrochemical and photoelectrochemical detection of dopamine based on titania-ceria-graphene quantum dots nanocomposite *Biosens. Bioelectron.* **151** 111977
[355] Fan C *et al* 2023 Graphene quantum dots as sulfiphilic and lithiophilic mediator toward high stability and durable life lithium-sulfur batteries *J. Energy Chem.* **85** 254–66
[356] Tian W, Zhu J, Dong Y, Zhao J, Li J, Guo N, Lin H, Zhang S and Jia D 2020 Micelle-induced assembly of graphene quantum dots into conductive porous carbon for high rate supercapacitor electrodes at high mass loadings *Carbon* **161** 89–96
[357] Baslak C, Demirel S, Kocyigit A, Erdal M O and Yıldırım M 2023 Electrolyte performance of green synthesized carbon quantum dots from fermented tea for high-speed capacitors *Diam. Relat. Mater.* **139** 110275
[358] Xia Q, Zeng W, Ji F, Chen X, Zhang Y, Ling F, Hu W, Fang L, Khisro S N and Zhou M 2019 Graphene quantum dot/$Co(OH)_2$ electrode on nanoporous Au–Ag alloy for superior hybrid micro-supercapacitors *J. Mater. Chem.* C **7** 11441–8
[359] Daugherty M C, Gu S, Aaron D S, Kelly R E, Gandomi Y A and Hsieh C-T 2020 Graphene quantum dot-decorated carbon electrodes for energy storage in vanadium redox flow batteries *Nanoscale* **12** 7834–42
[360] Yun X, Li J, Chen X, Chen H, Xiao L, Xiang K, Chen W, Liao H and Zhu Y 2019 Porous Fe_2O_3 modified by nitrogen-doped carbon quantum dots/reduced graphene oxide composite aerogel as a high-capacity and high-rate anode material for alkaline aqueous batteries *ACS Appl. Mater. Interfaces* **11** 36970–84
[361] Ganganboina A B, Park E Y and Doong R-A 2020 Boosting the energy storage performance of V_2O_5 nanosheets by intercalating conductive graphene quantum dots *Nanoscale* **12** 16944–55
[362] Qian J, Yang Z, Cui H, An K, Ren C, Liu Q and Wang K 2020 Fabricating a signal-off photoelectrochemical sensor based on $BiPO_4$-graphene quantum dots nanocomposites for sensitive and selective detection of hydroquinone *J. Electroanal. Chem.* **868** 114177
[363] Huo P, Zhao P, Shi X, Zhou Z and Liu B 2020 Enhanced photocatalytic performance of electrospun hollow titanium dioxide nanofibers decorated with graphene quantum dots *J. Mater. Sci.* **56** 2138–49
[364] Li K, Ji M, Chen R, Jiang Q, Xia J and Li H 2020 Construction of nitrogen and phosphorus co-doped graphene quantum dots/Bi_5O_7I composites for accelerated charge separation and enhanced photocatalytic degradation performance *Chin. J. Catal.* **41** 1230–9
[365] Wu Y, Yan M, Gao J, Lv P, Liu X, Li C and Yan Y 2018 Fabrication of nitrogen-doped graphene quantum dots-Cu_2O catalysts for enhanced photocatalytic hydrogen evolution *Nano* **13** 1850099
[366] Shtepliuk I and Yakimova R 2023 Nature of photoexcited states in ZnO-embedded graphene quantum dots *Phys. Chem. Chem. Phys.* **25** 10525–35
[367] Xie Y, Yu S, Zhong Y, Zhang Q and Zhou Y 2018 SnO_2/graphene quantum dots composited photocatalyst for efficient nitric oxide oxidation under visible light *Appl. Surf. Sci.* **448** 655–61
[368] Wang S, Li L, Zhu Z, Zhao M, Zhang L, Zhang N, Wu Q, Wang X and Li G 2019 Remarkable improvement in photocatalytic performance for tannery wastewater processing via SnS_2 modified with N-doped carbon quantum dots: synthesis, characterization, and 4-nitrophenol-aided Cr(VI) photoreduction *Small* **15** 1804515
[369] Li F, Li M, Luo Y, Li M, Li X, Zhang J and Wang L 2018 The synergistic effect of pyridinic nitrogen and graphitic nitrogen of nitrogen-foped graphene quantum dots for enhanced TiO_2 nanocomposites' photocatalytic performance *Catalysts* **8** 438
[370] Park M, Yoon H, Lee J, Kim J, Lee J, Lee S-E, Yoo S and Jeon S 2018 Efficient solid-state photoluminescence of graphene quantum dots embedded in boron oxynitride for AC-electroluminescent device *Adv. Mater.* **30** 1802951
[371] Murali G, Reddeppa M, Seshendra Reddy C, Park S, Chandrakalavathi T, Kim M-D and In I 2020 Enhancing the charge carrier separation and transport via nitrogen-doped graphene quantum dot-TiO_2 nanoplate hybrid structure for an efficient NO gas sensor *ACS Appl. Mater. Interfaces* **12** 13428–36
[372] Luo J, Wang J, Liu S, Wu W, Jia T, Yang Z, Mu S and Huang Y 2019 Graphene quantum dots encapsulated tremella-like $NiCo_2O_4$ for advanced asymmetric supercapacitors *Carbon* **146** 1–8
[373] Kadian S, Manik G, Das N, Nehra P, Chauhan R P and Roy P 2020 Synthesis, characterization and investigation of synergistic antibacterial activity and cell viability of silver–sulfur doped graphene quantum dot (Ag@S-GQDs) nanocomposites *J. Mater. Chem.* B **8** 3028–37
[374] Sun Y, Dong H, Wu K, Chen X, Wang S, Gu W, Hong Z, Liu M, Shen Y and Lu W 2020 Graphene quantum dots coated $LiCoO_2$ for improved cycling stability and thermal safety at high voltage *J. Electroanal. Chem.* **866** 114109
[375] Yuan A, Lei H, Xi F, Liu J, Qin L, Chen Z and Dong X 2019 Graphene quantum dots decorated graphitic carbon nitride nanorods for photocatalytic removal of antibiotics *J. Colloid Interface Sci.* **548** 56–65
[376] Arumugasamy S K, Govindaraju S and Yun K 2020 Electrochemical sensor for detecting dopamine using graphene quantum dots incorporated with multiwall carbon nanotubes *Appl. Surf. Sci.* **508** 145294
[377] Wang X, Li L, Fu Z and Cui F 2018 Carbon quantum dots decorated CuS nanocomposite for effective degradation of methylene blue and antibacterial performance *J. Mol. Liq.* **268** 578–86
[378] Nguyen D A, Oh H M, Duong N T, Bang S, Yoon S J and Jeong M S 2018 Highly enhanced photoresponsivity of a monolayer WSe_2 photodetector with nitrogen-doped graphene quantum dots *ACS Appl. Mater. Interfaces* **10** 10322–9
[379] Gupta P K, Chauhan D, Khan Z H and Solanki P R 2020 ZrO_2 nanoflowers decorated with graphene quantum dots for electrochemical immunosensing *ACS Appl. Nano Mater.* **3** 2506–16
[380] Majumder T and Mondal S P 2019 Graphene quantum dots as a green photosensitizer with carbon-doped ZnO nanorods for quantum-dot-sensitized solar cell applications *Bull. Mater. Sci.* **42** 65
[381] Jiménez-López J, Llorent-Martínez E J, Ortega-Barrales P and Ruiz-Medina A 2020 Graphene quantum dots-silver nanoparticles as a novel sensitive and selective luminescence probe for the detection of glyphosate in food samples *Talanta* **207** 120344
[382] Yang W, Xu W, Zhang N, Lai X, Peng J, Cao Y and Tu J 2020 TiO_2 nanotubes modified with polydopamine and graphene quantum dots as a photochemical biosensor for

the ultrasensitive detection of glucose *J. Mater. Sci.* **55** 6105–17
[383] Ganganboina A B and Doong R-A 2019 Graphene quantum dots decorated gold-polyaniline nanowire for impedimetric detection of carcinoembryonic antigen *Sci. Rep.* **9** 7214
[384] Ran Z, Yang H, Li Z, Wang K, Zhao J, Ran X, Du G and Yang L 2020 Pillar[6]arene@AuNPs functionalized N-CQDs@Co_3O_4 hybrid composite for ultrasensitive electrochemical detection of human epididymis protein 4 *ACS Sustain. Chem. Eng.* **8** 10161–72
[385] Huang Q, Lin X, Tong L and Tong Q-X 2020 Graphene quantum dots/multiwalled carbon nanotubes composite-based electrochemical sensor for detecting dopamine release from living cells *ACS Sustain. Chem. Eng.* **8** 1644–50
[386] Esfandiari M, Kareem Abbas A, Shahbazi-Alavi H and Safaei-Ghomi J 2020 Synthesis of benzodiazepines promoted by CeO_2/CuO@nitrogen graphene quantum dots@NH_2 nanocomposite *Polycycl. Aromat. Compd.* **42** 1235–48
[387] Jiang Z, Lei Y, Zhang M, Zhang Z and Ouyang Z 2019 Graphene quantum dots-modified ternary ZnCdS semiconductor for enhancing photoelectric properties *J. Nanomater.* **2019** 1–9
[388] Chihava R, Apath D, Moyo M, Shumba M, Chitsa V and Tshuma P 2020 One-pot synthesized nickel-cobalt sulfide-decorated graphene quantum dot composite for simultaneous electrochemical determination of antiretroviral drugs: lamivudine and tenofovir disoproxil fumarate *J. Sens.* **2020** 1–13
[389] Deilam R, Moeinpour F and Mohseni-Shahri F S 2020 Catalytic performance of Cu(II)-supported graphene quantum dots modified $NiFe_2O_4$ as a proficient nano-catalyst in the synthesis of 1,2,3-triazoles *Monatsh. Fur Chem.* **151** 1153–62
[390] Sarwar S, Lin M-C, Amezaga C, Wei Z, Iyayi E, Polk H, Wang R, Wang H and Zhang X 2023 High-performance and stable hybrid photodetector based on a monolayer molybdenum disulfide (MoS_2)/nitrogen doped graphene quantum dots (NH_2 GQDs)/all-inorganic ($CsPbBr_3$) perovskite nanocrystals triple junction *Adv. Compos. Hybrid Mater.* **6** 49
[391] Tang L *et al* 2014 Deep ultraviolet to near-infrared emission and photoresponse in layered N-doped graphene quantum dots *ACS Nano* **8** 6312–20
[392] Facure M H M, Schneider R, Mercante L A and Correa D S 2020 A review on graphene quantum dots and their nanocomposites: from laboratory synthesis towards agricultural and environmental applications *Environ. Sci. Nano* **7** 3710–34
[393] Ye Y, Zou Y, Jiang Z, Yang Q, Chen L, Guo S and Chen H 2020 An effective corrosion inhibitor of N doped carbon dots for q205 steel in 1 M HCl solution *J. Alloys Compd.* **815** 152338
[394] Cheng M, Wu Z, Liu G, Zhao L, Gao Y, Li S, Zhang B, Yan X and Geyu L 2020 Carbon dots decorated hierarchical litchi-like In_2O_3 nanospheres for highly sensitive and selective NO_2 detection *Sens. Actuators* B **304** 127272
[395] Jurado-Sánchez B, Pacheco M, Rojo J and Escarpa A 2017 Magnetocatalytic graphene quantum dots Janus micromotors for bacterial endotoxin detection *Angew. Chem., Int. Ed.* **56** 6957–61
[396] Le T H, Lee D H, Kim J H and Park S J 2020 Synthesis of enhanced fluorescent graphene quantum dots for catecholamine neurotransmitter sensing *Korean J. Chem. Eng.* **37** 1000–7
[397] Mohammadi A, Rahmandoust M, Mirzajani F, Azadkhah Shalmani A and Raoufi M 2020 Optimization of the interaction of graphene quantum dots with lipase for biological applications *J. Biomed. Mater. Res.* B **108** 2471–83
[398] Perini G, Palmieri V, Ciasca G, De Spirito M and Papi M 2020 Unravelling the potential of graphene quantum dots in biomedicine and neuroscience *Int. J. Mol. Sci.* **21** 3712
[399] Kuo W-S, Chang C-Y, Huang K-S, Liu J-C, Shao Y-T, Yang C-H and Wu P-C 2020 Amino-functionalized nitrogen-doped graphene-quantum-dot-based nanomaterials with nitrogen and amino-functionalized group content dependence for highly efficient two-photon bioimaging *Int. J. Mol. Sci.* **21** 2939
[400] Ashraf G, Asif M, Aziz A, Dao A Q, Zhang T, Iftikhar T, Wang Q and Liu H 2020 Facet-energy inspired metal oxide extended hexapods decorated with graphene quantum dots: sensitive detection of bisphenol A in live cells *Nanoscale* **12** 9014–23
[401] Deng M, Cao X, Guo L, Cao H, Wen Z, Mao C, Zuo K, Chen X, Yu X and Yuan W 2020 Graphene quantum dots: efficient mechanosynthesis, white-light and broad linear excitation-dependent photoluminescence and growth inhibition of bladder cancer cells *Dalton Trans.* **49** 2308–16
[402] Yu Z, Ma W, Wu T, Wen J, Zhang Y, Wang L, He Y, Chu H and Hu M 2020 Coumarin-modified graphene quantum dots as a sensing platform for multicomponent detection and its applications in fruits and living cells *ACS Omega* **5** 7369–78
[403] Kumawat M K, Thakur M, Gurung R B and Srivastava R 2017 Graphene quantum dots for cell proliferation, nucleus imaging, and photoluminescent sensing applications *Sci. Rep.* **7**
[404] Karimi S and Namazi H 2020 Simple preparation of maltose-functionalized dendrimer/graphene quantum dots as a pH-sensitive biocompatible carrier for targeted delivery of doxorubicin *Int. J. Biol. Macromol.* **156** 648–59
[405] Santos C I M *et al* 2020 Novel hybrids based on graphene quantum dots covalently linked to glycol corroles for multiphoton bioimaging *Carbon* **166** 164–74
[406] Wang Z, Liu Z, Gu B, Gao B, Wang T, Zheng X, Wang G, Guo Q and Chen D 2020 Ultraviolet light-driven controllable doping of graphene quantum dots with tunable emission wavelength for fluorescence bio-imaging *Mater. Lett.* **266** 127468
[407] Zhao S, Song X, Chai X, Zhao P, He H and Liu Z 2020 Green production of fluorescent carbon quantum dots based on pine wood and its application in the detection of Fe^{3+} *J. Clean. Prod.* **263** 121561
[408] Fan L, Wang Y, Li L and Zhou J 2020 Carbon quantum dots activated metal organic frameworks for selective detection of Cu(II) and Fe(III) *Colloids Surf.* A **588** 124378
[409] Fan Q, Li J, Wang J, Yang Z, Shen T, Guo Y, Wang L, Irshad M S, Mei T and Wang X 2020 Ultrasensitive Fe^{3+} ion detection based on carbon quantum dot-functionalized solution-gated graphene transistors *J. Mater. Chem.* C **8** 4685–9
[410] Li D Y, Wang S P, Azad F and Su S C 2020 Single-step synthesis of polychromatic carbon quantum dots for macroscopic detection of Hg^{2+} *Ecotoxicol. Environ. Saf.* **190** 110141
[411] Wang C, Shi H, Yang M, Yan Y, Liu E, Ji Z and Fan J 2020 Facile synthesis of novel carbon quantum dots from biomass waste for highly sensitive detection of iron ions *Mater. Res. Bull.* **124** 110730
[412] Li Q, Guo Z, Zhao X, Zhang T, Chen J and Wei Y 2020 One-pot synthesis of 2,2′-dipicolylamine derived highly photoluminescent nitrogen-doped carbon quantum dots for

Fe^{3+} detection and fingermark detection *Nanotechnology* **31** 335501
[413] Ruiyi L, Tinling P, Hongxia C, Jinsong S and Zaijun L 2020 Electrochemical detection of cancer cells in human blood using folic acid and glutamic acid-functionalized graphene quantum dot-palladium@gold as redox probe with excellent electrocatalytic activity and target recognition *Sens. Actuators* B **309** 127709
[414] Kadian S, Manik G, Das N and Roy P 2020 Targeted bioimaging and sensing of folate receptor-positive cancer cells using folic acid-conjugated sulfur-doped graphene quantum dots *Microchim. Acta* **187** 1–10
[415] Barati F, Arpanaei A and Mahmoudifard M 2020 Highly efficient detection of cancer-derived exosomes using modified core–shell electrospun nanofibers as a capture substrate and antibody immobilized-graphene quantum dots as a signaling agent *Anal. Methods* **12** 3670–81
[416] Iannazzo D, Celesti C and Espro C 2020 Recent advances on graphene quantum dots as multifunctional nanoplatforms for cancer treatment *Biotechnol. J.* **16** 1900422
[417] Lee B H, Hasan M T, Lichthardt D, Gonzalez-Rodriguez R and Naumov A V 2021 Manganese–nitrogen and gadolinium–nitrogen co-doped graphene quantum dots as bimodal magnetic resonance and fluorescence imaging nanoprobes *Nanotechnology* **32** 095103
[418] Pooresmaeil M, Namazi H and Salehi R 2020 Synthesis of photoluminescent glycodendrimer with terminal β-cyclodextrin molecules as a biocompatible pH-sensitive carrier for doxorubicin delivery *Carbohydr. Polym.* **246** 116658
[419] Dolatkhah M, Hashemzadeh N, Barar J, Adibkia K, Aghanejad A, Barzegar-Jalali M and Omidi Y 2020 Graphene-based multifunctional nanosystems for simultaneous detection and treatment of breast cancer *Colloids Surf.* B **193** 111104
[420] Muthusankar G, Devi R K and Gopu G 2020 Nitrogen-doped carbon quantum dots embedded Co_3O_4 with multiwall carbon nanotubes: an efficient probe for the simultaneous determination of anticancer and antibiotic drugs *Biosens. Bioelectron.* **150** 111947
[421] Ghorai S, Roy I, De S, Dash P S, Basu A and Chattopadhyay D 2020 Exploration of the potential efficacy of natural resource-derived blue-emitting graphene quantum dots in cancer therapeutic applications *New J. Chem.* **44** 5366–76
[422] Zheng S, Jin Z, Han C, Li J, Xu H, Park S, Park J-O, Choi E and Xu K 2019 Graphene quantum dots-decorated hollow copper sulfide nanoparticles for controlled intracellular drug release and enhanced photothermal-chemotherapy *J. Mater. Sci.* **55** 1184–97
[423] Sung S-Y, Su Y-L, Cheng W, Hu P-F, Chiang C-S, Chen W-T and Hu S-H 2018 Graphene quantum dots-mediated theranostic penetrative delivery of drug and photolytics in deep tumors by targeted biomimetic nanosponges *Nano Lett.* **19** 69–81
[424] Gao T, Wang X, Zhao J, Jiang P, Jiang F-L and Liu Y 2020 Bridge between temperature and light: bottom-up synthetic route to structure-defined graphene quantum dots as a temperature probe in vitro and in cells *ACS Appl. Mater. Interfaces* **12** 22002–11
[425] Zhang H, Ba S, Yang Z, Wang T, Lee J Y, Li T and Shao F 2020 Graphene quantum dot-based nanocomposites for diagnosing cancer biomarker APE1 in living cells *ACS Appl. Mater. Interfaces* **12** 13634–43
[426] Hashemi M S, Gharbi S, Jafarinejad-Farsangi S, Ansari-Asl Z and Dezfuli A S 2020 Secondary toxic effect of graphene oxide and graphene quantum dots alters the expression of miR-21 and miR-29a in human cell lines *Toxicol. In Vitro* **65** 104796
[427] Su W, Guo R, Yuan F, Li Y, Li X, Zhang Y, Zhou S and Fan L 2020 Red-emissive carbon quantum dots for nuclear drug delivery in cancer stem cells *J. Phys. Chem. Lett.* **11** 1357–63
[428] Xin Q, Jia X, Nawaz A, Xie W, Li L and Gong J R 2020 Mimicking peroxidase active site microenvironment by functionalized graphene quantum dots *Nano Res.* **13** 1427–33
[429] Jeong S, Pinals R L, Dharmadhikari B, Song H, Kalluri A, Debnath D, Wu Q, Ham M-H, Patra P and Landry M P 2020 Graphene quantum dot oxidation governs noncovalent biopolymer adsorption *Sci. Rep.* **10** 7074
[430] Kim D *et al* 2018 Graphene quantum dots prevent α-synucleinopathy in Parkinson's disease *Nat. Nanotechnol.* **13** 812–8
[431] Du J, Feng B, Dong Y, Zhao M and Yang X 2020 Vanadium coordination compounds loaded on graphene quantum dots (GQDs) exhibit improved pharmaceutical properties and enhanced anti-diabetic effects *Nanoscale* **12** 9219–30
[432] Jiang X L, Liu J H, Que Y T, Que Y M, Hu P P, Huang C Z and Tong X Y 2019 Multifunctional single-layered graphene quantum dots used for diagnosis of mitochondrial malfunction-related diseases *ACS Biomater. Sci. Eng.* **6** 1727–34
[433] Rakhshaei R, Namazi H, Hamishehkar H and Rahimi M 2020 Graphene quantum dot cross-linked carboxymethyl cellulose nanocomposite hydrogel for pH-sensitive oral anticancer drug delivery with potential bioimaging properties *Int. J. Biol. Macromol.* **150** 1121–9
[434] Li Y, Dong H, Tao Q, Ye C, Yu M, Li J, Zhou H, Yang S, Ding G and Xie X 2020 Enhancing the magnetic relaxivity of MRI contrast agents via the localized superacid microenvironment of graphene quantum dots *Biomaterials* **250** 120056
[435] Kappen J, Ponkarpagam S and John S A 2020 Study on the interactions between graphene quantum dots and Hg(II): unraveling the origin of photoluminescence quenching of graphene quantum dots by Hg(II) *Colloids Surf.* A **591** 124551
[436] Yang Y, Xing X, Zou T, Wang Z, Zhao R, Hong P, Peng S, Zhang X and Wang Y 2020 A novel and sensitive ratiometric fluorescence assay for carbendazim based on N-doped carbon quantum dots and gold nanocluster nanohybrid *J. Hazard. Mater.* **386** 121958
[437] Ren Q, Ga L and Ai J 2019 Rapid synthesis of highly fluorescent nitrogen-doped graphene quantum dots for effective detection of ferric ions and as fluorescent ink *ACS Omega* **4** 15842–8
[438] Mohagheghpour E, Farzin L and Sadjadi S 2023 Alendronate-functionalized graphene quantum dots as an effective fluorescent sensing platform for arsenic ion detection *Biol. Trace Elem. Res.* (https://doi.org/10.1007/s12011-023-03819-5)
[439] Wang Z, Chen D, Gu B, Gao B, Liu Z, Yang Y, Guo Q, Zheng X and Wang G 2020 Yellow emissive nitrogen-doped graphene quantum dots as a label-free fluorescent probe for Fe^{3+} sensing and bioimaging *Diam. Relat. Mater.* **104** 107749
[440] Fan Q, Li J, Zhu Y, Yang Z, Shen T, Guo Y, Wang L, Mei T, Wang J and Wang X 2020 Functional carbon quantum dots for highly sensitive graphene transistors for Cu^{2+} ion detection *ACS Appl. Mater. Interfaces* **12** 4797–803
[441] Tung F-I, Zheng L-J, Hou K-T, Chiang C-S, Chen M-H and Liu T-Y 2020 One-stop radiotherapeutic targeting of primary and distant osteosarcoma to inhibit cancer progression and metastasis using 2DG-grafted graphene quantum dots *Nanoscale* **12** 8809–18
[442] Feng S, Pan J, Li C and Zheng Y 2020 Folic acid-conjugated nitrogen-doped graphene quantum dots as a fluorescent

diagnostic material for MCF-7 cells *Nanotechnology* **31** 135701
[443] Wang Z, Chen D, Gu B, Gao B, Wang T, Guo Q and Wang G 2020 Biomass-derived nitrogen doped graphene quantum dots with color-tunable emission for sensing, fluorescence ink and multicolor cell imaging *Spectrochim. Acta* A **227** 117671
[444] Wu T, Liang X, Liu X, Li Y, Wang Y, Kong L and Tang M 2020 Induction of ferroptosis in response to graphene quantum dots through mitochondrial oxidative stress in microglia *Part. Fibre Toxicol.* **17**
[445] Kuo W-S *et al* 2023 Single-sized N-functionality graphene quantum dot in tunable dual-modality near infrared–I/II illumination detection and photodynamic therapy under multiphoton nonlinear excitation *Biosens. Bioelectron.* **241** 115648
[446] Cheng R, Yu C, Zhen Z, Tang S and Ou S 2020 Understanding the selective-sensing mechanism of lysine by fluorescent nanosensors based on graphene quantum dots *Spectrochim. Acta* A **242** 118732
[447] Sun B, Wang Y, Li D, Li W, Gou X, Gou Y and Hu F 2020 Development of a sensitive electrochemical immunosensor using polyaniline functionalized graphene quantum dots for detecting a depression marker *Mater. Sci. Eng.* C **111** 110797
[448] Fu -C-C, Hsieh C-T, Juang R-S, Gu S, Gandomi Y A, Kelly R E and Kihm K D 2020 Electrochemical sensing of mercury ions in electrolyte solutions by nitrogen-doped graphene quantum dot electrodes at ultralow concentrations *J. Mol. Liq.* **302** 112593
[449] Hong G-L, Deng H-H, Zhao H-L, Zou Z-Y, Huang K-Y, Peng H-P, Liu Y-H and Chen W 2020 Gold nanoclusters/graphene quantum dots complex-based dual-emitting ratiometric fluorescence probe for the determination of glucose *J. Pharm. Biomed. Anal.* **189** 113480
[450] Xia M, Zhao X-E, Sun J, Zheng Z and Zhu S 2020 Graphene quantum dots combined with the oxidase-mimicking activity of Ce^{4+} for ratiometric fluorescent detection of Ce^{4+} and alendronate sodium *Sens. Actuators* B **319** 128321
[451] Sheng L, Huangfu B, Xu Q, Tian W, Li Z, Meng A and Tan S 2020 A highly selective and sensitive fluorescent probe for detecting Cr(VI) and cell imaging based on nitrogen-doped graphene quantum dots *J. Alloys Compd.* **820** Sricharoen P, Limchoowong N, Nuengmatcha P and Chanthai S 2020 Ultrasonic-assisted recycling of Nile tilapia fish scale biowaste into low-cost nano-hydroxyapatite: Ultrasonic-assisted adsorption for Hg^{2+} removal from aqueous solution followed by "turn-off" fluorescent sensor based on Hg^{2+}-graphene quantum dots *Ultrason. Sonochem.***63**
[452] Sun D, Liu T, Wang C, Yang L, Yang S and Zhuo K 2020 Hydrothermal synthesis of fluorescent carbon dots from gardenia fruit for sensitive on-off-on detection of Hg^{2+} and cysteine *Spectrochim. Acta* A **240** 118598
[453] Chu X, Wang S and Cao Y 2020 A new fluorescence probe comprising nitrogen-doped graphene quantum dots for the selective and quantitative determination of cerium(IV) *New J. Chem.* **44** 797–806
[454] Nsibande S A and Forbes B C F 2020 Development of a turn-on graphene quantum dot-based fluorescent probe for sensing of pyrene in water *RSC Adv.* **10** 12119–28
[455] Le T H, Lee H J, Kim J H and Park S J 2020 Highly selective fluorescence sensor based on graphene quantum dots for sulfamethoxazole determination *Materials* **13** 2521
[456] Pinilla-Peñalver E, Soriano M L, Durán G M, Llorent-Martínez E J, Contento A M and Ríos Á 2020 Discrimination between nanocurcumin and free curcumin using graphene quantum dots as a selective fluorescence probe *Microchim. Acta* **187** 1–11
[457] Sharma S, Singh N, Nepovimova E, Korabecny J, Kuca K, Satnami M L and Ghosh K K 2019 Interaction of synthesized nitrogen enriched graphene quantum dots with novel anti-Alzheimer's drugs: spectroscopic insights *J. Biomol. Struct. Dyn.* **38** 1–16
[458] Batool M, Hussain D, Akrem A, Najam-ul-haq M, Saeed S, Zaka S M, Nawaz M S, Buck F and Saeed Q 2020 Graphene quantum dots as cysteine protease nanocarriers against stored grain insect pests *Sci. Rep.* **10** 3444
[459] Zhao C, Wu L, Wang X, Weng S, Ruan Z, Liu Q, Lin L and Lin X 2020 Quaternary ammonium carbon quantum dots as an antimicrobial agent against gram-positive bacteria for the treatment of MRSA-infected pneumonia in mice *Carbon* **163** 70–84
[460] Li P *et al* 2020 Carbon quantum dots derived from lysine and arginine simultaneously scavenge bacteria and promote tissue repair *Appl. Mater. Today* **19** 100601
[461] Malmir S, Karbalaei A, Pourmadadi M, Hamedi J, Yazdian F and Navaee M 2020 Antibacterial properties of a bacterial cellulose CQD-TiO_2 nanocomposite *Carbohydr. Polym.* 234
[462] Wang K, Liang L, Xu J, Li H, Du M, Zhao X, Zhang D, Feng H and Fan H 2019 Synthesis and bacterial inhibition of novel Ag_2S–N–CQD composite material *Chem. Pap.* **74** 1517–24
[463] Lee B *et al* 2020 Graphene quantum dots as anti-inflammatory therapy for colitis *Sci. Adv.* **6** z2630
[464] Wang N, Xu H, Sun S, Guo P, Wang Y, Qian C, Zhong Y and Yang D 2020 Wound therapy via a photo-responsively antibacterial nano-graphene quantum dots conjugate *J. Photochem. Photobiol.* B **210** 111978
[465] Yang S, Chu M, Du J, Li Y, Gai T, Tan X, Xia B and Wang S 2020 Graphene quantum dot electrochemiluminescence increase by bio-generated H_2O_2 and its application in direct biosensing *R. Soc. Open Sci.* **7** 191404
[466] Dos Reis S R R, Pinto S R, de Menezes F D, Martinez-Manez R, Ricci-Junior E, Alencar L M R, Helal-Neto E, da Silva de Barros A O, Lisboa P C and Santos-Oliveira R 2020 Senescence and the impact on biodistribution of different nanosystems: the discrepancy on tissue deposition of graphene quantum dots, polycaprolactone nanoparticle and magnetic mesoporous silica nanoparticles in young and elder animals *Pharm. Res.* **37** 1–12
[467] Shin D H, Jang C W, Ko J S and Choi S-H 2021 Enhancement of efficiency and stability in organic solar cells by employing MoS_2 transport layer, graphene electrode, and graphene quantum dots-added active layer *Appl. Surf. Sci.* **538** 148155
[468] Gao F, Yang C-L and Jiang G 2021 Effects of the coupling between electrode and GQD-anthoxanthin nanocomposites for dye-sensitized solar cell: DFT and TD-DFT investigations *J. Photochem. Photobiol.* A **407** 113080
[469] Gaffney E *et al* 2020 The role of GQDs additive in TiO_2 nanorods as an electron transfer layer on performance improvement of the perovskite solar cells *Electrochim. Acta* **337**
[470] Peter I J, Rajamanickam N, Vijaya S, Anandan S, Ramachandran K and Nithiananthi P 2020 TiO_2/graphene quantum dots core-shell based photo anodes with TTIP treatment–a perspective way of enhancing the short circuit current *Sol. Energy Mater. Sol. Cells* **205** 110239
[471] Shin D H, Shin S H, Kim S and Choi S-H 2020 High-performance and -stability graphene quantum dots-mixed conducting polymer/porous Si hybrid solar

cells with titanium oxide passivation layer *Nanotechnology* **31** 095202
[472] Geng C, Shang Y, Qiu J, Wang Q, Chen X, Li S, Ma W, Fan H-J, Omer A-A-A and Chen R 2020 Carbon quantum dots interfacial modified graphene/silicon Schottky barrier solar cell *J. Alloys Compd.* **835** 155268
[473] Pei H, Zhang H, Mo Z, Guo R, Liu N, Jia Q and Gao Q 2020 Highly efficient photocatalytic degradation of rhodamine B by conical graphene quantum dots/cerium oxide composite *Ceram. Int.* **46** 3827–36
[474] Zhou Q, Song Y, Li N, Chen D, Xu Q, Li H, He J and Lu J 2020 Direct dual Z-scheme Bi_2WO_6/GQDs/WO_3 inverse opals for enhanced photocatalytic activities under visible light *ACS Sustain. Chem. Eng.* **8** 7921–7
[475] Zhu J *et al* 2022 Graphene quantum dot inlaid carbon nanofibers: revealing the edge activity for ultrahigh rate pseudocapacitive energy storage *Energy Storage Mater.* **47** 158–66
[476] Zhang L, Xue J, Long L, Yang L, Liu F, Lv F, Kong W and Liu J 2020 Synergistic effect of nitrogen-doping and graphene quantum dot coupling for high-efficiency hydrogen production based on titanate nanotubes *Nanotechnology* **31** 115705
[477] Liao D *et al* 2023 Efficient photoelectrochemical aptasensing of di-2-ethylhexyl phthalate in environmental samples based on N, S co-doped graphene quantum dots/TiO_2 nanorods *Anal. Chim. Acta* **1271** 341477
[478] Zhu J, Dong Y, Zhang S and Fan Z 2020 Application of carbon-/graphene quantum dots for supercapacitors *Acta Phys. Chim. Sin.* **36** 1903052–0
[479] Payami E and Teimuri-Mofrad R 2023 Development of ternary nanocomposite based on ferrocenyl-modified graphene quantum dots for high-performance energy storage applications *J. Energy Storage* **72** 108346
[480] Qing Y *et al* 2019 Boosting the supercapacitor performance of activated carbon by constructing overall conductive networks using graphene quantum dots *J. Mater. Chem.* A **7** 6021–7
[481] Camellini A, Rebecchi L, Rubino A, Niu W, Kim S W, Ma J, Feng X and Kriegel I 2023 Improving the stability of photodoped metal oxide nanocrystals with electron donating graphene quantum dots *Nanoscale* **15** 17138–46
[482] Liu W *et al* 2020 Graphene quantum dots-based advanced electrode materials: design, synthesis and their applications in electrochemical energy storage and electrocatalysis *Adv. Energy Mater.* **10**
[483] Zhang X, Liu Y, Kuan C-H, Tang L, Krueger T D, Yeasmin S, Ullah A, Fang C and Cheng L-J 2023 Highly fluorescent nitrogen-doped carbon dots with large Stokes shifts *J. Mater. Chem.* C **11** 11476–85
[484] Yuan F *et al* 2019 Bright high-colour-purity deep-blue carbon dot light-emitting diodes via efficient edge amination *Nat. Photon.* **14** 171–6
[485] Li X, Wang Z, Liu Y, Zhang W, Zhu C and Meng X 2020 Bright tricolor ultrabroad-band emission carbon dots for white light-emitting diodes with a 96.5 high color rendering index *J. Mater. Chem.* C **8** 1286–91
[486] Jin L *et al* 2020 Orange-red, green, and blue fluorescence carbon dots for white light emitting diodes *J. Mater. Sci. Technol.* **50** 184–91
[487] Chen H, Luo Q, Liu T, Tai M, Lin J, Murugadoss V, Lin H, Wang J, Guo Z and Wang N 2020 Boosting multiple interfaces by co-doped graphene quantum dots for high efficiency and durability perovskite solar cells *ACS Appl. Mater. Interfaces* **12** 13941–9
[488] Yang L, Li Y, Wang L, Pei Y, Wang Z, Zhang Y, Lin H and Li X 2020 Exfoliated fluorographene quantum dots as outstanding passivants for improved flexible perovskite solar cells *ACS Appl. Mater. Interfaces* **12** 22992–3001
[489] Tsai K-A, Hsieh P-Y, Lai T-H, Tsao C-W, Pan H, Lin Y-G and Hsu Y-J 2020 Nitrogen-doped graphene quantum dots for remarkable solar hydrogen production *ACS Appl. Energy Mater.* **3** 5322–32
[490] Dejpasand M T, Saievar-Iranizad E, Bayat A, Montaghemi A and Ardekani S R 2020 Tuning HOMO and LUMO of three region (UV, Vis and IR) photoluminescent nitrogen doped graphene quantum dots for photodegradation of methylene blue *Mater. Res. Bull.* **128** 110886
[491] Pang S *et al* 2020 Boosting performance of perovskite solar cells with graphene quantum dots decorated SnO_2 electron transport layers *Appl. Surf. Sci.* **507** 145099
[492] Jahantigh F, Ghorashi S M B and Mozaffari S 2020 Orange photoluminescent N-doped graphene quantum dots as an effective co-sensitizer for dye-sensitized solar cells *J. Solid State Electrochem.* **24** 883–9
[493] Jahantigh F, Ghorashi S M B and Bayat A 2020 Hybrid dye sensitized solar cell based on single layer graphene quantum dots *Dyes Pigm.* **175** 108118
[494] Saedi A, Moradi A M, Kimiagar S and Panahi H A 2020 Efficiency enhancement of dye-sensitized solar cells based on gracilaria/ulva using graphene quantum dot *Int. J. Environ. Res.* **14** 393–402
[495] Ebrahimi M, Kermanpur A, Atapour M, Adhami S, Heidari R H, Khorshidi E, Irannejad N and Rezaie B 2020 Performance enhancement of mesoscopic perovskite solar cells with GQDs-doped TiO_2 electron transport layer *Sol. Energy Mater. Sol. Cells* **208** 110407
[496] Wang Z, Rong X, Wang L, Wang W, Lin H and Li X 2020 Dual role of amino-functionalized graphene quantum dots in NiO_x Films for efficient inverted flexible perovskite solar cells *ACS Appl. Mater. Interfaces* **12** 8342–50
[497] Zhou Y, Yang S, Yin X, Han J, Tai M, Zhao X, Chen H, Gu Y, Wang N and Lin H 2019 Enhancing electron transport via graphene quantum dot/SnO_2 composites for efficient and durable flexible perovskite photovoltaics *J. Mater. Chem.* A **7** 1878–88
[498] Kim J K, Nguyen D N, Lee J-H, Kang S, Kim Y, Kim S-S and Kim H-K 2020 Carbon quantum dot-incorporated nickel oxide for planar p-i-n type perovskite solar cells with enhanced efficiency and stability *J. Alloys Compd.* **818** 152887
[499] Zhao X, Wu Y, Xia Z, Chang S, Shang Y and Cao A 2021 A GQD-based composite film as photon down-converter in CNT/Si solar cells *Nano Res.* **14** 3893–9
[500] Fan W, Li H, Zhang H, Cai L, Wang J, Wang X, Wang Y, Tang Y and Song Y 2021 Study on the influence of embedded structure of carbon quantum dots of the organic solar cells with the territory active layer structure of P3HT: PC61BM: cQDs *J. Mater. Sci., Mater. Electron.* **32** 2293–301
[501] Ahmed D S, Mohammed M K A and Majeed S M 2020 Green synthesis of eco-friendly graphene quantum dots for highly efficient perovskite solar cells *ACS Appl. Energy Mater.* **3** 10863–71
[502] Mustafa M N and Sulaiman Y 2020 Fully flexible dye-sensitized solar cells photoanode modified with titanium dioxide-graphene quantum dot light scattering layer *Sol. Energy* **212** 332–8
[503] Ouarrad H, Ramadan F Z and Drissi L B 2020 Engineering silicon-carbide quantum dots for third generation photovoltaic cells *Opt. Express* **28** 36656
[504] Saeidi S, Rezaei B, Irannejad N and Ensafi A A 2020 Efficiency improvement of luminescent solar concentrators using upconversion nitrogen-doped graphene quantum dots *J. Power Sources* **476** 228647
[505] Sabetghadam S A, Hosseini Z, Zarei S and Ghanbari T 2020 Improvement of the current generation in silicon solar

cells by utilizing graphene quantum dot as spectral converter *Mater. Lett.* **279** 128515
[506] Zhang F, Yang C, Wang X-X, Li R, Wan Z, Wang X, Wan Y, Long Y-Z and Cai Z 2020 Graphene quantum dots doped PVDF(TBT)/PVP(TBT) fiber film with enhanced photocatalytic performance *Appl. Sci.* **10** 596
[507] Han M, Zhu S, Xia C and Yang B 2022 Photocatalytic upcycling of poly(ethylene terephthalate) plastic to high-value chemicals *Appl. Catal.* B **316** 121662
[508] Kanwal S, Jahan S and Mansoor F 2020 An ultrasonic-assisted synthesis of leather-derived luminescent graphene quantum dots: catalytic reduction and switch on–off probe for nitro-explosives *RSC Adv.* **10** 22959–65
[509] Sajjadizadeh H-S, Goharshadi E K and Karimi-Nazarabad M 2024 Highly efficient photoanode in visible light water splitting through development of Z-scheme structure between compositing TiO_2 with GQDs and Ba doped VO_2 (m) with smart selection of Ag nanoparticles sites *Fuel* **355** 129544
[510] Esmaeilzadeh M, Sadjadi S and Salehi Z 2020 Pd immobilized on hybrid of magnetic graphene quantum dots and cyclodextrin decorated chitosan: an efficient hydrogenation catalyst *Int. J. Biol. Macromol.* **150** 441–8
[511] Li S, Chen Z, Wu D, Qin Y and Kong Y 2020 Graphene quantum dots enhanced photocatalytic activity of Sb_2WO_6 under ultraviolet- and visible-light irradiation *Bull. Korean Chem. Soc.* **41** 552–7
[512] Lee H, Anwer H and Park J-W 2020 Graphene quantum dots on stainless-steel nanotubes for enhanced photocatalytic degradation of phenanthrene under visible light *Chemosphere* **246** 125761
[513] Liu N, Tang M, Wu J, Tang L, Huang W, Li Q, Lei J, Zhang X and Wang L 2020 Boosting visible-light photocatalytic performance for CO_2 reduction via hydroxylated graphene quantum dots sensitized MIL-101(Fe) *Adv. Mater. Interfaces* **7** 2000468
[514] Wang C, Zheng F, Zhang L, Yang J and Dong P 2023 Insight into the role of graphene quantum dots on the boosted photocatalytic H_2 production performance of a covalent organic framework *Appl. Surf. Sci.* **640** 158383
[515] Shin D H, Shin S H, Lee S G, Kim S and Choi S-H 2019 High-detectivity/-speed flexible and self-powered graphene quantum dots/perovskite photodiodes *ACS Sustain. Chem. Eng.* **7** 19961–8
[516] Ma Y *et al* 2018 Enhancing the performance of inverted perovskite solar cells via grain boundary passivation with carbon quantum dots *ACS Appl. Mater. Interfaces* **11** 3044–52
[517] Diao S, Zhang X, Shao Z, Ding K, Jie J and Zhang X 2017 12.35% efficient graphene quantum dots/silicon heterojunction solar cells using graphene transparent electrode *Nano Energy* **31** 359–66
[518] Huang J, Chen W, Yu X, Fu X, Zhu Y and Zhang Y 2020 Fabrication of a ternary BiOCl/CQDs/rGO photocatalyst: the roles of CQDs and rGO in adsorption-photocatalytic removal of ciprofloxacin *Colloids Surf.* A **597** 124758
[519] Chang Y-S, Hsieh P-Y, Mark Chang T-F, Chen C-Y, Sone M and Hsu Y-J 2020 Incorporating graphene quantum dots to enhance the photoactivity of CdSe-sensitized TiO_2 nanorods for solar hydrogen production *J. Mater. Chem.* A **8** 13971–9
[520] Xue J, Long L, Zhang L, Luo H, Yang L, Liu F, Lv F, Kong W and Liu J 2020 Enhanced H_2 evolution and the interfacial electron transfer mechanism of titanate nanotube sensitized with CdS quantum dots and graphene quantum dots *Int. J. Hydrog. Energy* **45** 6476–86
[521] Ibarbia A, Grande H J and Ruiz V 2020 On the factors behind the photocatalytic activity of graphene quantum dots for organic dye degradation *Part. Part. Syst. Charact.* **37** 2000061
[522] Pedrozo-Penafiel M J, Miranda-Andrades J R, Gutierrez-Beleño L M, Larrudé D G and Aucelio R Q 2020 Indirect voltammetric determination of thiomersal in influenza vaccine using photo-degradation and graphene quantum dots modified glassy carbon electrode *Talanta* **215** 120938
[523] Karimi H, Rajabi H R and Kavoshi L 2020 Application of decorated magnetic nanophotocatalysts for efficient photodegradation of organic dye: a comparison study on photocatalytic activity of magnetic zinc sulfide and graphene quantum dots *J. Photochem. Photobiol.* A **397** 112534
[524] Xu T, Wang D, Dong L, Shen H, Lu W and Chen W 2019 Graphitic carbon nitride co-modified by zinc phthalocyanine and graphene quantum dots for the efficient photocatalytic degradation of refractory contaminants *Appl. Catal.* B **244** 96–106
[525] Yoshino A 2012 The birth of the lithium-ion battery *Angew. Chem., Int. Ed.* **51** 5798–800
[526] Li Z, Bu F, Wei J, Yao W, Wang L, Chen Z, Pan D and Wu M 2018 Boosting the energy storage densities of supercapacitors by incorporating N-doped graphene quantum dots into cubic porous carbon *Nanoscale* **10** 22871–83
[527] Zhang W, Yang Y, Xia R, Li Y, Zhao J, Lin L, Cao J, Wang Q, Liu Y and Guo H 2020 Graphene-quantum-dots-induced MnO_2 with needle-like nanostructure grown on carbonized wood as advanced electrode for supercapacitors *Carbon* **162** 114–23
[528] Qiu H, Sun X, An S, Lan D, Cui J, Zhang Y and He W 2020 Microwave synthesis of histidine-functionalized graphene quantum dots/Ni-Co LDH with flower ball structure for supercapacitor *J. Colloid Interface Sci.* **567** 264–73
[529] Pang Y, Wei J, Wang Y and Xia Y 2018 Synergetic protective effect of the ultralight MWCNTs/NCQDs modified separator for highly stable lithium–sulfur batteries *Adv. Energy Mater.* **8** 1702288
[530] Hsiao Y-J and Lin L-Y 2020 Enhanced surface area, graphene quantum dots, and functional groups for the simple acid-treated carbon fiber electrode of flexible fiber-type solid-state supercapacitors without active materials *ACS Sustain. Chem. Eng.* **8** 2453–61
[531] Hu Y, Chen W, Lei T, Jiao Y, Wang H, Wang X, Rao G, Wang X, Chen B and Xiong J 2020 Graphene quantum dots as the nucleation sites and interfacial regulator to suppress lithium dendrites for high-loading lithium-sulfur battery *Nano Energy* **68** 104373
[532] Zhao X, Wu Y, Wang Y, Wu H, Yang Y, Wang Z, Dai L, Shang Y and Cao A 2020 High-performance Li-ion batteries based on graphene quantum dot wrapped carbon nanotube hybrid anodes *Nano Res.* **13** 1044–52
[533] Vijaya Kumar Saroja A P, Garapati M S, ShyiamalaDevi R, Kamaraj M and Ramaprabhu S 2020 Facile synthesis of heteroatom doped and undoped graphene quantum dots as active materials for reversible lithium and sodium ions storage *Appl. Surf. Sci.* **504** 144430
[534] Jia H, Cai Y, Lin J, Liang H, Qi J, Cao J, Feng J and Fei W 2018 Heterostructural graphene quantum dot/MnO_2 nanosheets toward high-potential window electrodes for high-performance supercapacitors *Adv. Sci.* **5** 1700887
[535] Singh A, Kumar S and Ojha A K 2020 Charcoal derived graphene quantum dots for flexible supercapacitor oriented applications *New J. Chem.* **44** 11085–91
[536] Li Z, Liu X, Wang L, Bu F, Wei J, Pan D and Wu M 2018 Hierarchical 3D all-carbon composite structure modified with N-doped graphene quantum dots for high-performance flexible supercapacitors *Small* **14**

[537] Chang H-W *et al* 2020 $NiCo_2O_4$/graphene quantum dots (GQDs) for use in efficient electrochemical energy devices: an electrochemical and x-ray absorption spectroscopic investigation *Catal. Today* **348** 290–8

[538] Ramadan A, Anas M, Ebrahim S, Soliman M and Abou-Aly A 2020 Effect of Co-doped graphene quantum dots to polyaniline ratio on performance of supercapacitor *J. Mater. Sci., Mater. Electron.* **31** 7247–59

[539] Yao W, Ren J, Mao J, Wang L, Chen Z, Pan D, Wu M and Li Z 2020 N-doped graphene quantum dots supported by carbon nanotubes grown on carbon clothes for lithium storage *J. Electrochem. Soc.* **167** 060513

[540] Pattarapongdilok N and Parasuk V 2020 Adsorptions of lithium ion/atom and packing of Li ions on graphene quantum dots: application for Li-ion battery *Comput. Theor. Chem.* **1177** 112779

[541] Li Y, Wu F, Jin X, Xu H, Liu X and Shi G 2020 Preparation and electrochemical properties of graphene quantum dots/biomass activated carbon electrodes *Inorg. Chem. Commun.* **112** 107718

[542] Sim Y *et al* 2020 The synergistic effect of nitrogen and fluorine co-doping in graphene quantum dot catalysts for full water splitting and supercapacitor *Appl. Surf. Sci.* **507** 145157

[543] Rahimpour K and Teimuri-Mofrad R 2020 Novel hybrid supercapacitor based on ferrocenyl modified graphene quantum dot and polypyrrole nanocomposite *Electrochim. Acta* **345** 136207

[544] Santana E R and Spinelli A 2020 Electrode modified with graphene quantum dots supported in chitosan for electrochemical methods and non-linear deconvolution of spectra for spectrometric methods: approaches for simultaneous determination of triclosan and methylparaben *Microchim. Acta* **187** 1–12

[545] Zhang Z, Lei Y, Zhao L, Jiang Z and Ouyang Z 2018 Graphene quantum dots decorated Al-doped ZnS for improved photoelectric performance *Materials* **11** 1452

[546] Ma Y, Yuan W, Bai Y, Wu H and Cheng L 2019 The toughening design of pseudocapacitive materials via graphene quantum dots: towards enhanced cycling stability for supercapacitors *Carbon* **154** 292–300

[547] Bao Y, Liu P, Zhang J, Wang L, Wang M, Mei H, Zhang Q, Chen C and Xiao Z 2020 Construction of carbon quantum dots embed α-Co/$Ni(OH)_2$ hollow nanocages with enhanced supercapacitor performance *J. Am. Ceram. Soc.* **103** 4342–51

[548] Liu F, Wang Y, Zhang Y, Lin J, Su Q, Shi J, Xie X, Liang S and Pan A 2020 A facile carbon quantum dot-modified reduction approach towards tunable Sb@CQDs nanoparticles for high performance sodium storage *Batter. Supercaps* **3** 463–9

[549] Kumar Y R, Deshmukh K, Sadasivuni K K and Pasha S K K 2020 Graphene quantum dot based materials for sensing, bio-imaging and energy storage applications: a review *RSC Adv.* **10** 23861–98

[550] Wang X-F, Wang G-G, Li J-B, Liu Z, Chen Y-X, Liu L-F and Han J-C 2019 Direct white emissive Cl-doped graphene quantum dots-based flexible film as a single luminophore for remote tunable UV-WLEDs *Chem. Eng. J.* **361** 773–82

[551] Shan H *et al* 2019 Electron transfer and cascade relaxation dynamics of graphene quantum dots/MoS_2 monolayer mixed-dimensional van der Waals heterostructures *Mater. Today* **24** 10–16

[552] Luo C, Xie H, Hou C, Zhang Q, Li Y and Wang H 2018 Flexible photodetector based on cotton coated with reduced graphene oxide and sulfur and nitrogen co-doped graphene quantum dots *J. Mater. Sci.* **54** 3242–51

[553] El Fatimy A, Myers-Ward R L, Boyd A K, Daniels K M, Gaskill D K and Barbara P 2016 Epitaxial graphene quantum dots for high-performance terahertz bolometers *Nat. Nanotechnol.* **11** 335–8

[554] Zhu W *et al* 2020 Graphene quantum dot-decorated vertically oriented graphene/germanium heterojunctions for near-infrared photodetectors *ACS Appl. Nano Mater.* **3** 6915–24

[555] Thakur M K, Fang C-Y, Yang Y-T, Effendi T A, Roy P K, Chen R-S, Ostrikov K K, Chiang W-H and Chattopadhyay S 2020 Microplasma-enabled graphene quantum dot-wrapped gold nanoparticles with synergistic enhancement for broad band photodetection *ACS Appl. Mater. Interfaces* **12** 28550–60

[556] Jang C W, Shin D H and Choi S-H 2019 Highly-flexible and -stable deep-ultraviolet photodiodes made of graphene quantum dots sandwiched between graphene layers *Dyes Pigm.* **163** 238–42

[557] Pramanik A, Biswas S, Tiwary C S, Sarkar R and Kumbhakar P 2018 Colloidal N-doped graphene quantum dots with tailored luminescent downshifting and detection of UVA radiation with enhanced responsivity *ACS Omega* **3** 16260–70

[558] Hasan M T, Gonzalez-Rodriguez R, Ryan C, Coffer J L and Naumov A V 2019 Variation of optical properties of nitrogen-doped graphene quantum dots with short/mid/long-wave ultraviolet for the development of the UV photodetector *ACS Appl. Mater. Interfaces* **11** 39035–45

[559] Hu X, Zhu W, Zhao M, Wang G, Yang S, Liu Z, Zheng L, Guo Q, Chen D and Ding G 2019 Graphene quantum dots promoted the synthesis of heavily n-type graphene for near-infrared photodetectors *J. Phys. Chem.* C **124** 1674–80

[560] Dey T, Mukherjee S, Ghorai A, Das S and Ray S K 2020 Effects of size and localized states in charge carrier dynamics and performance of solution-processed graphene quantum dots/silicon heterojunction near-UV photodetectors *J. Phys. Chem.* C **124** 12161–7

[561] Jana S, Dey T, Bhaktha BN S and Ray S K 2023 Probing the tunable optical properties of highly luminescent functionalized graphene quantum dots as downconverters for superior detection of ultraviolet radiation *Mater. Today Nano* **24** 100400

[562] Wu W T, Wu H X, Zhong M and Guo S W 2019 Dual role of graphene quantum dots in active layer of inverted bulk heterojunction organic photovoltaic devices *ACS Omega* **4** 16159–65

[563] Wu H H, Ding J S, Yang D Y, Li J T, Shi Y H and Zhou Y Y 2020 Graphene quantum dots doped ZnO superstructure (ZnO superstructure/GQDs) for weak UV intensity photodetector application *Ceram. Int.* **46** 17800–8

[564] Yang W, Park I-W, Lee J M and Choi H 2020 Influence of oxidized graphene quantum dots as photosensitizers *J. Nanosci. Nanotechnol.* **20** 3432–6

[565] Abid A, Sehrawat P and Islam , S S 2019 Graphene quantum dot arrays: pros and cons of photodetection in the Coulomb blockade regime *Carbon* **149** 499–511

[566] Riccardi E *et al* 2020 Ultrasensitive photoresponse of graphene quantum dots in the Coulomb blockade regime to THz radiation *Nano Lett.* **20** 5408–14

[567] Hoang Tran M, Park T and Hur J 2021 Solution-processed ZnO:graphene quantum dot/poly-TPD heterojunction for high-performance UV photodetectors *Appl. Surf. Sci.* **539** 148222

[568] Goswami L, Aggarwal N, Verma R, Bishnoi S, Husale S, Pandey R and Gupta G 2020 Graphene quantum dot-sensitized ZnO-nanorod/GaN-nanotower heterostructure-based high-performance UV photodetectors *ACS Appl. Mater. Interfaces* **12** 47038–47

[569] Arunragsa S, Seekaew Y, Pon-On W and Wongchoosuk C 2020 Hydroxyl edge-functionalized graphene quantum dots for gas-sensing applications *Diam. Relat. Mater.* **105** 107790
[570] Purbia R, Kwon Y M, Kim H-D, Lee Y S, Shin H and Baik J M 2020 Zero-dimensional heterostructures: n-doped graphene dots/SnO_2 for ultrasensitive and selective NO_2 gas sensing at low temperatures *J. Mater. Chem.* A **8** 11734–42
[571] Mohammadpour Z and Zare H R 2020 The effect of graphene oxide nanosheets (GONSs) and graphene oxide quantum dots (GOQDs) on corrosion resistance enhancement of Ni–Fe nanocomposite coatings *JOM* **72** 4495–504
[572] Pourhashem S, Rashidi A and Vaezi M R 2019 Comparing the corrosion protection performance of graphene nanosheets and graphene quantum dots as nanofiller in epoxy coatings *Ind. Lubr. Tribol.* **71** 653–6
[573] Ye Y W, Jiang Z L, Zou Y J, Chen H, Guo S D, Yang Q M and Chen L Y 2020 Evaluation of the inhibition behavior of carbon dots on carbon steel in HCl and NaCl solutions *J. Mater. Sci. Technol.* **43** 144–53
[574] Keerthana A K and Ashraf P M 2019 Carbon nanodots synthesized from chitosan and its application as a corrosion inhibitor in boat-building carbon steel BIS2062 *Appl. Nanosci.* **10** 1061–71
[575] Jiang B K, Chen A Y, Gu J F, Fan J T, Liu Y, Wang P, Li H J, Sun H, Yang J H and Wang X Y 2020 Corrosion resistance enhancement of magnesium alloy by N-doped graphene quantum dots and polymethyltrimethoxysilane composite coating *Carbon* **157** 537–48
[576] Xu Y, Lu Y H, Li J G, Liu R L and Zhu X 2020 Effect of graphene quantum dot size on plant growth *Nanoscale* **12** 15045–9
[577] Maria-Hormigos R, Jurado-Sánchez B and Escarpa A 2019 Graphene quantum dot based micromotors: a size matter *Chem. Commun.* **55** 6795–8
[578] Mohamad Nor N A, Nakao H, Jaafar J and Kim J-D 2020 Crosslinked carbon nanodots with highly sulfonated polyphenylsulfone as proton exchange membrane for fuel cell applications *Int. J. Hydrog. Energy* **45** 9979–88
[579] Borah M J, Sarmah H J, Bhuyan N, Mohanta D and Deka D 2022 Application of Box-Behnken design in optimization of biodiesel yield using WO/graphene quantum dot (GQD) system and its kinetics analysis *Biomass Convers. Biorefin.* **12** 221–32
[580] Heidari-Maleni A, Gundoshmian T M, Jahanbakhshi A and Ghobadian B 2020 Performance improvement and exhaust emissions reduction in diesel engine through the use of graphene quantum dot (GQD) nanoparticles and ethanol-biodiesel blends *Fuel* **267** 117116
[581] Gu Q L, Ng T C A, Zain I, Liu X M, Zhang L, Zhang Z X, Lyu Z Y, He Z M, Ng H Y and Wang J 2020 Chemical-grafting of graphene oxide quantum dots (GOQDs) onto ceramic microfiltration membranes for enhanced water permeability and anti-organic fouling potential *Appl. Surf. Sci.* **502** 144128